Newfoundland Labrador

Natural Resources

Mines

TILL GEOCHEMISTRY OF THE GREAT BURNT LAKE (NTS 12A/08), BURNT HILL (NTS 2D/05), NORTHERN COLD SPRING POND (NTS 12A/01) AND ADJACENT MAP AREAS

H.E. Campbell

Open File NFLD/3358

St. John's, Newfoundland
May, 2019

NOTE

The purchaser agrees not to provide a digital reproduction or copy of this product to a third party. Derivative products should acknowledge the source of the data.

DISCLAIMER

The Geological Survey, a division of the Department of Natural Resources (the "authors and publishers"), retains the sole right to the original data and information found in any product produced. The authors and publishers assume no legal liability or responsibility for any alterations, changes or misrepresentations made by third parties with respect to these products or the original data. Furthermore, the Geological Survey assumes no liability with respect to digital reproductions or copies of original products or for derivative products made by third parties. Please consult with the Geological Survey in order to ensure originality and correctness of data and/or products.

Recommended citation:
Campbell, H.E.

2019: Till geochemistry of the Great Burnt Lake (NTS 12A/08), Burnt Hill (NTS 2D/05), Northern Cold Spring Pond (NTS 12A/01) and adjacent map areas. Government of Newfoundland and Labrador, Department of Natural Resources, Geological Survey, St. John's, Open File NFLD/3358, 53 pages.

Cover image:
"the appearance of a vast ruin, which is really its true character"
Howley (1881) on boulder fields around Meelpaeg, Great Burnt and Crooked lakes (looking westward toward the Pipestone Pond Complex; photograph by J.S. Organ, overcast day, June 2016).

Newfoundland Labrador

Natural Resources

Mines

TILL GEOCHEMISTRY OF THE GREAT BURNT LAKE (NTS 12A/08), BURNT HILL (NTS 2D/05), NORTHERN COLD SPRING POND (NTS 12A/01) AND ADJACENT MAP AREAS

H.E. Campbell

Open File NFLD/3358

St. John's, Newfoundland
2019

CONTENTS

Page

FIGURES

Page

PLATE

TABLES

ABSTRACT

This report provides standard and duplicate data for 821 till-geochemical samples collected in 2016, and for 269 till-geochemical samples collected in 1987–88. Also presented are discussions and selected geochemical distribution maps displaying anomalous till values and the results of standard and duplicate data for the 2016 and 1987–88 surveys.

The data in this study include analyses by inductively coupled plasma-optical emission spectrometry (ICP-OES) after 4-acid digestion for aluminum, arsenic, barium, beryllium, cadmium, calcium, cerium, chromium, cobalt, copper, dysprosium, iron, lanthanum, lead, lithium, magnesium, manganese, molybdenum, nickel, niobium, phosphorus, potassium, rubidium, scandium, sodium, strontium, titanium, vanadium, yttrium, zinc, and zirconium; and by instrumental neutron activation analysis (INAA) for antimony, arsenic, barium, bromine, cerium, cesium, chromium, cobalt, europium, gold, iron, hafnium, lanthanum, lutetium, molybdenum, rubidium, scandium, samarium, selenium, sodium, tantalum, terbium, thorium, tungsten, uranium, ytterbium, and zirconium. Silver is analyzed by ICP-OES finish after nitric acid digestion. The data also include analyses of fluoride by ion-selective electrode after alkaline fusion and loss-on-ignition (LOI) by gravimetry. Similar analyses are reported for the 1987–88 survey, excluding silver, which was not analyzed, and gold, which was analyzed by neutron activation. The gold results are considered problematic and have been omitted. Results from these analyses are displayed on individual element-distribution maps that are superimposed on a bedrock-geology base map. Control charts of the analytical results (including recommended values and ranges of 60 elements with the exception of fluoride) for certified reference materials (CRM's) TILL-1, TILL-2, TILL-3 and TILL4 from 1987–88, and 2016 and analysis of CRM's from 2017 are included. Visual analysis of field-duplicate and lab-duplicate data in the form of Thompson-Howarth plots is presented. Field duplicate data were not collected for the 1987–88 surveys.

Spearman rank correlation coefficients from the 2016 till-geochemistry data highlight elemental associations that appear to reflect regional bedrock units; the results indicate correlations between Ni, Co and Mg, and Cr, Fe, Sc and V from elements that are likely derived from the Pipestone Pond Complex (PPC) and the Coy Pond Complex (CPC); correlations between Al, Ba, Rb, K, Be and Cs suggest the Meelpaeg Lake Granite as the source for these elemental anomalies.

Anomalous Au was returned in tills overlying the PPC and the CPC. Anomalous gold in the CPC most likely reflects dispersal from the Huxter Lane/Mosquito Hill deposit, with 98 ppb in a sample 825 m east of the deposit. Several Au anomalies are noted proximal to known showings in the PPC, but the source of an 81 ppb Au anomaly in till 12 km south of the Pipestone Pond gold showing is not certain. Anomalous Zn (624 ppm) is noted southeast of the PPC, and near the contact of the Through Hill granite and the Spruce Brook Formation (471 ppm). A single anomalous value of 1326 ppm Pb is possibly derived from the Pipestone Rapids indication but is located several kilometres southeast of the PPC. Anomalous concentrations of Ni and Cr, dispersed from an unknown source, are abundant in tills near, and dispersed from, the chromite showings hosted in the PPC and CPC. A single W anomaly of 186 ppm is located in the southwest of the study area in tills above the Meelpaeg Lake Granite. Anomalous Co, Sc, V, Cu, Zn, Pb and As are associated with samples taken alongside the Bay d'Espoir highway. The anomalies in this section may be the result of anthropogenic disturbance, as there are 3 quarries used for roadbuilding near the anomalous sample locations. Thus, caution is necessary when interpreting these anomalies. Elsewhere, there is elevated and anomalous F, Pb and W in tills southeast of the Bay d'Espoir highway, and over the Ackley Granite, and anomalous Sb (125–131 ppm) directly south of the Wolf Pond prospect. Anomalous F results from the 1987–88 survey are much higher than samples in the same proximity from the 2016 survey, possibly due to the difference in collection depths (backhoe vs. *hand-dug pits), and sieve sizes (177µm* vs. *63 µm).*

Future work will include the integration and discussion of these data with respect to ice flow and geochemical dispersal. Aerial photo mapping of NTS map area 12A/08 will assist in the interpretation of geochemical results from this study.

INTRODUCTION

Standard and duplicate data analyses from the results of a 2016 till-geochemistry and surficial-mapping program conducted in central Newfoundland are presented (NTS map areas 12A/08, 2D/05, 06), along with supplemental sites in NTS map areas 2D/06, 11, 12; and from an earlier till-geochemistry and mapping survey in NTS map areas 01M/13, 2D/03, 04, 05, 06, 11, 12 (Proudfoot *et al.*, 1990). Individual results from the sampling program have been released in Open File NFLD/3341 (Campbell, 2018; Appendix A). The standard and duplicate data are included in Appendices B–P). Also included in this report are internal control charts from data collected in 1987–88, 2016 and 2017 (Appendix Q), and Thompson-Howarth plots of duplicate distribution (Appendices R and S). Elemental correlations and anomalous till-geochemical values are discussed in this report supplementing Campbell, 2018, including dot plots of selected elements demonstrating the distribution of geochemical anomalies.

OBJECTIVES

The 2016 mapping and sampling study was initiated to investigate till-geochemical signatures and the Quaternary geology of NTS map areas 12A/08 and 2D/05, and to provide data for the provincial till-geochemical database to assist in ongoing exploration efforts within the study area. This program is a continuation of regional till-geochemical and surficial-mapping studies aimed at understanding the glacial geology of, and identifying mineralized material in till in NTS map areas inclusive of the Gander and Exploits subzones (Brushett, 2015; Brushett and Amor, 2016). The 1987–88 study, in which detailed landform and pebble orientation analyses were conducted (Proudfoot *et al.*, 1990), was aimed at better understanding landforms and ice-flow regime from Burnt Hill toward St. Alban's.

LOCATION AND ACCESS

The Great Burnt Lake (NTS map area 12A/08), northern Cold Spring Pond (NTS map area 12A/01), Burnt Hill (NTS map area 2D/05), Great Gull Lake (NTS map area 2D/06), Miguels Pond (NTS map area 2D/12), Eastern Pond (NTS map area 2D/11), Twillick Brook (NTS map area 2D/04) and St. Alban's (NTS map area 1M/13) are located south of the Trans-Canada Highway (TCH), northeast of Meelpaeg and north of Jeddore Lake (Figure 1). The Bay d'Espoir highway (Route 360) bounds the study area to the east.

A small portion of the eastern study area can be accessed through Route 360, and a network of logging roads in various conditions leading off of Route 360. Due to lack of roads in the central and western portion of the study area, sites were accessed by helicopter.

PHYSIOGRAPHY

The study area straddles the drainage basins of Newfoundland's northeastern (Atlantic Ocean) and southern (Gulf of St. Lawrence) coasts. The western portion of the survey contains Great Burnt Lake, Crooked Lake and Island Pond Lake. A ridge separates the lakes from the relatively elevated central study area, extending from the northernmost point, east of Great Burnt Lake, through the Jamieson Hills to the east of Gulp Pond. To the east of this ridge, wetlands are interspersed between hills and ridges with Mount Cormack (320 m) to the west, and Burnt Hill (298 m) and the Partridgeberry Hills forming the highlands to the south. The Northwest Gander River cuts through a plain on the eastern portion of the study area, and east of the river, the land slopes gently southeast toward Berry Hill Pond (Figure 1). The survey area is bounded to the south by east–west-trending ridges and hills, and wetlands on the east-southern boundary of map area 2D/05. Lakes to the southwest have been dammed as part of the Burnt Pond–Granite Lake–Meelpaeg Lake hydroelectric reservoir system (Batterson and Taylor, 2008).

North of the Burnt Hill and Great Burnt Lake in map areas 2D/11 and /12, the topography is characterized by rolling hills dissected by northeast–southwest-oriented valleys; the highest elevations are at Miguel Hill (400 m) and Pot Hill (308 m) (Brushett, 2015).

BEDROCK GEOLOGY

The following bedrock geology descriptions have been derived from earlier work: map areas 2D/05, 08 and 12 (Colman-Sadd and Swinden, 1982, 1984a, b; Colman-Sadd, 1985; Colman-Sadd and Russell, 1988; Swinden, 1988; McNicoll *et al.*, 2006 and Sandeman *et al.*, 2012, 2013); map area 2D/06 (Blackwood and Green, 1983); map area 2D/11 (Blackwood, 1981; Dickson, 1996; Sandeman *et al.*, 2017, 2018); map area 2D/03 (Dickson,1983, 2000); map area 1M/13 (Colman-Sadd, 1976, 1980; Westhues, 2017; Westhues and Hamilton, 2018); map areas 12A/07, 10 (Evans *et al.*, 1994). The study area is too large to include a detailed map of the separate bedrock units and legend; Figure 2 illustrates the larger bedrock groupings for the study area. For more detail, the reader is referred to the above references, or to the bedrock compilation of Colman-Sadd *et al.* (2000).

The study area is underlain by bedrock of the base- and precious-metal-rich Exploits Subzone of the Dunnage Zone, and the Gander Zone (Sandeman *et al.*, 2013; Westhues and Hamilton, 2018). To the north of Coy Pond, the area straddles the Dog Bay Line, a major structural feature spatially associated with mineralization (Sandeman *et al.*, 2018). The mapped rock types and their estimated percentage relative to the 2016 study area are as follows: metamorphosed siliciclas-

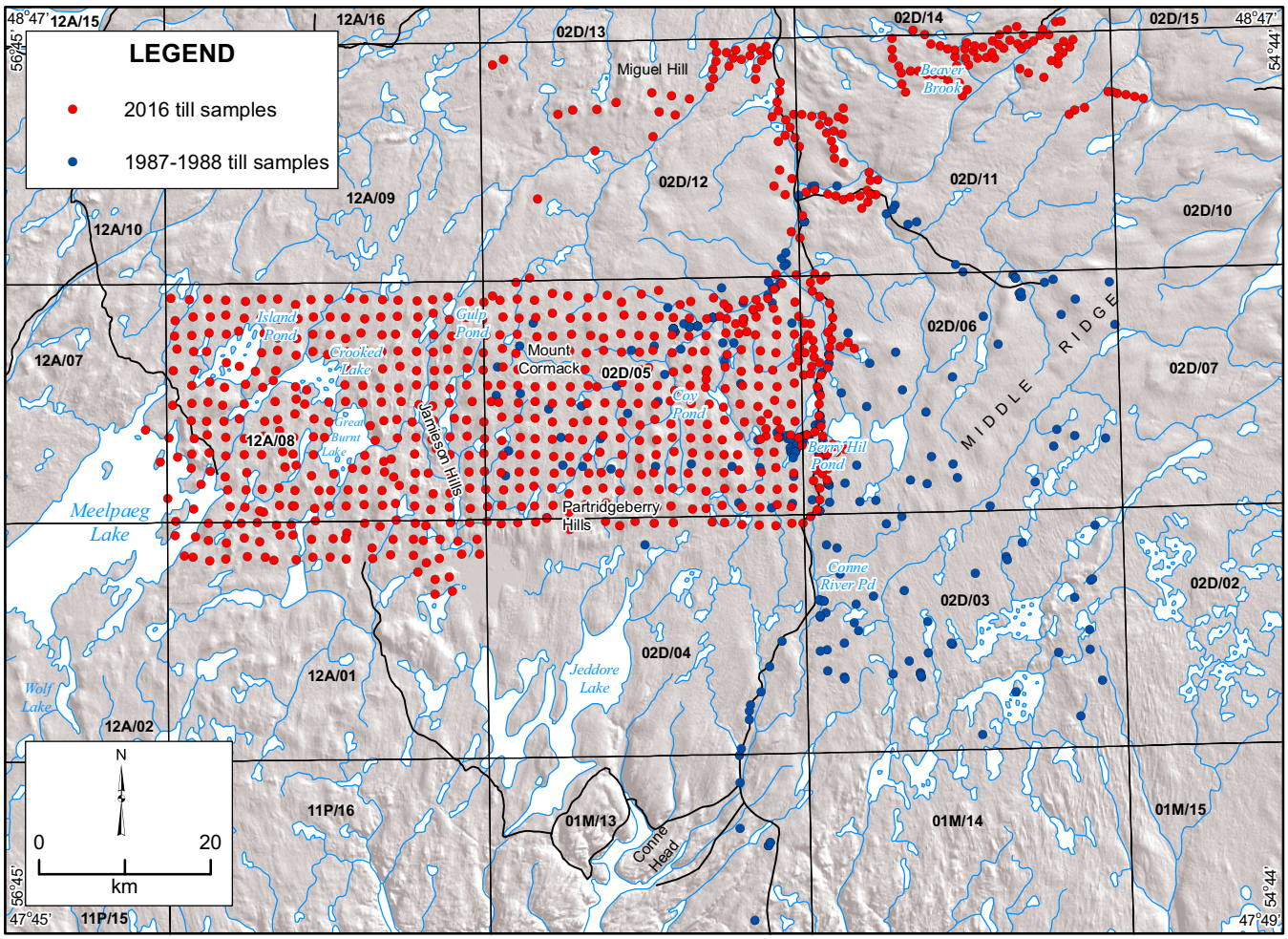

Figure 1. *Location map of the study area. Till samples taken in 1987–88 and 2016 are located south of Miguel Hill to Conne Head.*

tic sediments (55%), felsic intrusive rocks (35%) and ophiolite complexes including mafic and ultramafic plutonic rocks (10%).

Many of the sample sites overlie variably metamorphosed quartzites and semipelitic schists of the Spruce Brook Formation, which is intruded by the Through Hill granite (Figure 2). These rocks form the Mount Cormack Subzone, an elliptically shaped feature that is surrounded by the ophiolitic rocks of the Pipestone Pond and Coy Pond complexes to the west and east (Colman-Sadd and Swinden, 1982, 1984a, b; Colman-Sadd, 1985; Swinden, 1988; Sandeman *et al.*, 2012, 2013). The doughnut-like appearance of this bedrock configuration has led to the informal nickname of the "Tim Horton's complex" (J. Clarke, personal communication, March, 2018).

Clastic sedimentary, volcaniclastic and intermediate to felsic volcanic rocks of the North Steady Pond Formation (Baie d'Espoir Group) are exposed to the east of the Coy Pond Complex and to the south of the Mount Cormack Subzone and Pipestone Pond Complex toward Round Pond. Basalt, conglomerate and greywacke of the Cold Spring Pond formation (of uncertain stratigraphic affinity) outcrop to the southwest of the North Steady Pond Formation. The Meelpaeg Lake Granite of the Silurian North Bay Granite Suite intrudes the Spruce Brook Formation to the west in the Great Burnt Lake area. The Early Ordovician Partridgeberry Hills Granite underlies the southern half of map area, intruding the Coy Pond Complex, the Baie d'Espoir Group and the North Steady Pond Formation (Colman-Sadd and Swinden, 1982, 1984a, b; Colman-Sadd, 1985; Swinden, 1988; Sandeman *et al.*, 2012, 2013).

The main structural fabric trends northeast to southwest, including the faulted contacts of the Pipestone Pond and Coy Pond complexes, with smaller ophiolite slivers oriented to the east–west (Colman Sadd and Swinden, 1984a, b).

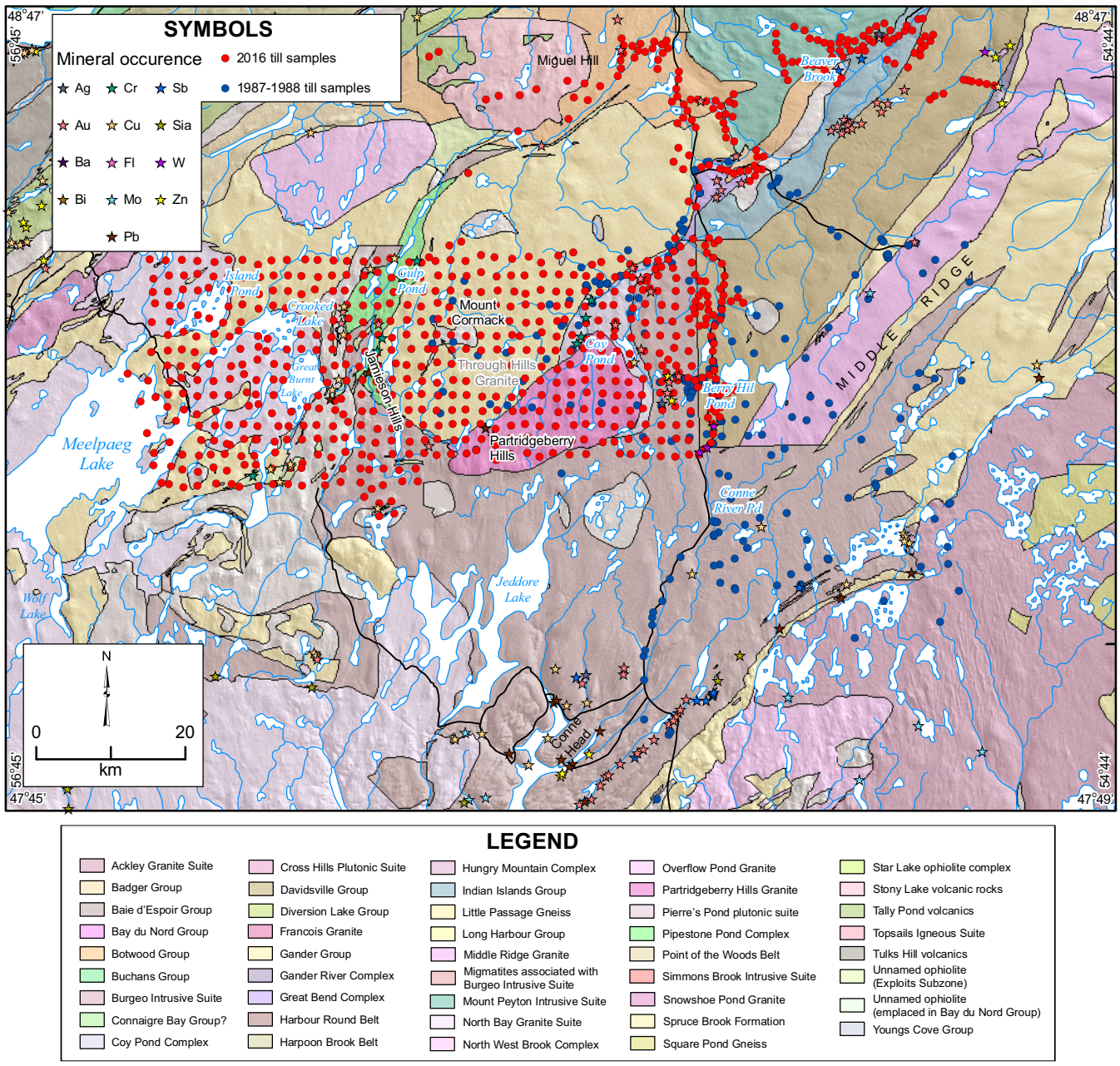

Figure 2. *Bedrock and mineral occurrence map of the study area (after Colman Sadd* et al.*, 2000; Stapleton and Smith, 2018).*

The Spruce Brook Formation underlies the southern half of NTS map area 2D/12, north of the Mount Cormack Complex. This unit is intruded by the Devonian Overflow Pond Granite (Colman-Sadd and Russell, 1988) and the Ordovician Snowshoe Pond Granite (Evans *et al.*, 1994) to the east in NTS map area 12A/09. The Pipestone Pond Complex runs through the boundary of NTS map areas 2D/11 and 12. Siliciclastic sedimentary marine units attributed to the Baie d'Espoir Group, and ophiolite slivers are mapped to the north of the Spruce Brook Formation in NTS map area 2D/12. Siliciclastic non-marine sedimentary units of the Botwood Group outcrop along the North Great Rattling Brook, with Stony Lake volcanic rocks mapped north of NTS map area 2D/12 (Colman-Sadd and Russell, 1988).

East of the Mount Cormack Complex, siliciclastic marine sediments of the Davidsville Group, and psammites, semipelites and quartzites of the Gander Group are intruded by the Middle Ridge Granite (Blackwood and Green, 1983). Northwest of the study area, volcanic rocks of Tally Pond and the Point of the Woods Belt of the Victoria Lake Supergroup outcrop northwest of the immediate study area, north of Noel

Paul's Line (Brown and Colman-Sadd, 1976; Evans *et al.*, 1994). The Silurian to Devonian Mount Peyton intrusive suite outcrops in the northern part of NTS map area 2D/11 and consists of pink, massive medium-grained granite to the east and grey fine-medium gabbro to the west. Sandstone and conglomerate rocks of the Indian Islands Group, and semipelites, pelites and quartzites of the Gander Group (Dickson, 1996) outcrop to the east of the Mount Peyton intrusive suite. South of the study area, siliciclastic marine sediments and volcanic rocks of the Baie D'Espoir Group are intruded by granites from the Silurian North Bay Granite Suite (Colman-Sadd, 1976, 1980; Westhues, 2017; Westhues and Hamilton, 2018).

REGIONAL GLACIAL HISTORY

The regional glacial history of Newfoundland has been summarized by MacClintock and Twenhofel (1940), Murray (1955), Jenness (1960), Grant (1974, 1977, 1989) and Shaw *et al.* (2006). Murray (1955) and Grant (1974) postulated the existence of coalescing ice caps in Newfoundland during the Late Glacial Maximum (Figure 3A). Later work by Rogerson, (1982), Grant (1989) and Shaw *et al.* (2006) described a deglaciation sequence in Newfoundland that was initiated by radial flow of ice towards the sea; from an east-west central divide (Figure 3B). This resulted in the formation of independent ice centres throughout the island. In addition, paleo-ice streams, which flowed toward the coast, were identified (*see* Blundon *et al.*, 2010 and references therein; Figure 3C). The conceptual models of glaciation on the island remain valid, amidst minor revisions and refinements to the locations of ice centres and the timing of deglaciation. Reconciliation of striation data from the past and present (Taylor, 2001) with large-scale landform mapping from satellite imagery and digital elevation models (Liverman *et al.*, 2006), and regional mapping studies, have refined the locations of the ice caps and their centres throughout the island.

MINERALIZATION

Mineralization in the Pipestone Pond and Coy Pond complexes consists of base metals (*e.g.*, Cr, Cu, Pb and Zn) and precious metals (Au) (*e.g.*, Coleman Sadd and Swinden, 1980, 1982; Swinden and Collins, 1982; Swinden, 1988; Dean and Wilton, 2002; Evans, 1996; Sandeman *et al.*, 2012, 2013). Most mineral occurrences are hosted in the Coy Pond and Pipestone Pond (ophiolite) complexes, and in the rocks of the North Steady Pond Formation and the Cold Spring Pond Formation. Antimony and gold mineralization occur in the northwest (*see* Evans, 1996; Lake and Wilton, 2006 and Sandeman *et al.*, 2018 and references therein), and to the south, mineralization consists of base-metal sulphides, gold and antimony (*e.g.*, Colman-Sadd, 1976, 1980; Evans, 1996; Westhues, 2017; Westhues and Hamilton, 2018). Individual occurrences are shown in Figure 2 (Stapleton and Smith, 2018); for brevity, only the prospects and developed prospects are displayed in Table 1.

Chromite occurrences are numerous in the Coy Pond and Pipestone Pond complexes. Heavily disseminated to massive lenses of chromite are typically found throughout the ultramafic rocks of the Pipestone Pond Complex (Swinden, 1988), and disseminated and massive pods of chromite in serpentine, in the ultramafic unit of the Coy Pond Complex (Colman-Sadd and Swinden, 1982). The Coy Pond Complex is also host to gold mineralization in association with arsenopyrite, notably at the Reid deposit (Sandeman *et al.*, 2012), that has an inferred resource of 5.99 million tonnes averaging 0.558 g/t Au (Golden Dory Resources, Press Release, September 28, 2010). The Cold Spring Pond Formation hosts volcanogenic massive sulphide mineralization at the Great Burnt Lake deposit. Mineralization occurs as a tabular, conformable, massive pyrrhotite and chalcopyrite body (Swinden and Collins, 1982), and a 43-101-compliant resource estimate by Pavey Ark Minerals Inc. returned 441 000 tonnes at 2.5% Cu (Puritch and Barry, 2015). Additional mineralization occurs in a similar stratigraphic setting approximately 10 km to the north at the South Pond deposit, where disseminations and blebs of chalcopyrite in semi-massive zones of pyrrhotite occur in association with elevated gold mineralization of uncertain genesis (Puritch and Barry, 2015; J. Hinchey, personal communication, 2016). The North Steady Pond Formation also hosts precious- and base-metal mineralization (McBride, 1988; J. Hinchey, personal communication, 2016). The Mosquito Hill deposit contains gold mineralization in association with arsenopyrite (Sandeman *et al.*, 2013). A 43-101-compliant resource calculation (Giroux and Froude, 2010) returned 11.18 million tonnes averaging 0.546 g/t Au for 196 257 ounces gold. VMS mineralization occurs at the Katie property (south of the Mosquito Hill and Reid deposits) where mineralized outcrop samples have returned grades of 17% combined Zn, Pb and Cu (J. Hinchey, personal communication, 2016), and trenching has returned 15.1% Zn, 0.45% Pb, 0.27% Cu, 42g/t Ag and 2.4g/t Au (Canstar Resources Inc., 2018) website-https://www.canstarresources.com/projects/the-katie-project/geology).

No known occurrences are noted in the Meelpaeg Lake Granite of the North Bay Granite Suite, which underlies Island Pond, Meelpaeg, Crooked and Great Burnt lakes, in the western portion of the study area. Wolframite, molybdenite and bismuthinite occur in quartz, quartz-greisen and quartz-pegmatite veins at Granite Lake, 25 km west of the study area (Tuach and Delaney, 1987).

Mineralization to the northeast of Coy Pond includes Au–Ag–Sb–As associated with the Dog Bay Line, including the Beaver Brook antimony mine, which has produced nearly 20 000 dry metric tonnes of ore (Sandeman *et al.*, 2018). Fur-

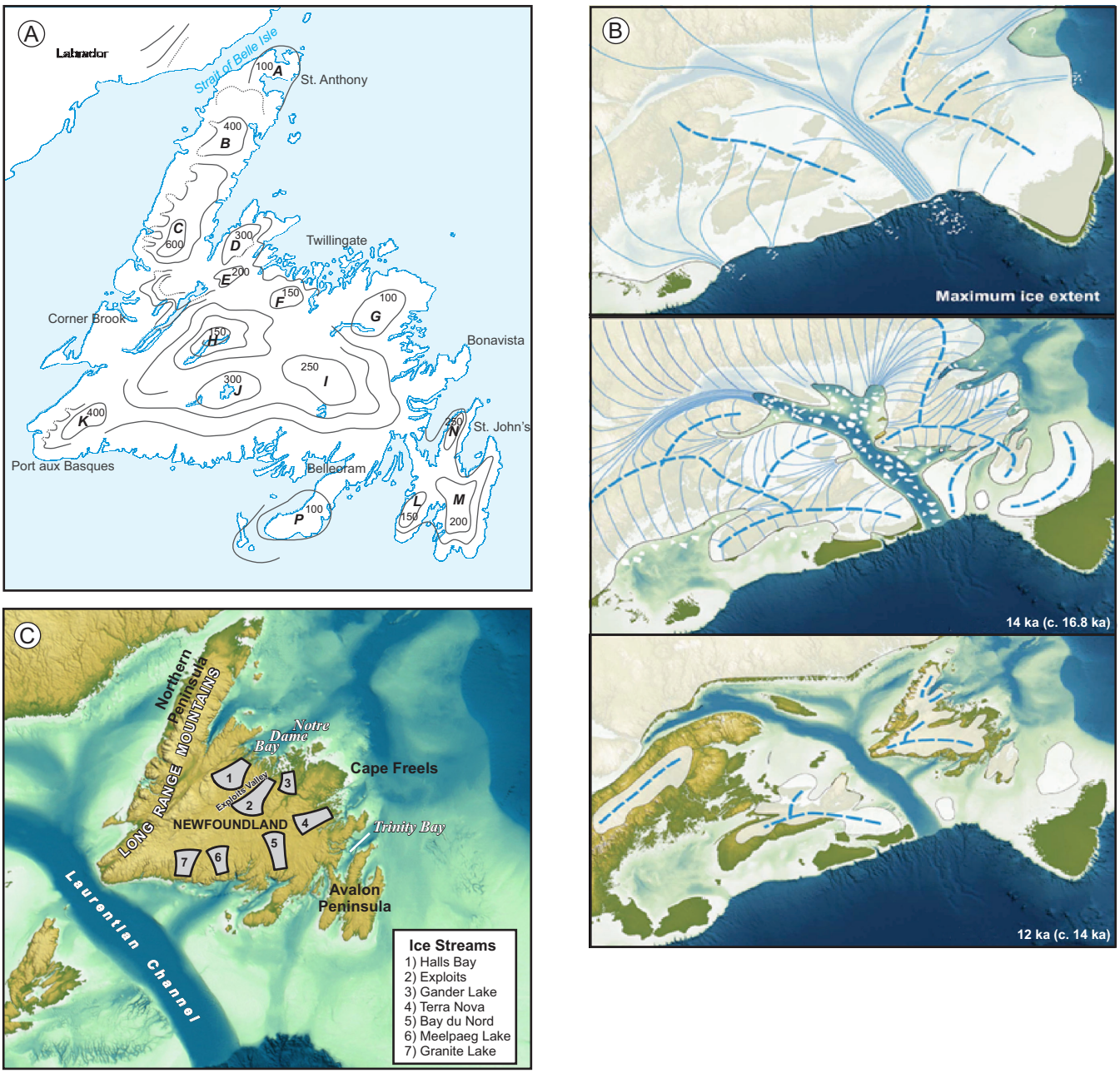

Figure 3. *Main regional-scale synthesis of events thought to have effected erosion and dispersal in the study area. A) Locations of multiple ice caps proposed by Grant (1974). The letters mark the location of the ice caps, end moraines and other ice-marginal features are shown by dotted lines, numbers represent average ground elevation in metres; B) Deglacial model of Newfoundland from maximum extent until 12 000 Ka (Shaw* et al.*, 2006) indicating a large east–west arcuate ice divide across the Province; C) Ice streams identified by Blundon* et al. *(2010).*

ther exploration around the mine, including drilling, has uncovered Sb–Au–As mineralized zones and Sb and Au in soil samples (*ibid.*).

Mineral exploration activity in the southern part of the survey, toward St. Albans, was initially focused on base-metal prospects, but has recently focused on structurally controlled quartz veins hosting Au–Sb–As mineralization (Evans, 1996; Westhues, 2017; Westhues and Hamilton, 2018). Abundant mineral showings and occurrences are mapped in this area (Figure 2), with active exploration history throughout the Little River, True Grit, Wolf Pond and other areas. Recent grab samples taken during the regional bedrock-mapping program in the St. Alban's area contain up

Table 1. Listing of past producers, developed prospects and prospects throughout the study area (Stapleton and Smith, 2018). Showings and indications are not listed, for brevity

Deposit Name	MODS Reference	Major Commodity	Commodity	Stratigraphic Unit	Status	NTS	UTMZONE	EAST	NORTH
Benton Granite Quarry	002D/16/Stn001	Stn		Gander Lake Pluton	Past Producer (Dormant)	02D/16	21	695790	5414390
Bay d'Espoir Quarry	002D/04/Stn001	Stn	Stn	St.Josephs Cove Fm - Bay d'Espoir Gp	Past Producer (Dormant)	02D/04	21	605000	5320500
Beaver Brook	002D/11/Sb 003	Sb	Au	Davidsville Group	Past Producer (Dormant)	02D/11	21	633050	5397150
Great Burnt Lake Deposit	012A/08/Cu 001	Cu		Cold Spring Pond Formation of the Baie d'Espoir Group	Developed Prospect	12A/08	21	562870	5354080
Mosquito Hill	002D/05/Au 008	Au	Cu	North Steady Pond Fm-Baie d'Espoir Gp	Developed Prospect	02D/05	21	603374	5367646
South Pond Copper	012A/08/Cu 002	Cu	Au	Baie d'Espoir Group	Developed Prospect	12A/08	21	563640	5363860
Hunan	002D/11/Sb 001	Sb	Au, Zn, Cu, As	Davidsville Group	Developed Prospect	02D/11	21	629950	5395550
Bruce Pond - Katie Property	002D/05/Au 004	Au		North Steady Pond Fm- Baie d'Espoir Gp	Prospect	02D/05	21	607000	5352300
Bullet	002D/15/Au 002	Au	Pb, Sb, Cu	Davidsville Group	Prospect	02D/15	21	657690	5425570
The Knob	002D/15/Au 004	Au	Cu, Pb, Sb	Davidsville Group	Prospect	02D/15	21	657440	5425500
Baseline Showing	002D/15/Au 008	Au		Davidsville Group	Prospect	02D/15	21	658030	5427200
Lazyman	001M/13/Au 022	Au		Bay d'Espoir Group - Riches Island Formation	Prospect	01M/13	21	608924	5312320
Chrome Pond	012A/08/Cr 001	Cr	Fe, Mg, Pt, Tlc	Pipestone Pond Complex	Prospect	12A/08	21	568080	5357900
Careless Cove	002D/15/Au 006	Au	Ag	Davidsville Group	Prospect	02D/15	21	649340	5418980
Kim Lake #2	002D/03/Sb 001	Sb	Au	Isle Galet Formation - Baie d'Espoir Group	Prospect	02D/03	21	624710	5326130
Tall Tree Zone - Katie Property	002D/05/Zn 002	Zn	Au	North Steady Pond Formation, Baie d'Espoir Group	Prospect	02D/05	21	607550	5351300
Chiouk Brook	002D/11/Au 001	Au	Cu, Pb, Sb	Great Bend Complex	Prospect	02D/11	21	616200	5384000
Lizard Pond South	002D/11/Au 002	Au	Cr, Mg	Great Bend Complex	Prospect	02D/11	21	614220	5379500
Little River No. 5	001M/13/Au 007	Au		Isle Galet Formation - Baie d'Espoir Group	Prospect	01M/13	21	607800	5308350
Xingchang	002D/11/Sb 002	Sb	Au	Davidsville Group	Prospect	02D/11	21	629200	5395050
Peyton	002D/14/Au 004	Au	Ag, Cu, Pb, Zn	Mt Peyton Intrusive Suite	Prospect	02D/14	21	644850	5425500
Dome	002D/15/Au 007	Au		Hunt's Cove Formation (Davidsville Group)	Prospect	02D/15	21	658650	5428550
Red Rocks Steady No 1	002D/05/Asb002	Asb	Mg	Coy Pond Complex	Prospect	02D/05	21	597020	5360530
Mystery Pond Zone - Katie Property	002D/05/Au 005	Au	Ag, Cu, Pb, Zn, W	North Steady Pond Formation, Baie d'Espoir Group	Prospect	02D/05	21	603500	5358150
A-Zone Extension	002D/11/Au 007	Au		Davidsville Group	Prospect	02D/11	21	631080	5388880
Bowater	002D/15/Au 003	Au		Davidsville Group	Prospect	02D/15	21	656100	5426900
Pocket Pond	002D/15/Au 012	Au	Zn, Cu, Pb, Sb	Hunts Cove Fm-Davidsville Gp	Prospect	02D/15	21	662450	5427700
Little River Antimony	001M/13/Sb 003	Sb	Au	Isle Galet Formation - Baie D'Espoire Group	Prospect	01M/13	21	602587	5303341
Startrack	002D/16/Au 002	Au	Sb	Gander Group, Indian Bay Big Pond Formation	Prospect	02D/16	21	694841	5417330
Black Bart VMS System - Katie Property	002D/05/Zn 001	Zn	Pb, Au, Ag	North Steady Pond Formation, Baie d'Espoir Group	Prospect	02D/05	21	607100	5354550
Aztec	002D/11/Au 006	Au		Davidsville Group	Prospect	02D/11	21	630650	5388950
Rolling Pond	002D/11/Au 019	Au	Sb, As, Ba	Botwood Group	Prospect	02D/11	21	611475	5391400
Lotto Zone	002D/15/Au 011	Au		Davidsville Group	Prospect	02D/15	21	658760	5428920
The MacDonald Zone - Katie Property	002D/05/Au 003	Au	Ag, Zn, Cu, Pb	North Steady Pond Formation, Baie d'Espoir Group	Prospect	02D/05	21	607200	5353700
South Pond B-Zone	012A/08/Au 002	Au	Cu	Cold Spring Pond Formation	Prospect	12A/08	21	563230	5361650
Breccia Pond	002D/11/Au 004	Au	Ni, Fe	Great Bend Complex	Prospect	02D/11	21	616900	5380400
Wolf Pond	001M/13/Au 008	Au	Sb	Isle Galet Formation - Baie d'Espoir Group	Prospect	01M/13	21	607200	5307800
Great Bend Magnesite Pit	002D/11/Mg 008	Mg	Cr, Asb, Tlc	Great Bend Complex	Prospect	02D/11	21	611520	5377950
Hurricane	002D/14/Au 002	Au	Ag	Mt Peyton Intrusive Suite	Prospect	02D/14	21	645150	5425150
22 West	001M/13/Au 009	Au	Ag, Sb	Isle Galet Formation - Baie d'Espoir Group	Prospect	01M/13	21	605200	5305700
Grouse	002D/15/Au 017	Au			Prospect	02D/15	21	656739	5425030
Little River Three	001M/13/Au 021	Au	Au, Sb, Zn	Isle Galet Formation - Baie D'Espoire Group	Prospect	01M/13	21	600674	5302514
West Tower Pond	002D/16/Au 001	Au	Sb	Gander Group, Indian Bay Big Pond Formation	Prospect	02D/16	21	696580	5415680
Great Gull Lake Tungsten #2	002D/03/W 001	W		Baie d'Espoir Group - North Steady Pond Formation	Prospect	02D/03	21	612350	5344920
The Outflow	002D/15/Au 001	Au	As, Sb	Davidsville Group	Prospect	02D/15	21	653550	5422550
Keats Showing	002D/15/Au 010	Au		Davidsville Group	Prospect	02D/15	21	658040	5427140
Twillick Brook	002D/04/Sla001	Sla		Twillick Brook Member - St Josephs Cove Formation	Prospect	02D/04	21	604850	5320850
Reid Porphyry Zone	002D/05/Au 006	Au		Coy Pond Complex	Prospect	02D/05	21	602332	5369083
South Pond A-Zone	012A/08/Au 001	Au	Cu	Cold Spring Pond Formation of the Baie D'Espoir Group	Prospect	12A/08	21	563430	5363150
Caribou River North	002D/10/Mg 001	Mg	Tlc	Gander River Ultrabasic Belt	Prospect	02D/10	21	650850	5393130
Goose	002D/11/Au 011	Au		Davidsville Group	Prospect	02D/11	21	635750	5390000
Corsair	002D/14/Au 003	Au		Mt Peyton Intrusive Suite	Prospect	02D/14	21	644350	5425300
Road Showing	002D/15/Au 009	Au		Davidsville Group	Prospect	02D/15	21	658880	5428110
End Zone	012A/08/Cu 006	Cu		Cold Springs Pond Fm-North Salmon Dam Basalt	Prospect	12A/08	21	563520	5360130

to 7000 ppb gold (Westhues, 2017). Farther to the southeast, along the Bay d'Espoir highway, a sample containing 51 ppb Au from the government regional-till program (Brushett and Amor, 2016) was taken from till above the Simmon's Brook Intrusive Suite (O'Brien, 1998).

GLACIAL DISPERSAL

In general, mineral dispersal trains are much shorter (*i.e.*, <5 km long) and more diffuse in Newfoundland than in Labrador. Dispersal trains on the island reflect erosion and transport of material from small topographically controlled ice centres, rather than the km-scale glacial dispersal of material observed in Labrador from large-scale continental ice-sheets (Batterson and Liverman, 2000). Dispersal trains on the island are less easily defined, due to chemical similarities in adjacent bedrock types, and complexities in ice-flow directions from shifting ice centres (*ibid.*). The previously mentioned east-west ice-divide (Shaw *et al.*, 2006; Figure 3B) cuts through the northeastern corner of the study. Glacial dispersal around the ice divide would be minimal as: 1) the horizontal component of ice flow velocity would be zero, and 2) ice-flow directions would shift in response to ice accumulation and decay (Benn and Evans, 2010).

The south-southeast oriented landforms associated with the Meelpaeg Lake paleo ice-stream (Blundon *et al.*, 2010), and the north-northeast landforms associated with the Terra Nova paleo ice-stream (*ibid.*) bound the study area to the extreme west and northeast respectively. In these regions, till may be transported 5 to 10 times farther than till in regions that has been dispersed by normal ice-flow (Primmer *et al.*, 2015).

SEDIMENTARY CHARACTERISTICS

Sediment composition and characteristics of the study area are detailed in Campbell *et al.* (2017) and briefly summarized below.

The sediment is poorly sorted, ranging between clay and boulders. The observed clast angularity (subangular to subrounded) and shape (bullet, cigar and triangle), and the presence of striations on clasts indicates that the material was eroded, transported and deposited by glaciers, and thus is a till. Only one till unit was identified during the 2016 survey through the hand-dug sample pits, and in the 1987–1988 survey over NTS map areas 1M/13, 2D/03, 04, 05, 06, 11, 12 where some sample pits were excavated by backhoe (Proudfoot *et al.*, 1990).

In some places, till has been eroded and fines removed by melting water from retreating glaciers (*i.e.*, NTS map areas 12A/08; northeast corner of 2D/05). In others (*i.e.*, over ultramafic rocks of the Pipestone Pond and Coy Pond complexes), till cover is very shallow and samples were commonly taken from mudboils. The southeastern and south central areas of both map areas appear to be overlain by hummocky meltout tills (*i.e.*, tills deposited by melting glaciers) that are composed of sandy matrices and rounded clasts. In areas where granite is present, tills tend to have a coarser matrix due to the competency of the granite and its characteristic minerals (quartz and feldspars). In the eastern portion of NTS map areas 2D/05 up into 2D/11 and 2D/06, where less competent sedimentary rocks (particularly mudstones and shales) are present, the erosion is pervasive and tills tend to be clay-rich. These aforementioned variations are reflected in the distribution of surficial material (Figure 4) where the western half of the 2016 study area is composed of hummocky tills, with areas of eroded tills and till veneer, and the eastern half is composed of till blanket deposits, hummocky tills and till veneer, and minor till ridges.

Small eskers and minor glaciofluvial outwash are observed to the southwest of the survey (Plate 1A), interspersed among ridges, and composed of sandy tills derived from granites. Poorly sorted, hummocky landforms consisting of boulders and sand, interpreted as disintegration moraine, are noted southeast of Crooked Lake (Plate 1B), as well as minor eskers.

The tills are predominantly grey-brown having a slight pink tinge (Munsell Soil Classification 2.5 YR3/2-4 to 2.5YR5/2-4) and yellow-brown (10YR2/2/2, 10RYR32-6, 10YR4/2-4). These colours reflect the dominant bedrock: tills dispersed from sedimentary units tend to have a more yellowish tinge; tills dispersed from plutonic rocks have a pink to dark-green tinge, reflecting the mineral abundances in the underlying felsic and mafic rock units.

SAMPLING METHODS

A total of 821 samples (including duplicates) were collected from the C-, BC-, and B-horizons (Figure 1; Appendix A); most were collected from test pits (40 to 70 cm deep) and roadcuts (50 to 100 cm deep). Mudboils were sampled at shallower depths (~25 cm). In the absence of surface sediment, samples were collected from bedrock detritus. Marine, fluvial or glaciofluvial sediments were avoided because of possible reworking, and the difficulty in determining distances and directions of sediment transport. Some samples around Great Burnt Lake and Crooked Lake were taken from the B-horizon. Care was taken to sample below the iron oxide-rich horizon present in soils in the lowlands near these lakes.

Sample spacing was constrained by access as well as surficial geology; generally about one sample every kilometre in road-accessible areas, and 1 sample every 4 km^2 in more remote areas, where helicopter support was required. Handheld Trimble Juno devices recorded site observations and downloaded each night to examine site and sample data. Duplicate samples from 47 sites were used to test for field re-

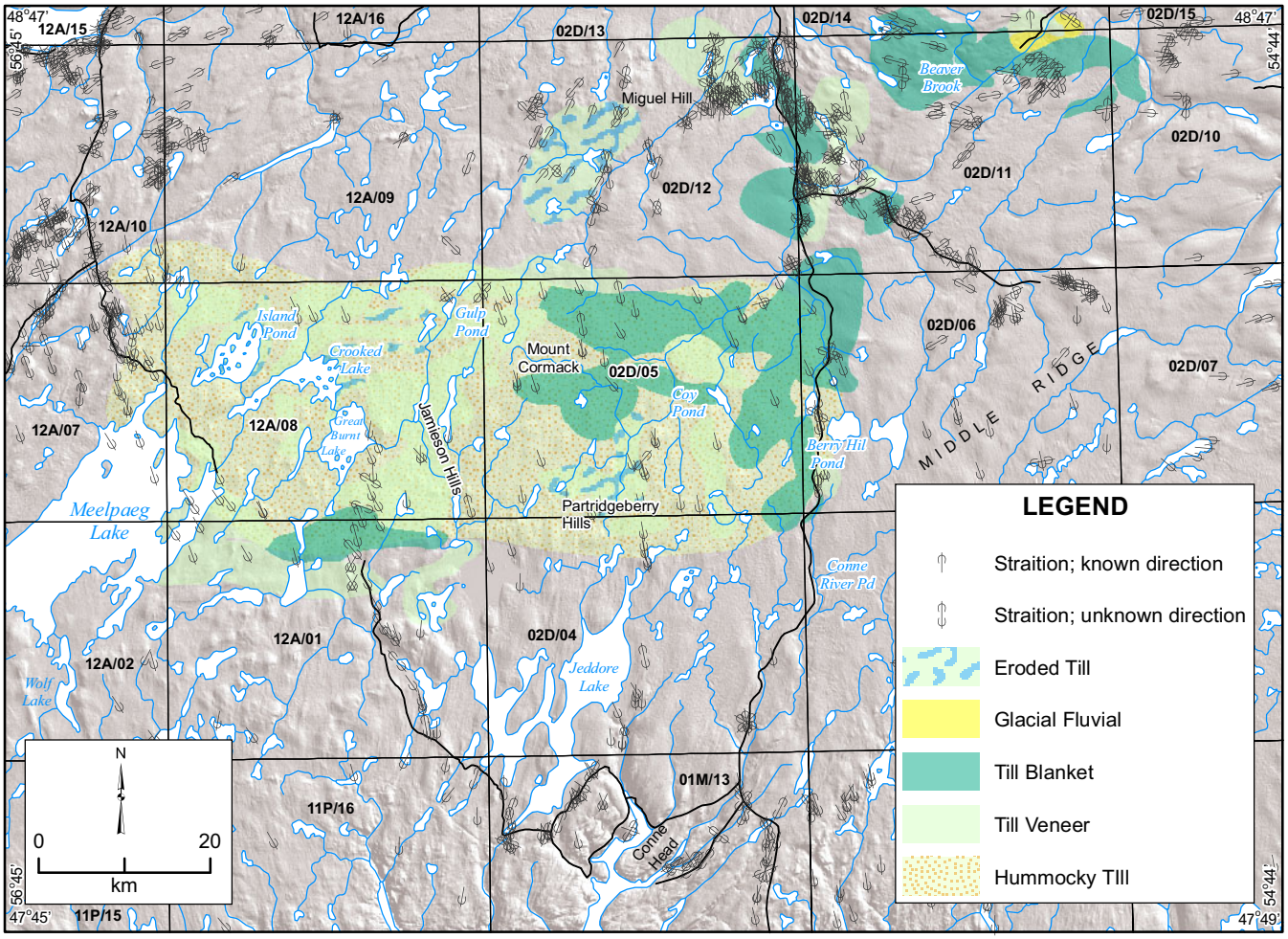

Figure 4. *General surficial materials map for the 2016 study area, based on individual site observations only. NTS map areas 12A/08 and 2D/05 are predominantly composed of hummocky tills (stippled light yellow unit), with areas of eroded till (light yellow with blue stippling), till veneer (lime green) and till blanket (dark green) with minor glaciofluvial units (yellow).*

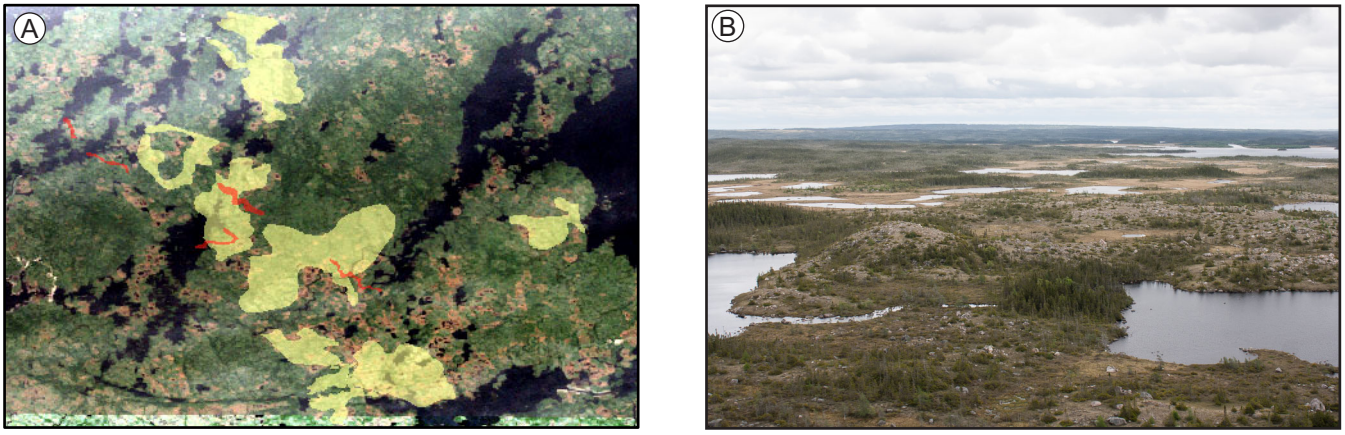

Plate 1. *A) Glacial deposits south of Great Burnt Lake and Crooked Lake composed of sandy, boulder tills (light green) and eskers (red outline); B) Close-up of disintegration moraine with abundant boulders. This type of terrain reflects* in-situ *melting of ice, with material being slightly washed and sorted in areas.*

producibility. Samples were placed in Kraft-paper sample bags, and sent to the Geological Survey's Geochemical Laboratory in St. John's; here they were air-dried in ovens at 60°C and dry-sieved through 177 µm stainless-steel sieves.

Samples from the 1987–88 survey were taken from backhoe and hand-dug pits; sample spacing was less uniform (Figure 1), as the survey was broader in scope (Proudfoot *et al.*, 1990), incorporating sites from NTS map areas 1M/13, 2D/03, 04, 05, 06, 11, 12. Duplicate field samples were not collected during this survey. Preparation methods were the same, except that the sieve mesh size was 63 µm.

GEOCHEMISTRY

Analytical work was carried out at the Geological Survey's Geochemical Laboratory, with samples sent out, for additional analyses, to Maxxam Analytics Laboratories of Mississauga, Ontario. Samples were digested using a mixture of hydrochloric (HCl), nitric (HNO_3), perchloric ($HClO_4$) and hydrofluoric (HF) acid and analyzed with inductively coupled plasma-optical emission spectrometry (ICP-OES) for 31 elements. Silver was analyzed by ICP-OES after HNO_3 digestion. Data also include analyses of fluoride by alkaline fusion and ion-selective electrode, and loss-on-ignition (LOI) by gravimetric means (Tables 2 and 3). Samples that were sent out were analyzed by Instrumental Neutron Activation Analysis (INAA) for 27 elements. A detailed description of the above analytical methods is provided in Finch *et al.* (2018). To distinguish the different analytical methods, the trace-element variables are labelled using a combination of the element name and a numeric suffix indicating the type of digestion or preparation (where appropriate) and finish, as follows:

- 1 for INAA with no digestion,
- 2 for ICP-OES after 4-acid digestion,
- 6 for ICP-OES after HNO_3 digestion, and
- 9 for ion-selective electrode after alkaline fusion.

(*See* http://geoatlas.gov.nl.ca/Custom/help/Till_geochem_help_tables/Table2_AnalyticalMethods.html for an explanation of the codes.) A complete list of variables are given in Tables 2 and 3, along with the detection limits of each element, and a full listing of field and geochemical data is contained in Open File NFLD/3341 (Campbell, 2018), a link to which is provided in Appendix A.

QUALITY ASSURANCE/QUALITY CONTROL

Certified Reference Samples: 2016 Study

The data for 12 analyses of 60 elements for each Certified Reference Materials (CRM) TILL-1, TILL-2, TILL-3, and TILL-4 from the 2016 survey are presented in Appendices B−F. Values less than the detection limit are represented by the negative of the detection limit (rather than ½ the detection limit as they are represented in the till values). The code -99 indicates that the sample was not analyzed for that element. The accuracies or "recoveries" of the 12 analyses of 60 elements in Certified Reference Materials (CRM) TILL-1, TILL-2, TILL-3, and TILL-4 from the 2016 survey are summarized in Tables 4 to 6. The recovery is calculated as the ratio of the arithmetic mean of each standard's analyses to its respective recommended value (Lynch, 1996). In the case of fluoride, for which no certified reference values are available, the arithmetic means of multiple analyses of the certified reference materials at the GSNL laboratory were used (Finch *et al.*, 2018). Individual control charts showing analysis for the CRM's for each of the elements from 2016 are in Appendix Q. Control charts from 7 analyses of 60 elements in CRM's taken from a 2017 study are also included in Appendix Q for comparison.

More than half of the elements analyzed by ICP-OES show recoveries greater than 95%, although those of certain elements (notably Be2, Y2, and Zr2) are lower, indicating that these elements are hosted in mineral phases that are only partially digested by the multi-acid digestion. Overestimation (greater than 100% recovery) is observed in Co, Cu, Ni, Sc, Sr and V, with the maximum recovery displayed by Sr (118%).

Recoveries of approximately half of the elements analyzed by INAA are within 5% of 100%. Selenium is rarely detected in these standards, and thus is omitted from Table 5.

In general, recoveries are similar to those reported in other till-sampling programs (*e.g.*, Brushett and Amor, 2016; Organ and Amor, 2016a, b).

Certified Reference Samples: 1987–88 Study

Results of five analyses of 59 elements in CRMs TILL-1, TILL-2, TILL-3 and TILL-4 from the 1987–88 survey are compiled in Tables 7 to 9 and in Appendices B−F). Individual control charts showing the analysis for the CRM's for each of the elements are in Appendix Q. For elements analyzed by ICP-OES (Table 7), recoveries are similar to those of the 2016 survey, with the exception of Cu and Ni. Recoveries of elements analyzed by INAA are almost identical to those of the 2016 survey (Compare Tables 4 and 8).

Duplicate Analyses

Analyses of field and lab duplicates (Appendices G–P) from the 2016 survey were tabulated to examine analytical precision (Table 10). Absolute differences of duplicate pairs

Table 2. Geochemical elements for the 2016 survey, their analysis method, measurement units, detection limits (D.L.), number of samples that are less than the DL (<D.L.) and range of data values

Element	Method	Units	D.L.	<D.L.	Max	Min	Element	Method	Units	D.L.	<D.L.	Max	Min
Ag6	ICP-OES	ppm	0.1	760	0.6	<0.1	Mg2	ICP-OES	%	0.01	0	13.26	0.05
Al2	ICP-OES	%	0.01	0	9.65	1.16	Mn2	ICP-OES	ppm	1	0	11672	170
As1	INAA	ppm	0.5	2	1040.0	<0.5	Mo1	INAA	ppm	1	736	131	<1
As2	ICP-OES	ppm	2	16	923	<2	Mo2	ICP-OES	ppm	1	710	119	<1
Au1	INAA	ppb	1	557	98	<1	Na1	INAA	%	0.1	0	3.7	0.5
Ba1	INAA	ppm	50	0	790	58	Na2	ICP-OES	%	0.01	0	3.78	0.37
Ba2	ICP-OES	ppm	1	0	781	54	Nb2	ICP-OES	ppm	1	4	34	<1
Be2	ICP-OES	ppm	0.1	0	3.2	0.3	Ni2	ICP-OES	ppm	1	0	1790	4
Br1	INAA	ppm	1	30	228	<1	P2	ICP-OES	ppm	1	0	4194	59
Ca2	ICP-OES	%	0.01	0	3.14	0.08	Pb2	ICP-OES	ppm	1	7	1326	<1
Cd2	ICP-OES	ppm	0.1	447	1.6	<0.1	Rb1	INAA	ppm	5	0	200	7
Ce1	INAA	ppm	3	0	270	11	Rb2	ICP-OES	ppm	1	0	212	11
Ce2	ICP-OES	ppm	1	0	190	7	Sb1	INAA	ppm	0.1	2	16.8	<0.1
Co1	INAA	ppm	2	160	160	<2	Sc1	INAA	ppm	0.1	0	41.8	4.8
Co2	ICP-OES	ppm	1	1	181	<1	Sc2	ICP-OES	ppm	0.1	0	37.6	2.2
Cr1	INAA	ppm	10	1	1430	<10	Se1	INAA	ppm	1	771	<1	<1
Cr2	ICP-OES	ppm	1	0	518	9	Sm1	INAA	ppm	0.1	0	25.8	1.7
Cs1	INAA	ppm	0.5	4	60.3	0.9	Sr2	ICP-OES	ppm	1	0	242	28
Cu2	ICP-OES	ppm	1	5	160	<1	Ta1	INAA	ppm	0.2	1	3	<0.2
Dy2	ICP-OES	ppm	0.1	0	11.5	1	Tb1	INAA	ppm	0.5	9	4.3	<0.5
Eu1	INAA	ppm	0.5	189	3.6	<0.5	Th1	INAA	ppm	0.5	0	52.3	1.4
F9	ISE	ppm	40	0	687	29	Ti2	ICP-OES	ppm	1	0	17153	950
Fe1	INAA	%	0.1	0	25.6	0.7	U1	INAA	ppm	0.1	0	10.1	0.8
Fe2	ICP-OES	%	0.01	0	25.55	0.65	V2	ICP-OES	ppm	1	0	477	18
Hf1	INAA	ppm	1	2	44	<1	W1	INAA	ppm	1	157	186	<1
K2	ICP-OES	%	0.01	0	3.07	0.15	Y2	ICP-OES	ppm	1	0	52	5
La1	INAA	ppm	1	0	130	4	Yb1	INAA	ppm	0.5	1	14	<0.5
La2	ICP-OES	ppm	1	0	93	4	Zn2	ICP-OES	ppm	1	0	624	10
Li2	ICP-OES	ppm	0.1	0	102.7	2.7	Zr1	INAA	ppm	100	190	1500	<100
LOI	Gravimetric	%	0.1	0	38.6	1.0	Zr2	ICP-OES	ppm	1	0	147	14
Lu1	INAA	ppm	0.05	0	2.1	0.1							

Table 3. Geochemical elements for the 1987−88 survey, their analysis method, measurement units, detection limits (D.L.), number of samples that are less than the DL (<D.L.) and range of data values

Element	Method	Units	D.L.	<D.L.	Max	Min	Element	Method	Units	D.L.	<D.L.	Max	Min
Al2	ICP-OES	%	0.01	0	8.41	1.00	Mn2	ICP-OES	ppm	1	0	2730	336
As1	INAA	ppm	0.5	0	656.0	3.1	Mo1	INAA	ppm	1.5	212	9	<1
As2	ICP-OES	ppm	0.5	0	635	5	Mo2	ICP-OES	ppm	1	264	7	<1
Ba1	INAA	ppm	50	0	850	85	Na1	INAA	%	0.1	0	2.3	0.30
Ba2	ICP-OES	ppm	1	0	1319	95	Na2	ICP-OES	%	0.01	0	2.52	0.18
Be2	ICP-OES	ppm	0.1	0	11.5	0.4	Nb2	ICP-OES	ppm	1	0	30	3
Br1	INAA	ppm	1	134	74	<0.1	Ni2	ICP-OES	ppm	1	0	2061	6
Ca2	ICP-OES	%	0.01	0	1.43	0.07	P2	ICP-OES	ppm	1	0	1283	115
Cd2	ICP-OES	ppm	0.1	210	0.9	<0.1	Pb2	ICP-OES	ppm	1	0	203	6
Ce1	INAA	ppm	3	0	210	19	Rb1	INAA	ppm	5	0	410	25
Ce2	ICP-OES	ppm	1	0	217	24	Rb2	ICP-OES	ppm	1	0	497	30
Co1	INAA	ppm	2	0	100	1	Sb1	INAA	ppm	0.1	0	131.0	0.2
Co2	ICP-OES	ppm	1	0	94	5	Sc1	INAA	ppm	0.1	0	33.1	3.7
Cr1	INAA	ppm	10	0	750	48	Sc2	ICP-OES	ppm	0.1	0	32.8	3.5
Cr2	ICP-OES	ppm	1	0	405	11	Se1	INAA	ppm	1	325	<1	<1
Cs1	INAA	ppm	0.5	0	40.0	1.4	Sm1	INAA	ppm	0.1	0	16.9	1.7
Cu2	ICP-OES	ppm	1	0	195	4	Sr2	ICP-OES	ppm	1	0	236	16
Dy2	ICP-OES	ppm	0.1	2	9.9	<0.1	Ta1	INAA	ppm	0.2	0	5.4	0
Eu1	INAA	ppm	0.5	6	2.5	<0.1	Tb1	INAA	ppm	0.5	0	2.4	<0.5
F9	ISE	ppm	40	0	1754	0	Th1	INAA	ppm	0.5	0	102.0	2.7
Fe1	INAA	%	0.1	0	7.7	0.70	Ti2	ICP-OES	ppm	1	0	7244	925
Fe2	ICP-OES	%	0.01	0	7.33	0.81	U1	INAA	ppm	0.1	0	23.4	0.6
Hf1	INAA	ppm	1	1	28	2	V2	ICP-OES	ppm	1	0	231	13
K2	ICP-OES	%	0.01	0	4.12	0.50	W1	INAA	ppm	1	24	54	<1
La1	INAA	ppm	1	0	95	9	Y2	ICP-OES	ppm	1	0	56	4
La2	ICP-OES	ppm	1	0	58	9	Yb1	INAA	ppm	0.5	0	8.4	0.9
Li2	ICP-OES	ppm	0.1	0	119.1	8.3	Zn2	ICP-OES	ppm	1	0	115	18
LOI	Gravimetric	%	0.1	0	32.4	0.6	Zr1	INAA	ppm	100	3	1000	100
Lu1	INAA	ppm	0.05	2	1.1	<0.05	Zr2	ICP-OES	ppm	1	0	201	20
Mg2	ICP-OES	%	0.01	0	15.86	0.20							

Table 4. Recoveries of ICP-OES analysis for the 2016 study

Elements	TILL-1	TILL-2	TILL-3	TILL-4	Average
Al2	0.94	0.94	0.94	0.95	94%
As2	0.93	0.95	0.93	0.94	94%
Ba2	1.00	0.99	1.00	0.98	100%
Be2	0.53	0.71	0.55	0.70	62%
Ca2	0.94	0.97	0.97	0.99	97%
Ce2	0.95	0.88	0.95	0.85	91%
Co2	1.12	1.13	1.12	1.15	113%
Cr2	0.97	0.93	0.90	0.84	91%
Cu2	1.04	1.06	1.05	1.09	106%
Fe2	1.00	1.00	1.01	1.00	100%
K2	0.94	0.92	0.93	0.93	93%
La2	0.95	0.93	0.92	0.89	92%
Li2	0.99	0.96	1.00	0.94	97%
Mg2	0.96	0.97	0.97	0.95	96%
Mn2	1.00	0.99	0.97	1.01	99%
Mo2	0.33	0.93	0.25	0.93	61%
Na2	1.02	1.00	1.01	0.99	101%
Nb2	0.87	0.82	0.85	0.92	86%
Ni2	1.12	1.03	0.98	1.17	108%
P2	0.99	0.95	0.99	0.99	98%
Pb2	0.64	0.74	0.71	0.83	73%
Rb2	1.02	1.01	1.00	0.99	101%
Sc2	1.16	1.11	1.11	1.17	114%
Sr2	1.15	1.18	1.15	1.23	118%
Ti2	0.86	0.92	0.99	0.95	93%
V2	1.06	1.07	1.08	1.06	107%
Y2	0.73	0.45	0.75	0.48	60%
Zn2	0.92	0.93	0.91	0.97	93%
Zr2	0.15	0.19	0.27	0.18	20%

Table 5. Recoveries of INAA analysis for the 2016 study

Elements	TILL-1	TILL-2	TILL-3	TILL-4	Average
As1	1.01	0.95	1.01	1.01	100%
Au1	1.23	1.00	1.08	1.15	112%
Ba1	1.03	0.92	1.02	1.00	99%
Br1	0.94	0.93	0.94	0.93	94%
Ce1	1.07	0.97	1.00	1.08	103%
Co1	0.98	0.89	0.90	0.94	93%
Cr1	1.06	1.00	1.00	1.06	103%
Cs1	1.06	0.97	1.13	1.08	106%
Eu1	1.20	1.10			115%
Fe1	1.04	0.94	1.02	1.01	100%
Hf1	1.08	0.91	0.75	1.10	96%
La1	1.02	0.96	0.88	1.02	97%
Lu1	0.94	0.59	0.79	0.82	78%
Mo1	0.20	1.07	0.30	1.14	68%
Na1	1.04	0.94	1.01	1.00	100%
Rb1	1.00	0.98	0.97	1.02	99%
Sb1	1.00	0.96	0.92	0.90	94%
Sc1	1.11	0.95	0.97	1.09	103%
Sm1	1.06	0.95	1.05	1.03	103%
Ta1	1.09	1.05		1.02	105%
Tb1	0.93	0.92		0.89	91%
Th1	1.05	0.95	1.07	1.01	102%
U1	0.96	0.92	0.94	0.99	95%
W1		1.00		0.98	99%
Yb1	1.06	0.89	1.00	0.92	97%
Zr1	0.96	0.96	1.03	1.13	102%

are plotted against their respective means in Thompson-Howarth (1978) plots (Appendix R and S) to give a visual impression of how precision varies with concentration level. For most elements, the precision of lab duplicates, analyzed by both INAA and ICP-OES, is better (*i.e.*, smaller in absolute magnitude) than their corresponding field duplicates. It is to be expected that the absolute magnitude of the precision of two field duplicates, collected at least 1 m apart and incorporating the natural inhomogeneity of the sample medium as well the analytical repeatability, would exceed the analytical precision alone.

The discrepancies between precision estimates for duplicate field and lab analyses of Ba1 La1, Lu1, Rb1 and Sc1, are relatively small overall. On the other hand, Au1, Co1, Cr1, Sb1, Ta1, Tb1, Eu1, W1 Yb1 and Cu2 show poor precision at concentrations near their respective detection limits; the precision improves with increasing concentration, with the exception of Au1. Poor repeatability of Au analysis is common in regional surveys as distribution of Au grains is particularly inhomogeneous (the 'nugget effect'; Clifton *et al.*, 1969).

Precision estimates calculated from lab duplicates in 1987–88 (of which the raw data is included in Appendices G–P) are summarized in Table 11. No precision estimates are included for field duplicates as they were not collected during this program.

DATA ANALYSIS

As a first step, the frequency distributions of each element were examined for analyses below the detection limits. Selenium returned no detectable values, and Ag6, Au1, Cd2, Mo1, and Mo2 all show a significant number of undetectables (Appendix A).

Assignment of Map Symbols

Geochemical results from the survey for each element are represented by circular symbols of differing sizes, with

Table 6. Recoveries of LOI and F analysis for the 2016 study

Elements	TILL-1	TILL-2	TILL-3	TILL-4	Average
LOI	1.01	0.98	1.07	1.21	107%
F9*	0.99	1.03	1.05	1.01	102%

* Arithmetic mean of all GSNL standard measurements (n=89) Finch *et al.*, 2018

Table 7. Recoveries of ICP-OES analysis for the 1987–88 study

Elements	TILL-1	TILL-2	TILL-3	TILL-4	Average
Al2	0.84	0.86	0.89	0.88	87%
As2	0.95	1.01	0.93	1.12	100%
Ba2	1.00	1.00	1.01	0.98	100%
Be2	0.53	0.77	0.58	0.75	66%
Ca2	0.03	0.97	0.99	0.99	74%
Cd2					
Ce2	1.06	0.85	1.01	0.87	95%
Co2	1.16	1.23	1.04	1.66	127%
Cr2	1.03	0.75	0.75	0.68	80%
Cu2	0.84	0.93	0.80	0.95	88%
Dy2					
Fe2	0.99	1.02	1.03	1.01	101%
K2	0.94	0.98	0.97	0.98	97%
La2	0.90	0.80	0.91	0.82	86%
Li2	0.99	0.97	1.01	0.94	98%
Mg2	0.99	0.99	1.04	1.02	101%
Mn2	1.00	0.99	0.99	1.02	100%
Mo2	-0.50	0.89	-0.24	0.89	26%
Na2	0.96	0.96	0.97	0.95	96%
Nb2	0.99	0.66	0.96	0.80	85%
Ni2	0.78	0.86	0.92	0.79	84%
P2	1.01	0.97	1.03	1.02	101%
Pb2	0.63	0.73	0.75	0.89	75%
Rb2	0.95	1.29	1.02	1.29	114%
Sc2	1.12	1.07	1.11	1.15	111%
Sr2	1.08	1.10	1.10	1.15	110%
Ti2	0.82	0.85	0.97	0.95	90%
V2	1.03	1.04	1.05	1.06	104%
Y2	0.70	0.42	0.74	0.47	58%
Zn2	0.86	0.85	0.94	0.92	89%
Zr2	0.17	0.21	0.31	0.20	22%

the size of the symbols representing the magnitude of the analysis. The break points for the symbols were determined by the 90th and 97.5 percentile of each element's frequency distribution, with the largest symbols assigned to values greater than the 97.5 percentile, intermediate symbols represent values that fall between the 90.5–97.5 percentile and smaller circles representing values lower than the 90th percentile. The data are presented in Tables 12 and 13, for the 2016 and 1987–88 surveys respectively, with the terms "anomalous" and "elevated" used to describe the 90th and 97.5 percentiles. The justification, advantages and limitations of using percentiles to define the classifications above are described by Amor (2013).

Table 8. Recoveries of INAA analysis for the 1987–88 study

Elements	TILL-1	TILL-2	TILL-3	TILL-4	Average
As1	1.01	0.95	1.01	1.01	100%
Au1	1.23	1.00	1.08	1.15	112%
Ba1	1.03	0.92	1.02	1.00	99%
Br1	0.94	0.93	0.94	0.93	94%
Ce1	1.07	0.97	1.00	1.08	103%
Co1	0.98	0.89	0.90	0.94	93%
Cr1	1.06	1.00	1.00	1.06	103%
Cs1	1.06	0.97	1.13	1.08	106%
Eu1	1.20	1.10			115%
Fe1	1.04	0.94	1.02	1.01	100%
Hf1	1.08	0.91	0.75	1.10	96%
La1	1.02	0.96	0.88	1.02	97%
Lu1	0.94	0.59	0.79	0.82	78%
Mo1		1.07	0.13	1.14	78%
Na1	1.04	0.94	1.01	1.00	100%
Rb1	1.00	0.98	0.97	1.02	99%
Sb1	1.00	0.96	0.92	0.90	94%
Sc1	1.11	0.95	0.97	1.09	103%
Sm1	1.06	0.95	1.05	1.03	103%
Ta1	1.09	1.05		1.02	105%
Tb1	0.93	0.92		0.89	91%
Th1	1.05	0.95	1.07	1.01	102%
U1	0.96	0.92	0.94	0.99	95%
W1		1.00		0.98	99%
Yb1	1.06	0.89	1.00	0.92	97%
Zr1	0.96	0.96	1.03	1.13	102%

Table 9. Recoveries of LOI and F analysis for the 1987–88 study

Elements	TILL-1	TILL-2	TILL-3	TILL-4	Average
LOI	1.04	1.01	1.10	1.32	112%
F9*	0.92	.90	.80	1.02	91%

* Arithmetic mean of all GSNL standard measurements (n=89) Finch *et al.*, 2018

Table 10. Overall precision of duplicate samples from the lab and field from the 2016 survey

Element	Precision (95% C.L.) Analytical	Field	Element	Precision (95% C.L.) Analytical	Field
Al2	2.9%	24.0%	Mg2	3.5%	44.8%
As1	10.2%	79.0%	Mn2	5.4%	28.9%
As2	22.2%	63.0%	Mo1	66.7%	112.0%
Au	161.7%	152.1%	Mo2	53.3%	66.7%
Ba1	10.2%	28.3%	Na1	9.5%	17.6%
Ba2	3.2%	30.0%	Na2	4.2%	24.6%
Be2	8.0%	31.4%	Nb2	11.4%	35.3%
Br1	11.5%	101.4%	Ni2	10.1%	55.4%
Ca2	3.6%	31.4%	P2	4.1%	60.0%
Cd2	66.7%	66.7%	Pb2	12.9%	58.6%
Ce1	15.8%	42.6%	Rb1	23.5%	30.2%
Ce2	8.5%	41.0%	Rb2	8.6%	24.6%
Co1	50.0%	120.0%	Sb1	21.0%	40.0%
Co2	9.5%	63.0%	Sc1	10.6%	36.4%
Cr1	27.0%	62.4%	Sc2	3.2%	38.0%
Cr2	3.7%	59.3%	Sm1	8.3%	32.2%
Cs1	17.6%	37.0%	Sr2	3.1%	23.4%
Cu2	6.9%	65.3%	Ta1	40.0%	46.7%
Dy2	10.2%	26.6%	Tb1	21.0%	38.0%
Eu1	144.6%	130.8%	Th1	10.0%	28.6%
F9	23.5%	89.6%	Ti2	7.7%	26.7%
Fe1	9.7%	42.3%	U1	10.9%	36.6%
Fe2	2.9%	35.3%	V2	3.5%	27.0%
Hf1	13.1%	41.7%	W1	120.0%	120.0%
K2	2.8%	26.2%	Y2	10.2%	27.5%
La1	12.7%	28.6%	Yb	30.7%	29.8%
La2	7.6%	38.2%	Zn2	4.3%	35.2%
Li2	4.6%	40.4%	Zr1	154.7%	148.3%
LOI	8.9%	68.1%	Zr2	7.4%	32.6%
Lu1	21.3%	31.7%			

Table 11. Overall precision of duplicate samples from the lab from the 1987–88 survey

Element	Precision (95% C.L.) Analytical	Element	Precision (95% C.L.) Analytical
Al2	1.9%	Mn2	3.4%
As1	12.8%	Mo1	64.7%
As2	16.1%	Mo2	62.8%
Ba1	10.6%	Na1	19.9%
Ba2	3.6%	Na2	2.3%
Be2	5.1%	Nb2	16.5%
Br1	27.9%	Ni2	3.5%
Ca2	3.6%	P2	3.9%
Cd2	114.6%	Pb2	10.1%
Ce1	24.4%	Rb1	10.0%
Ce2	22.5%	Rb2	16.9%
Co1	15.9%	Sb1	10.8%
Co2	7.4%	Sc1	27.1%
Cr1	22.0%	Sc2	3.6%
Cr2	4.5%	Se1	8.0%
Cs1	13.0%	Sm1	12.0%
Cu2	4.6%	Sr2	3.9%
Dy2	29.8%	Ta1	16.5%
Eu1	24.5%	Tb1	15.1%
Fe1	17.5%	Th1	14.9%
Fe2	2.9%	Ti2	16.1%
F9	27.9%	U1	9.0%
Hf1	16.4%	V2	5.8%
K2	2.6%	W1	45.3%
La1	21.3%	Y2	8.7%
La2	25.5%	Yb1	46.3%
Li2	4.2%	Zn2	2.9%
LOI	3.8%	Zr1	34.8%
Lu1	34.6%	Zr2	8.4%
Mg2	2.4%		

RESULTS

GEOCHEMICAL ANOMALIES IN TILL

Correlations

2016 Study

Correlations between elements were determined by using Spearman rank correlation coefficients of symmetrical coordinates (*see* Kynčlová *et al.*, 2017; Garrett *et al.*, 2017) using version 1.1.14 of the .rgr package in R package (R-PROJECT 2016; The R Project for Statistical Computing (http://www.r-project.org; accessed June 2018)). The resulting correlations in till (Figure 5) appear to show strong positive correlations in Ni, Cr, Co and Mg thought to be related to the mafic and multramafic rocks of the ophiolite complexes, and in Al, Ba, Rb, K, Be and Cs thought to be associated with felsic granitic rocks of the study area. There is a moderate to strong positive correlation between Fe, Sc, V, and between Al, Fe, Sc and V. Strong positive correlations exist between Hf, Tb, Lu, Yb, U, Th, Ce, La and Sm; these elements are negatively correlated with Co, Cu and Fe. Lead and thorium are moderately positively correlated, and Ca and Na, Zn and Fe, Cs and Rb are highly positively correlated. Arsenic and Sb are moderately positively correlated.

1987–88 Study

The resulting correlations in till (Figure 6) are similar to the 2016 study, and are more clearly defined in the correlations of symmetrical distances; although the heirarchical clustering of the elements differs. Strong positive correlations exist between Ce, Th, La, Sm, Tb, Hf, Lu and Yb, and between Sc, V, Fe and Zn. Cobalt, Mg and Ni show moderate positive correlations with one another, and are positively correlated with Sc, V, Fe, Zn, As and Cu. Uranium and Ta are strongly correlated but are negativelly correlated with Sc, V,

Table 12. 90 and 97.5 percentiles of geochemical variables (2016). Values exceeding the 90-percentile are considered "elevated"; those exceeding the 97.5-percentile "anomalous"

Element	Elevated (90%)	Anomalous (97.5%)	Element	Elevated (90%)	Anomalous (97.5%)
Al2 pct	7.75	8.57	Lu1 ppm	0.85	1.18
As1 ppm	34.0	87.3	Mg2 pct	1.27	2.43
As2 ppm	31	80	Mn2 ppm	886	1419
Au1 ppb	3	7	Mo1 ppm	1	2
Ba1 ppm	450	560	Mo2 ppm	1	2
Ba2 ppm	452	584	Na1 pct	1.9	2.3
Be2 ppm	1.9	2.2	Na2 pct	1.80	2.16
Br1 ppm	48	77	Nb2 ppm	16	22
Ca2 pct	1.26	2.32	Ni2 ppm	67	154
Cd2 ppm	0.2	0.3	P2 ppm	613	933
Ce1 ppm	120	158	Pb2 ppm	18	26
Ce2 ppm	81	109	Rb1 ppm	95	130
Co1 ppm	18	33	Rb2 ppm	93	122
Co2 ppm	22	42	Sb1 ppm	2.1	3.7
Cr1 ppm	420	810	Sc1 ppm	17.3	21.4
Cr2 ppm	116	207	Sc2 ppm	17.9	22.7
Cs1 ppm	5.8	10	Sm1 ppm	10	13.5
Cu2 ppm	43	69	Sr2 ppm	131	157
Dy2 ppm	4.4	6.1	Ta1 ppm	1.4	1.7
Eu1 ppm	1.8	2.2	Tb1 ppm	1.5	2.1
F9 ppm	301	394	Th1 ppm	19.2	26.7
Fe1 pct	4.6	6.0	Ti2 ppm	5901	7606
Fe2 pct	4.55	5.90	U1 ppm	4.1	5.1
Hf1 ppm	16	23	V2 ppm	106	136
K2 pct	2.12	2.60	W1 ppm	3	6
La1 ppm	59	72	Y2 ppm	21	30
La2 ppm	37	50	Yb1 ppm	5.8	8.2
Li2 ppm	31.7	48.7	Zn2 ppm	66	87
LOI pct	11.8	20.6	Zr2 ppm	81	106

Table 13. 90 and 97.5 percentiles of geochemical variables (1987–88). Values exceeding the 90-percentile are considered "elevated"; those exceeding the 97.5-percentile "anomalous"

Element	Elevated (90%)	Anomalous (97.5%)	Element	Elevated (90%)	Anomalous (97.5%)
Al2 pct	6.77	7.48	Mg2 pct	1.38	2.71
As1 ppm	76.0	179.3	Mn2 ppm	1228	1809
As2 ppm	69	165	Mo1 ppm	2	4
Ba1 ppm	513	563	Mo2 ppm	1	3
Ba2 ppm	493	560	Na1 pct	1.9	2.1
Be2 ppm	3.6	5.4	Na2 pct	1.78	1.94
Br1 ppm	14	29	Nb2 ppm	11	15.65
Ca2 pct	0.84	1.03	Ni2 ppm	104	262
Cd2 ppm	0.3	0.5	P2 ppm	968	1069
Ce1 ppm	150	173	Pb2 ppm	33	45
Ce2 ppm	102	127	Rb1 ppm	120	180
Co1 ppm	27	48	Rb2 ppm	143	214
Co2 ppm	30	48	Sb1 ppm	3.2	4.7
Cr1 ppm	300	410	Sc1 ppm	16.0	19.7
Cr2 ppm	89	136	Sc2 ppm	16.7	20.4
Cs1 ppm	11	16	Sm1 ppm	12.1	14.5
Cu2 ppm	62	96	Sr2 ppm	152	180
Dy2 ppm	4.3	5.7	Ta1 ppm	1.8	3.0
Eu1 ppm	2.0	2.4	Tb1 ppm	1.8	2.2
F9 ppm	340	989	Th1 ppm	23.4	30.5
Fe1 pct	4.4	5.1	Ti2 ppm	5416	5882
Fe2 pct	4.25	4.89	U1 ppm	6.1	7.3
Hf1 ppm	19	223	V2 ppm	101	125
K2 pct	2.14	2.68	W1 ppm	6	10
La1 ppm	65	78	Y2 ppm	21	29
La2 ppm	41	50	Yb1 ppm	5.9	7.2
Li2 ppm	42.8	59.9	Zn2 ppm	77	96
LOI pct	4.6	8.4	Zr2 ppm	96	119
Lu1 ppm	0.77	1.00			

Fe, As and Cu. Aluminium is moderately positively correlated to K, Rb and Sc. Cesium and Li are strongly positively correlated, and As, Cu, Zn and Co, and Pb and Br are moderately positively correlated.

Dotplots

Spatial concentrations of elements are represented by selected dot plots of elevated and anomalous concentrations of elements from the 2016 and 1987–88 studies, plotted above bedrock units on individual maps (Figures 7–25). As more than one method of analysis was used for several of the elements, the method that showed the best recovery was plotted.

Au1 (Figure 7)

Most of the tills containing elevated and anomalous Au are located above the Pipestone Pond Complex. The highest Au values are 98 ppb, in a sample located 825 m east of the Huxter Lane/Mosquito Hill deposit (2D/05/Au008) and 81 ppb, in a sample located 12 km southeast of the Pipestone Pond gold occurrence (12A/08/Au003). Most of the other gold anomalies in till from this study are single sample anomalies; some located near known mineral occurrences and bedrock units hosting mineral occurrences. Others, such as the 22 ppb located west of Great Burnt Lake, and the 8 ppb northwest of Island Pond Lake, occur in bedrock units not known to host mineral occurrences. A 10 ppb value in tills is located 1.5 km up-ice (northwest) of the Mosquito Hill (2D/05/Au008) prospect. Anomalous Au values of 14 and 12 ppb are located to the northwest and southwest of the Rolling Pond (2D/11/Au019) prospect. Other anomalous values of Au include; 15 ppb, 1.7 km northeast (down-ice) of the O'Reilly prospect (2D/11/ Au021), 8 ppb Au, 5.9 km down-ice (northeast) of North Paul's Pond (2D/11/Au020), 11 ppb Au, 5.6 km east-northeast (down-ice) of LBNL (2D/11/Au010), and 8 ppb Au, 630 m up-ice (west) of the Dead Wolf Brook Junction No 1 (2D/10/Cu001) showing.

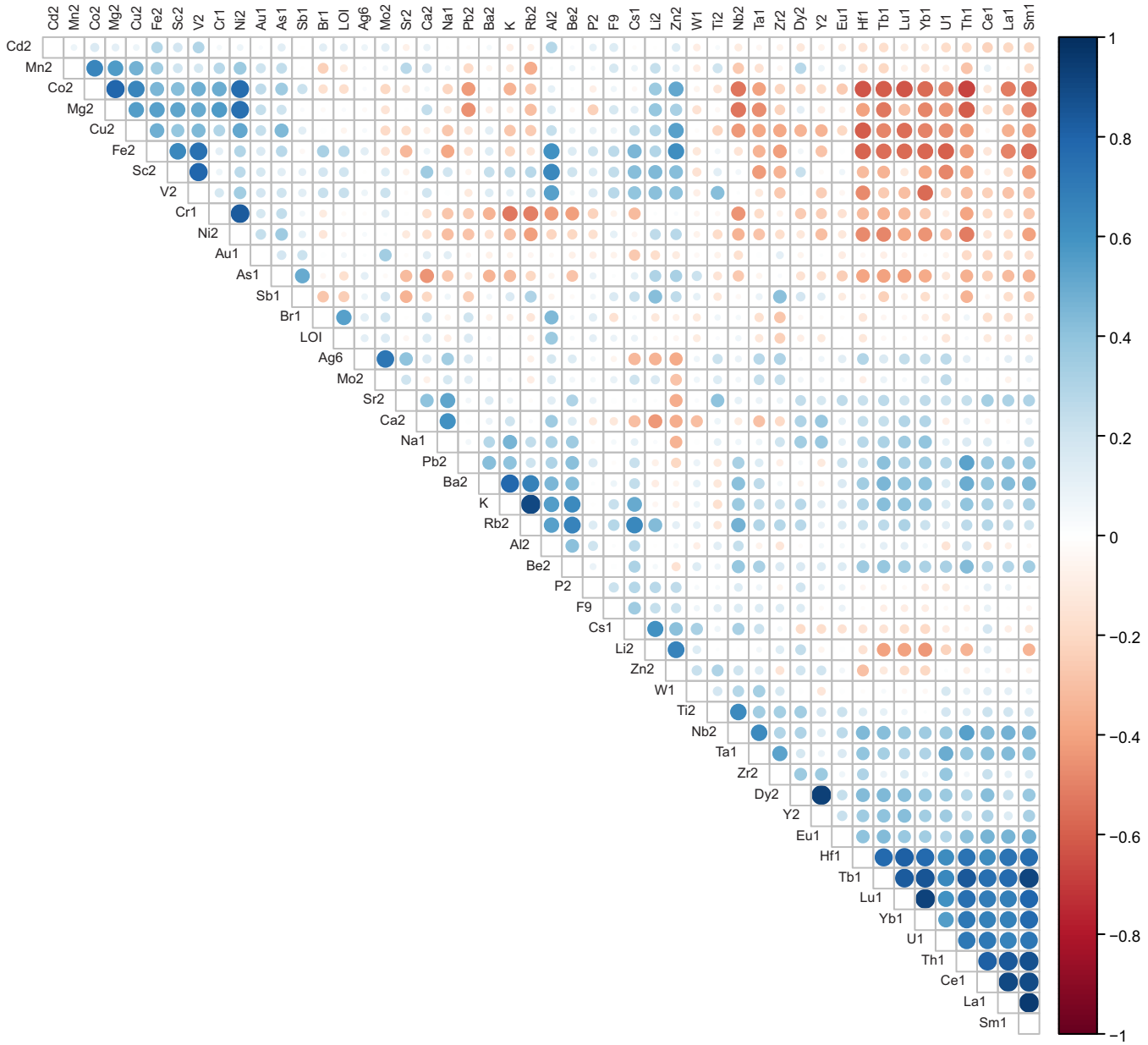

Figure 5. *Spearman rank correlation matrix of symmetric coordinates (Kynčlová* et al.*, 2017; Garrett* et al.*, 2017) for the 2016 till-geochemistry results. The results are clustered to show major-element associations; with the colour representing the magnitude of associations (dark blue represents positive correlations and brownish red represents negative correlations). The size of the dots represents the significance of the correlation at the 0.95 confidence level.*

Cr2, Co2 and Ni2 (Figures 8–10)

Anomalous values of Cr, Co and Ni are: 1) distributed in tills overlying the Pipestone Pond Complex and Coy Pond Complex, near known chromite showings, 2) extending south of the Pipestone Pond Complex, 3) extending to the southeast of the Coy Pond Complex, and 4) extending east of the Coy Pond Complex, toward the Baie du Nord Wilderness refuge. Till samples located next to the Bay d'Espoir highway north and south of Berry Hill Pond returned anomalous Co. An 8-km-southeastward linear extent of anomalous and elevated Co is located south of Conne River Pond.

Sc2, V2 and Cu2, Zn2 and Pb2 (Figures 11–15)

Anomalies in till of Sc, V and Cu are overlying and west of the Pipestone Pond Complex, the Coy Brook indication (2D/05/Cu001), southeast of the Partridgeberry Hills Granite

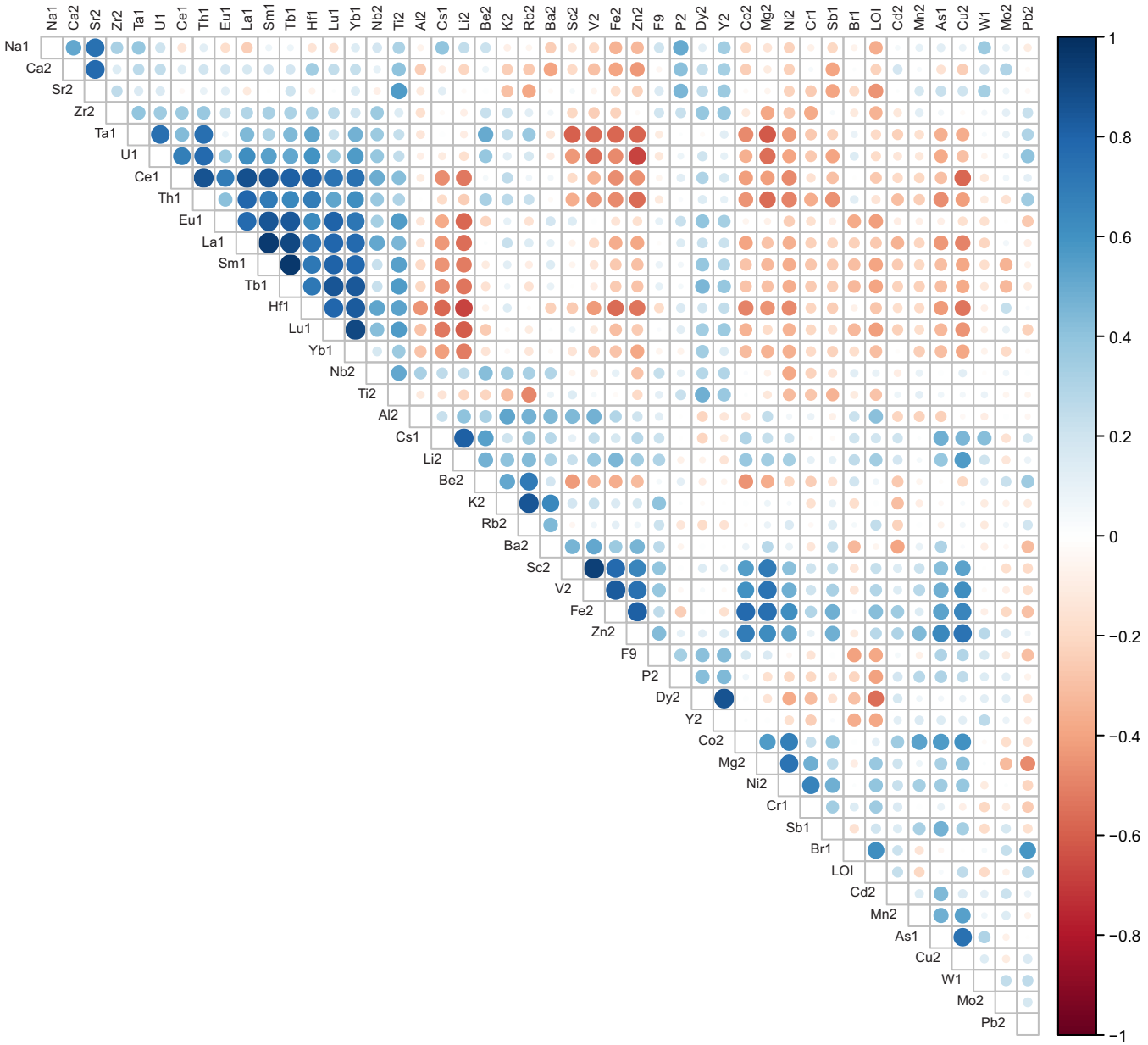

Figure 6. *Spearman rank correlation matrix of symmetric coordinates (Kynčlová* et al.*, 2017; Garrett* et al.*, 2017) for the 1987–88 till-geochemistry results. The results are clustered to show major-element associations; with the colour representing the magnitude of associations (dark blue represents positive correlations and brownish red represents negative correlations. The size of the dots represents the significance of the correlation at the 0.95 confidence level.*

and in samples taken south of Berry Hill Pond next to the Bay D'Espoir highway. Anomalous Zn, Cu and Pb are noted in tills overlying the Pipestone Pond Complex extending 5 km southeast of the Great Burnt Lake Lead (12A/08/Pb001), 3 and 8 km southeast of the Pipestone Rapids indication (12A/08/Pb003), respectively.

Anomalous and elevated Cu, Zn and Pb are located south of Conne River Pond, extending 6–8 km in the same 8-km-long extent mentioned immediately above with respect to Co. Elevated and anomalous values of these elements are noted north of Meelpaeg Lake, 1 and 9 km south and southeast of the Wolf Pond prospect (1M/13/Au008), west-northwest of the Dead Wolf Brook Junction No 1 (2D/10/Cu001) showing, and dispersed from the Beaver Brook antimony mine (2D/11/Sb003). The highest Zn anomaly in till (624 ppm) is located 5.5 km south-southeast of Great Burnt Lake Lead (12A/08/Pb001), with 471 ppm Zn in tills on the contact of

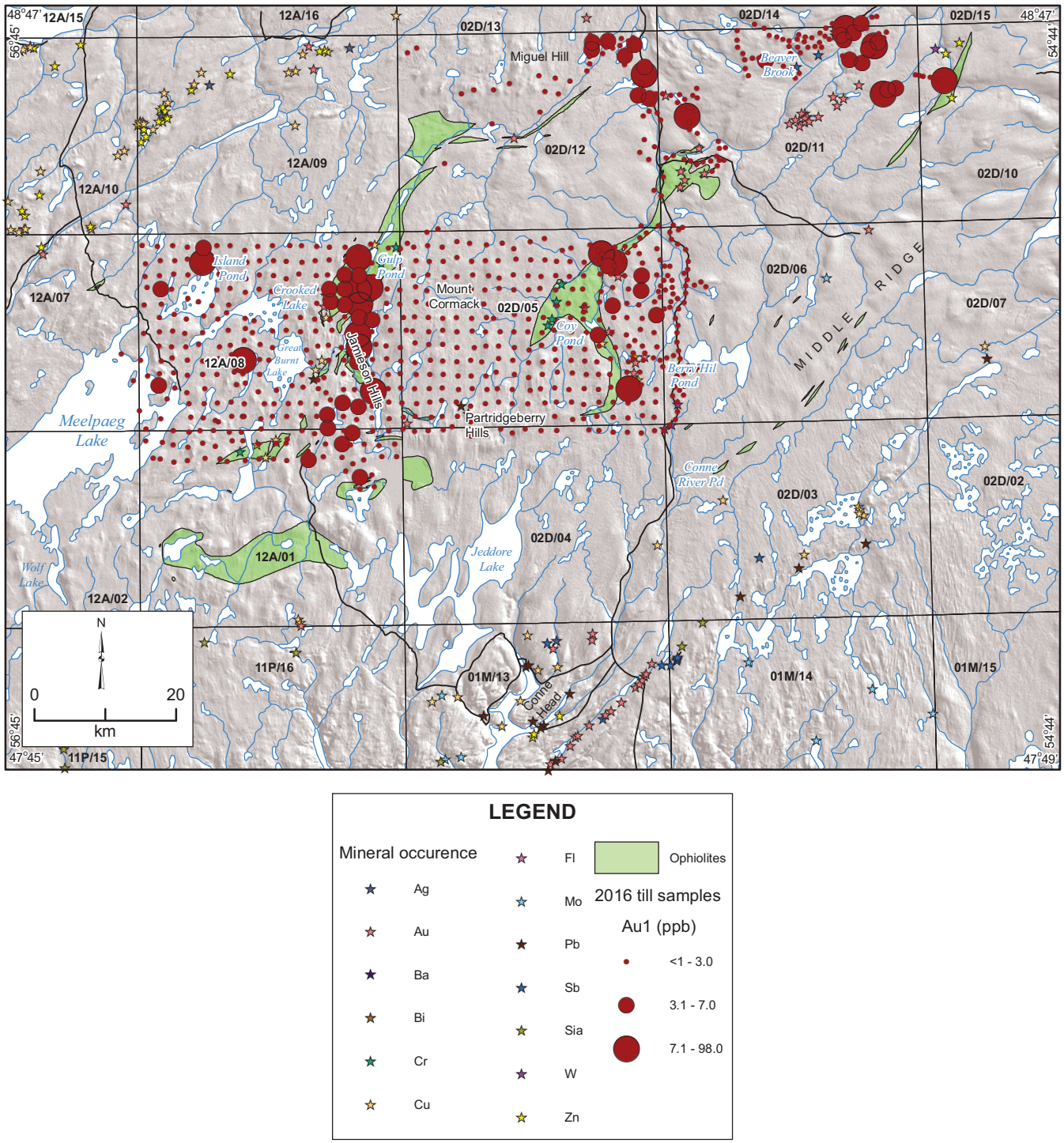

LEGEND

Mineral occurence

Ag
Au
Ba
Bi
Cr
Cu
Fl
Mo
Pb
Sb
Sia
W
Zn

Ophiolites

2016 till samples

Au1 (ppb)

<1 - 3.0
3.1 - 7.0
7.1 - 98.0

Figure 7. *Distribution of Au in tills from the 2016 study.*

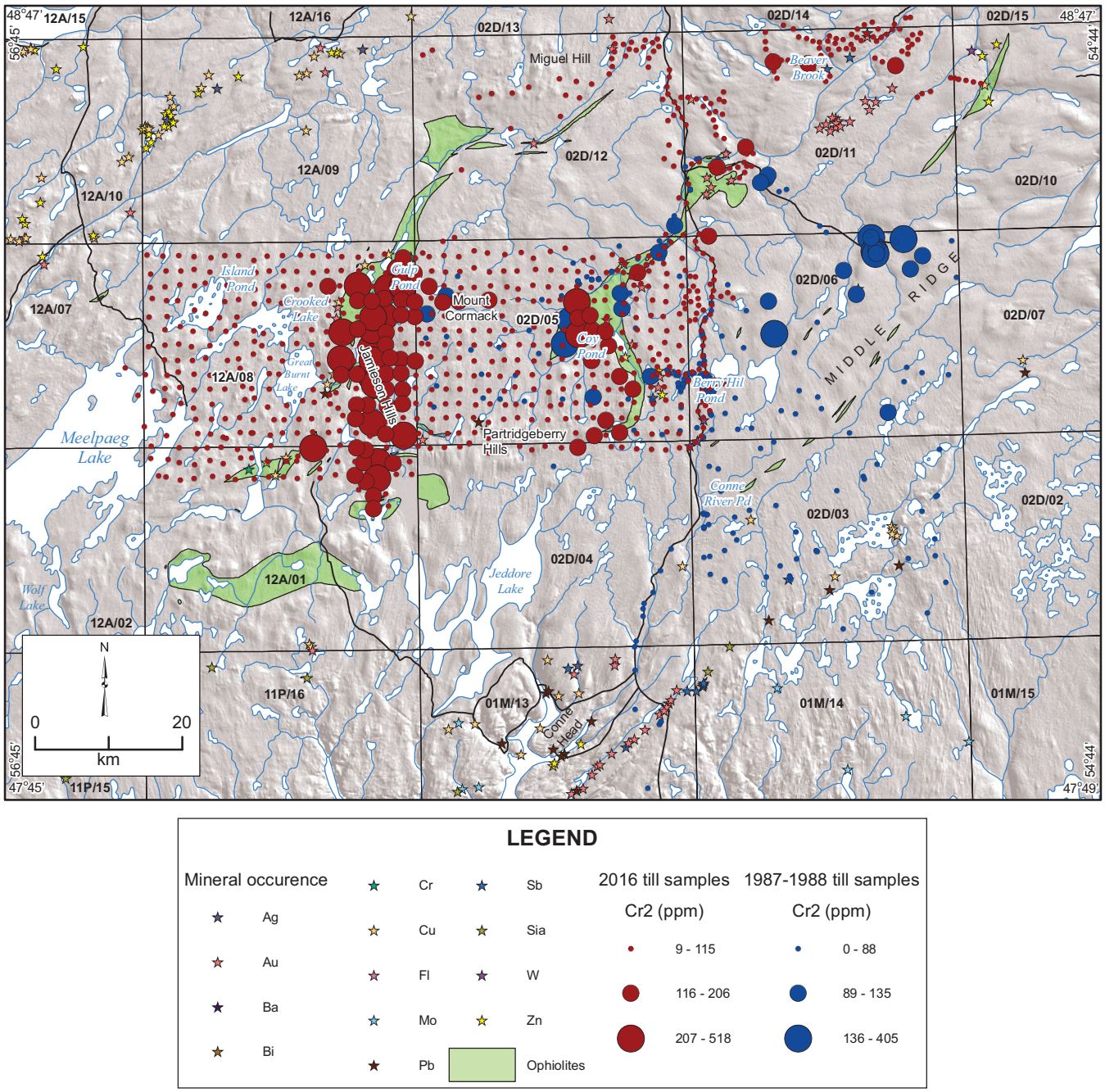

Figure 8. *Distribution of Cr2 in tills from the 2016 and 1987–88 studies.*

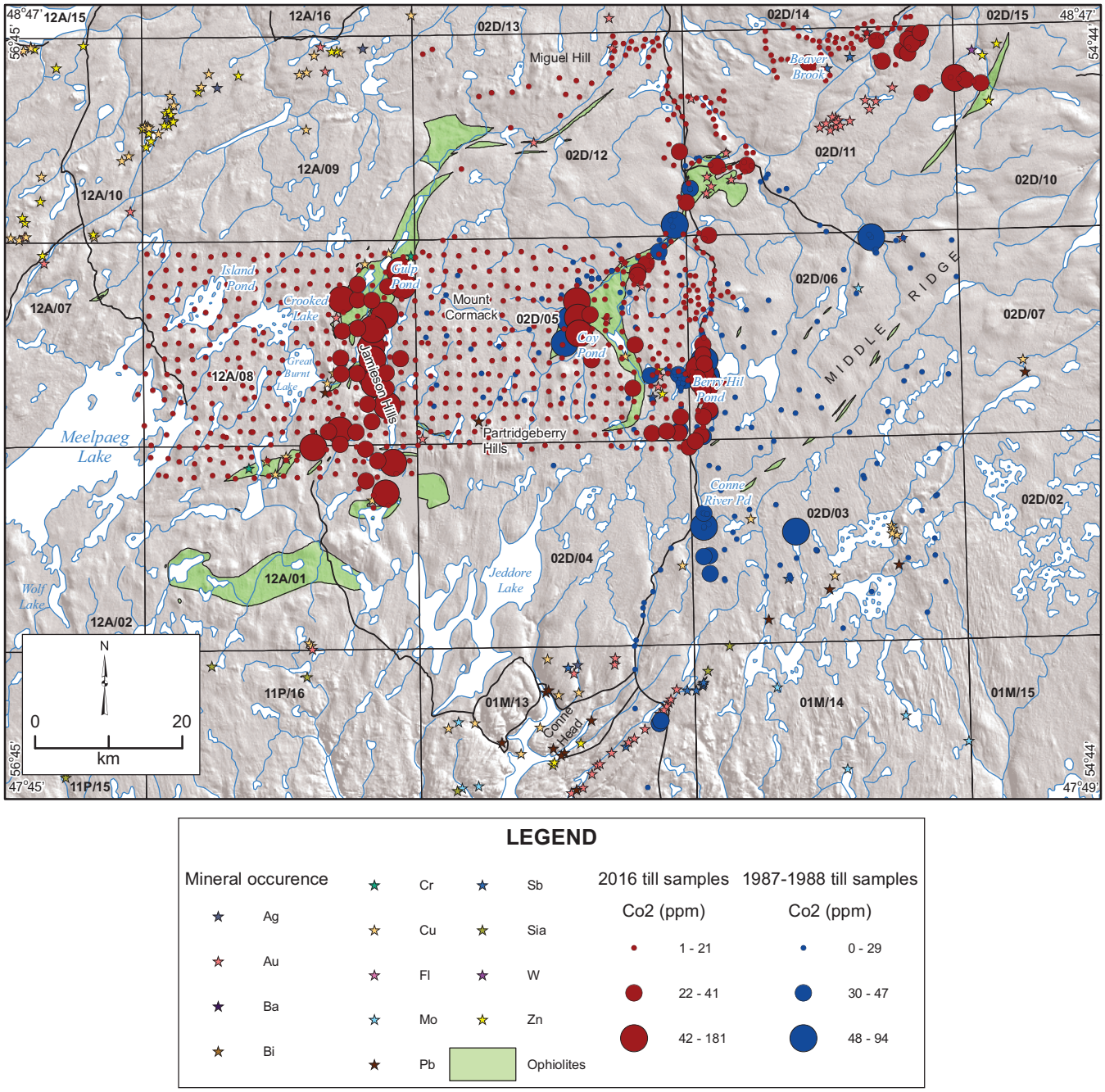

LEGEND

Mineral occurence

Ag
Au
Ba
Bi
Cr
Cu
Fl
Mo
Pb
Sb
Sia
W
Zn
Ophiolites

2016 till samples Co2 (ppm)
1 - 21
22 - 41
42 - 181

1987-1988 till samples Co2 (ppm)
0 - 29
30 - 47
48 - 94

Figure 9. *Distribution of Co2 in tills from the 2016 and 1987–88 studies.*

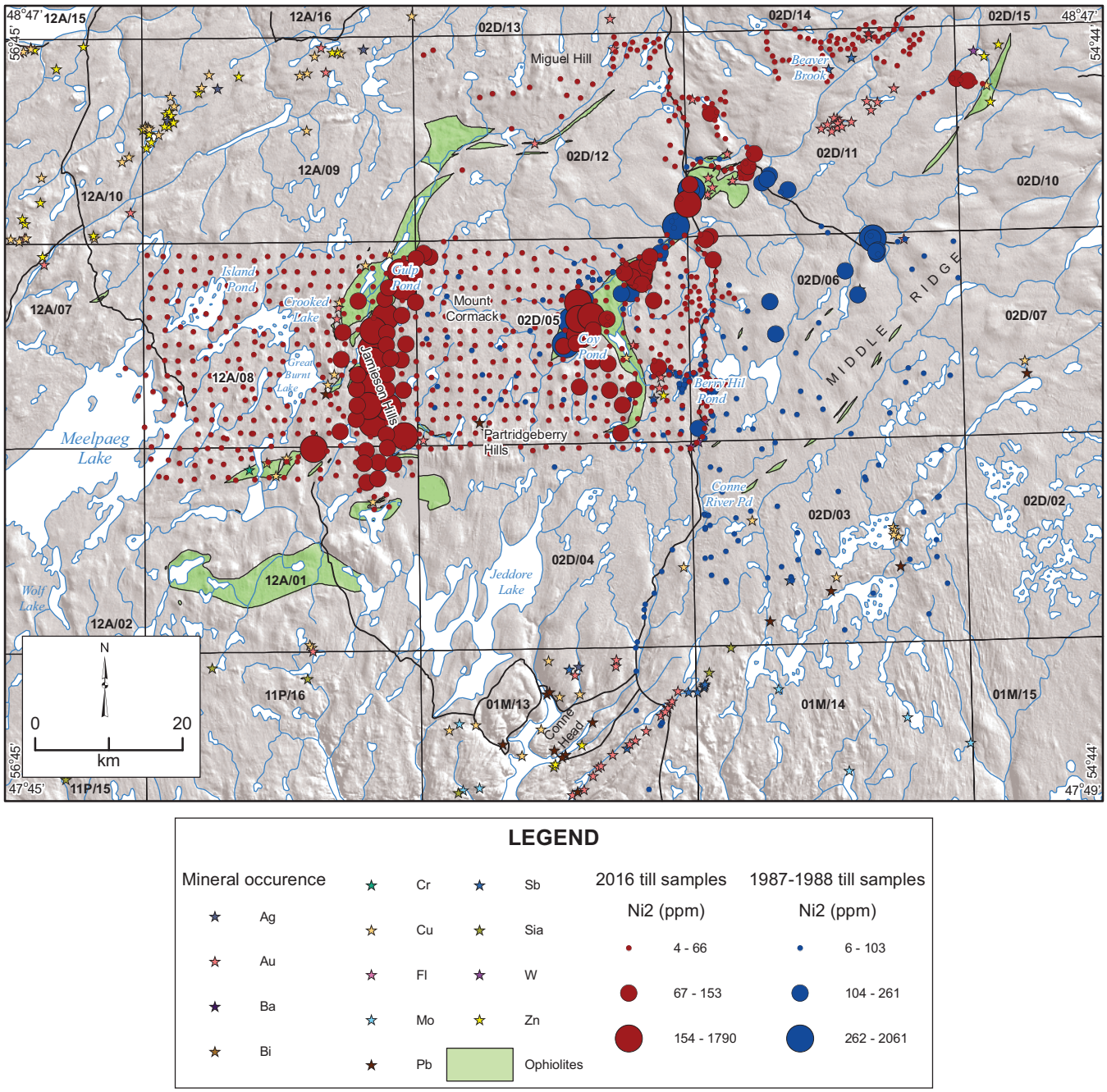

LEGEND

Mineral occurence

Ag
Au
Ba
Bi
Cr
Cu
Fl
Mo
Pb
Sb
Sia
W
Zn
Ophiolites

2016 till samples
Ni2 (ppm)
4 - 66
67 - 153
154 - 1790

1987-1988 till samples
Ni2 (ppm)
6 - 103
104 - 261
262 - 2061

Figure 10. *Distribution of Ni2 in tills from the 2016 and 1987–88 studies.*

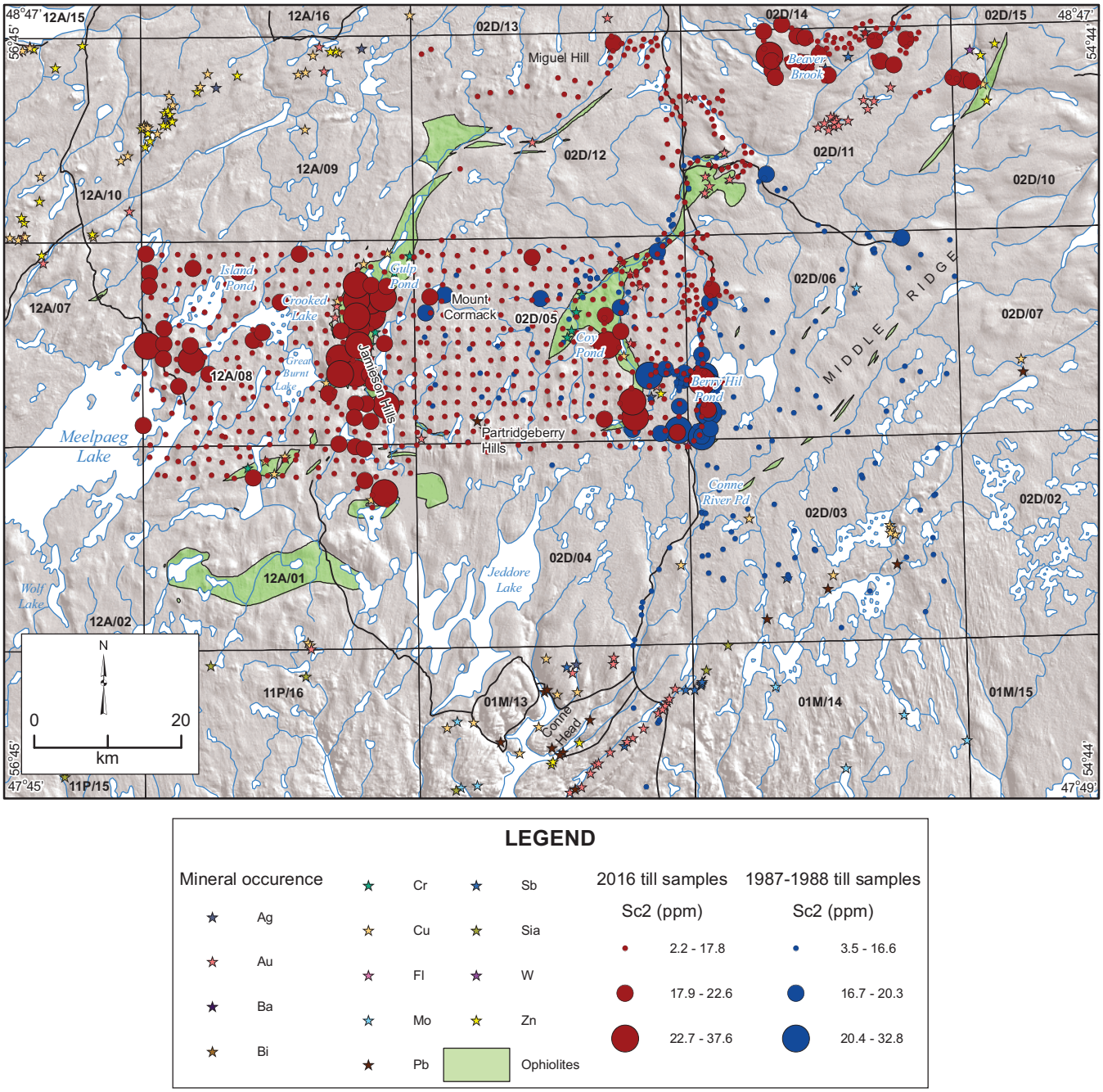

Figure 11. *Distribution of Sc2 in tills from the 2016 and 1987–88 studies.*

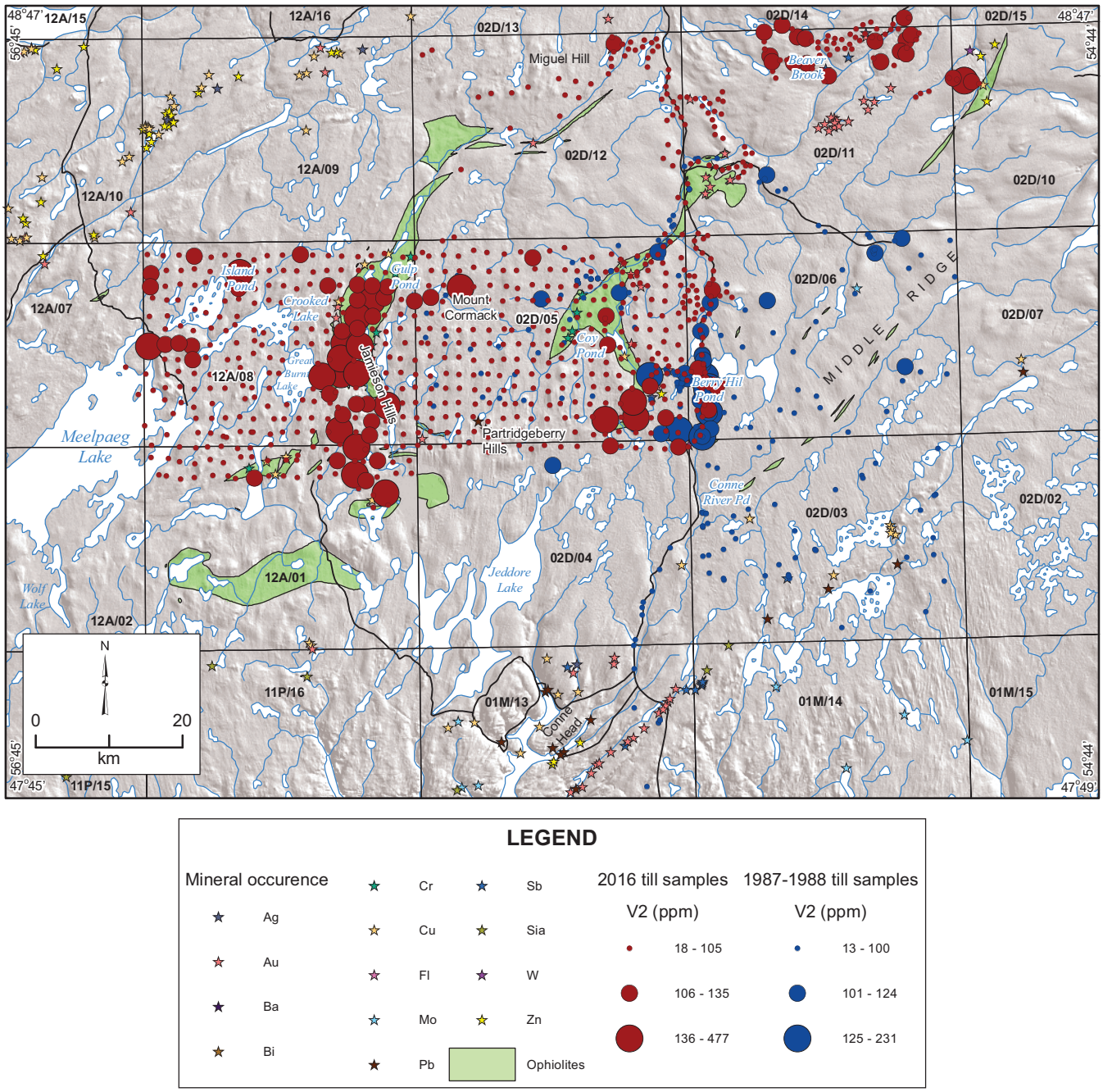

LEGEND

Mineral occurence

Ag
Au
Ba
Bi
Cr
Cu
Fl
Mo
Pb
Sb
Sia
W
Zn
Ophiolites

2016 till samples V2 (ppm)	1987-1988 till samples V2 (ppm)
18 - 105	13 - 100
106 - 135	101 - 124
136 - 477	125 - 231

Figure 12. *Distribution of V2 in tills from the 2016 and 1987–88 studies.*

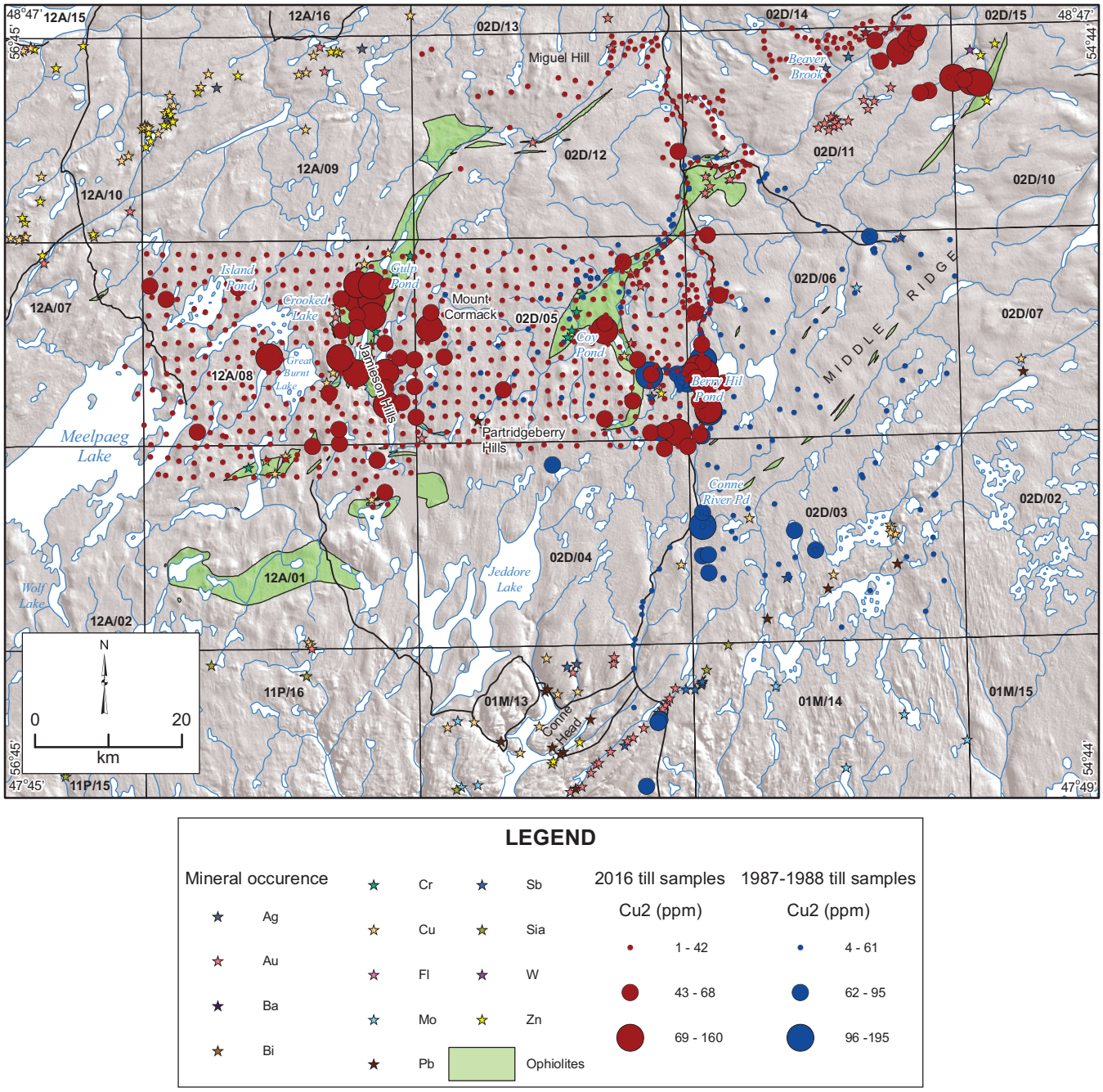

Figure 13. *Distribution of Cu2 in tills from the 2016 and 1987–88 studies.*

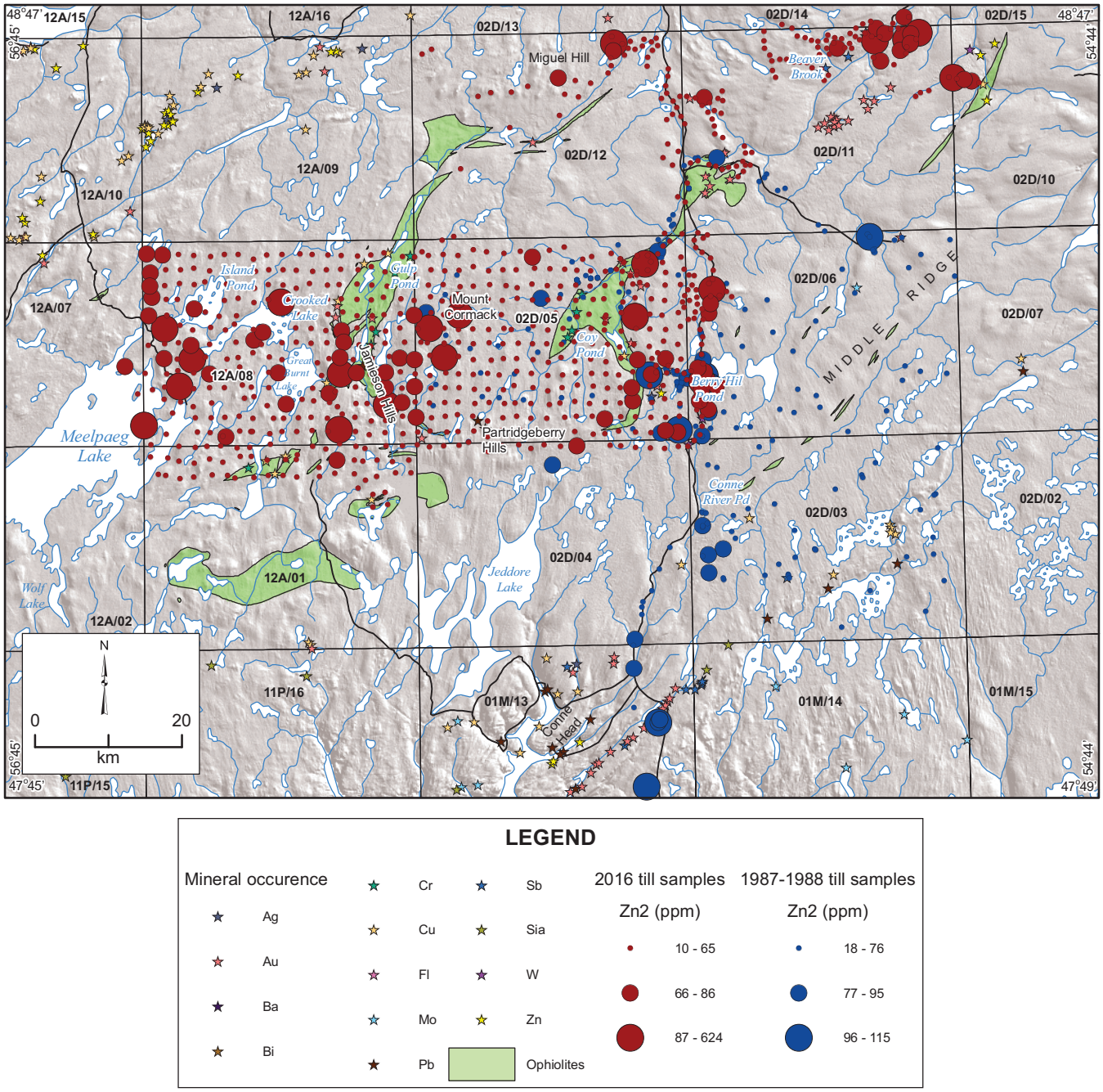

Figure 14. *Distribution of Zn2 in tills from the 2016 and 1987–88 studies.*

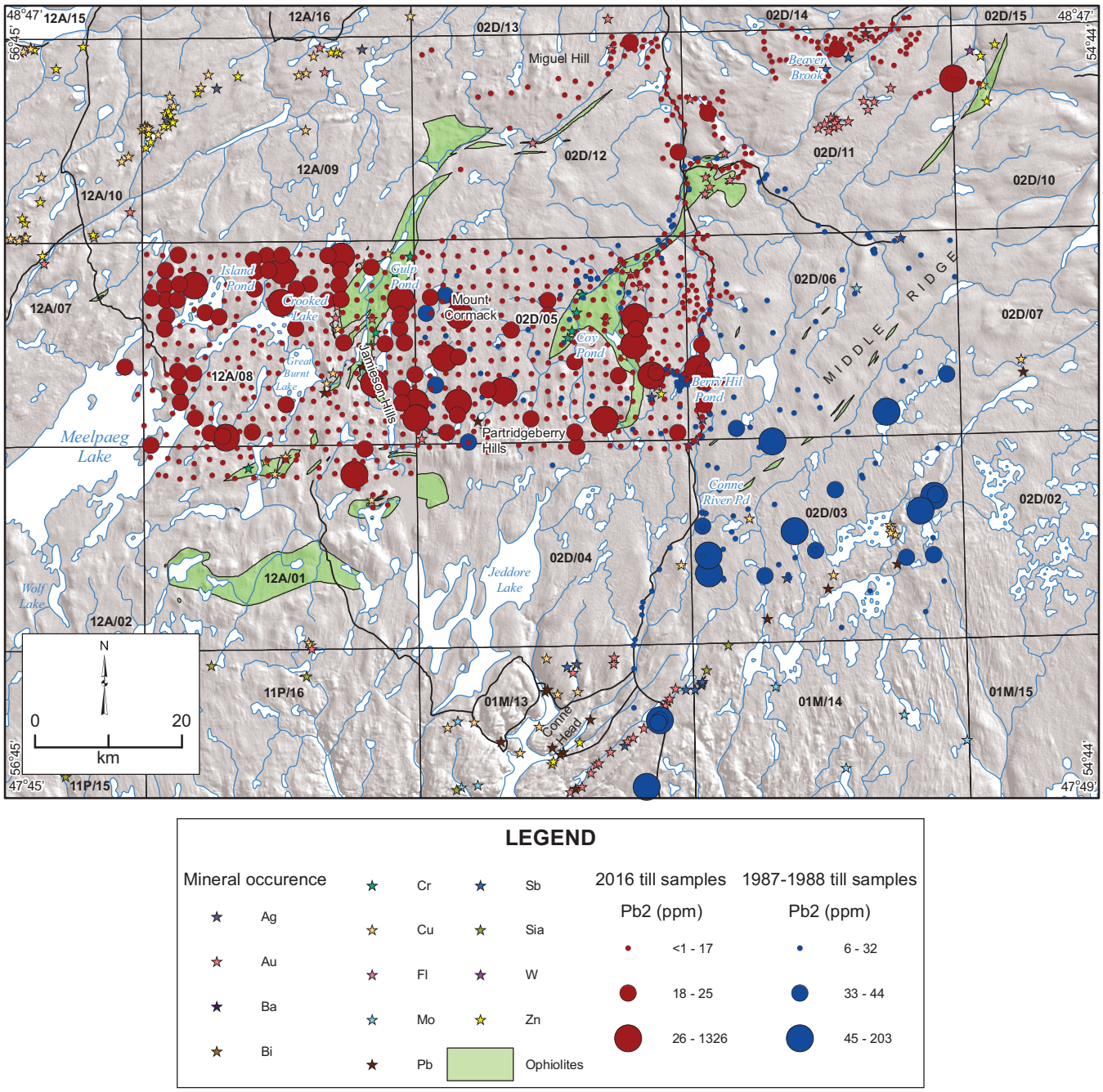

Figure 15. *Distribution of Pb2 in tills from the 2016 and 1987–88 studies with different underlying bedrock units.*

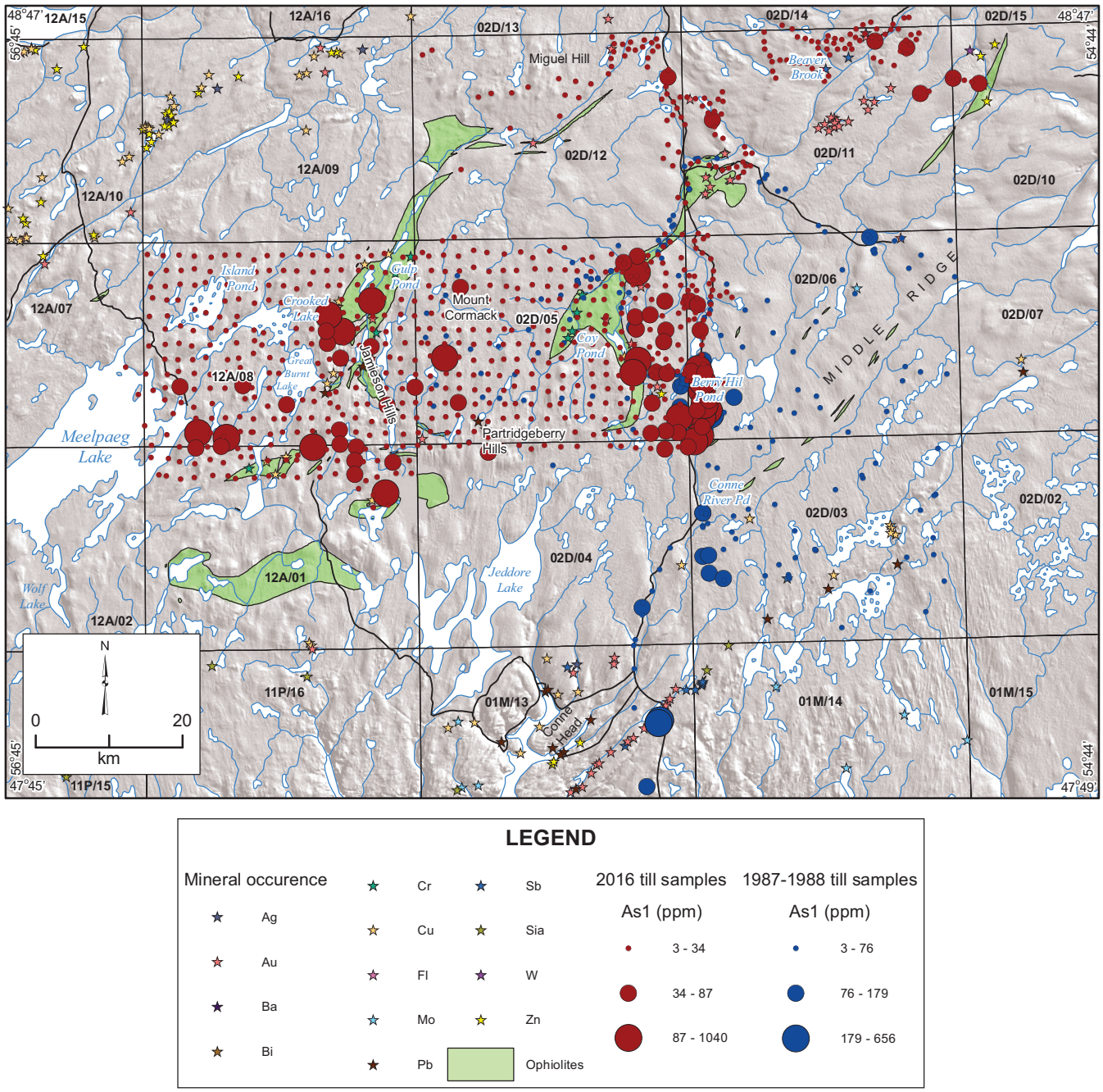

LEGEND

Mineral occurence

Ag
Au
Ba
Bi
Cr
Cu
Fl
Mo
Pb
Sb
Sia
W
Zn
Ophiolites

2016 till samples
As1 (ppm)
3 - 34
34 - 87
87 - 1040

1987-1988 till samples
As1 (ppm)
3 - 76
76 - 179
179 - 656

Figure 16. *Distribution of As1 in tills from the 2016 and 1987–88 studies.*

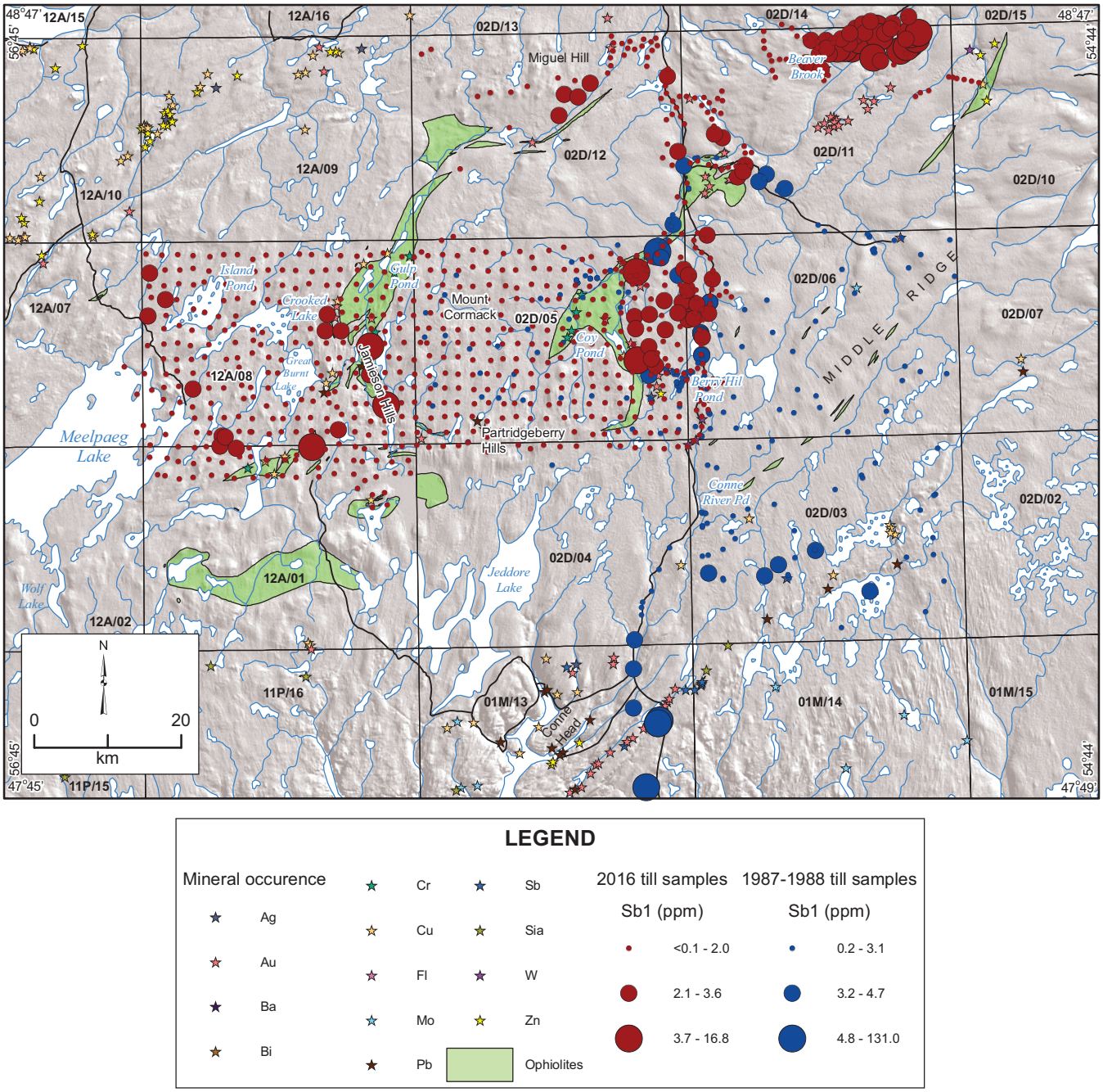

LEGEND

Mineral occurence

Ag
Au
Ba
Bi
Cr
Cu
Fl
Mo
Pb
Sb
Sia
W
Zn
Ophiolites

2016 till samples
Sb1 (ppm)
<0.1 - 2.0
2.1 - 3.6
3.7 - 16.8

1987-1988 till samples
Sb1 (ppm)
0.2 - 3.1
3.2 - 4.7
4.8 - 131.0

Figure 17. *Distribution of Sb1 in tills from the 2016 and 1987–88 studies.*

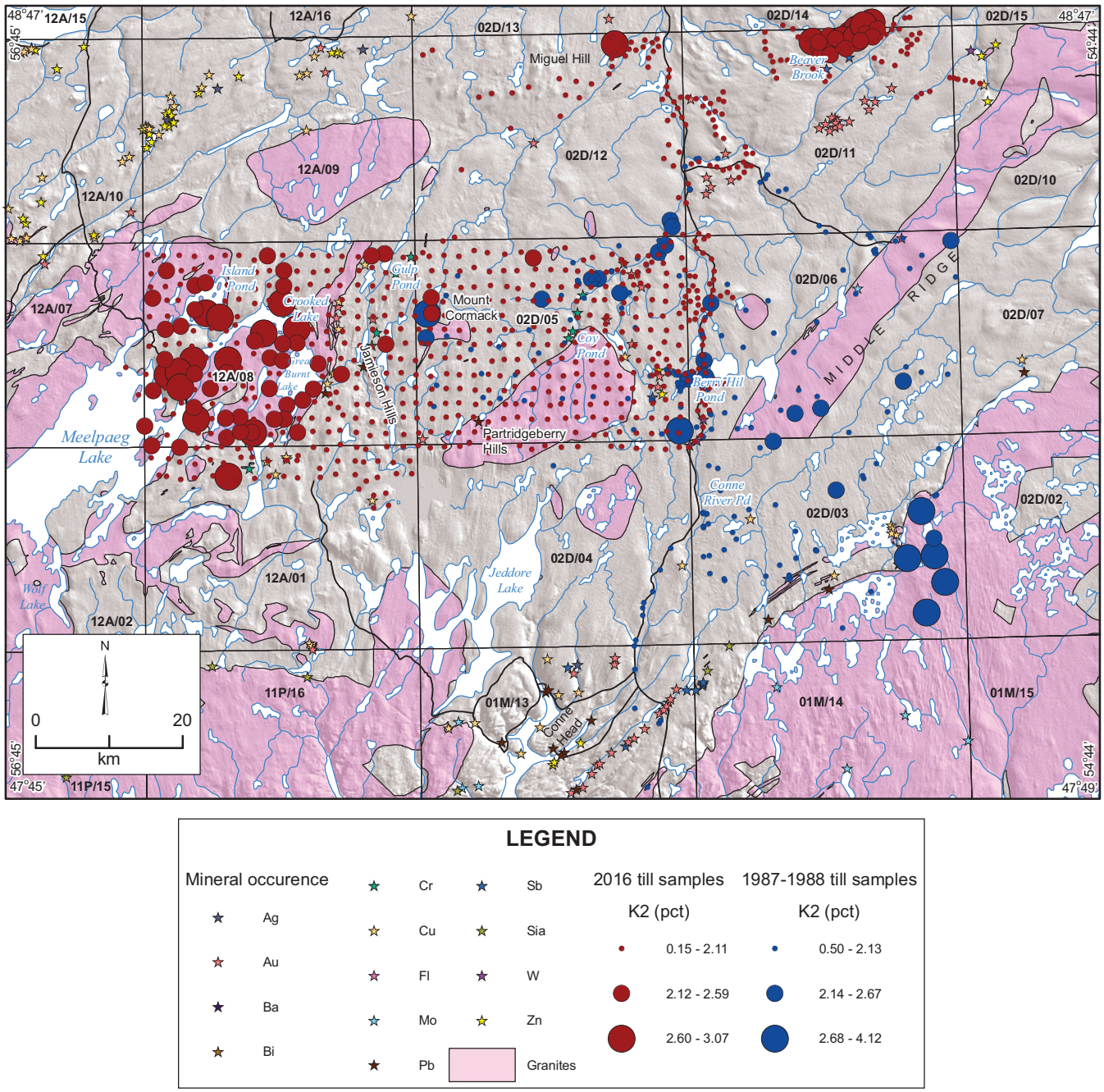

LEGEND

Mineral occurence

Ag
Au
Ba
Bi
Cr
Cu
Fl
Mo
Pb
Sb
Sia
W
Zn
Granites

2016 till samples
K2 (pct)
0.15 - 2.11
2.12 - 2.59
2.60 - 3.07

1987-1988 till samples
K2 (pct)
0.50 - 2.13
2.14 - 2.67
2.68 - 4.12

Figure 18. *Distribution of K2 in tills from the 2016 and 1987–88 studies.*

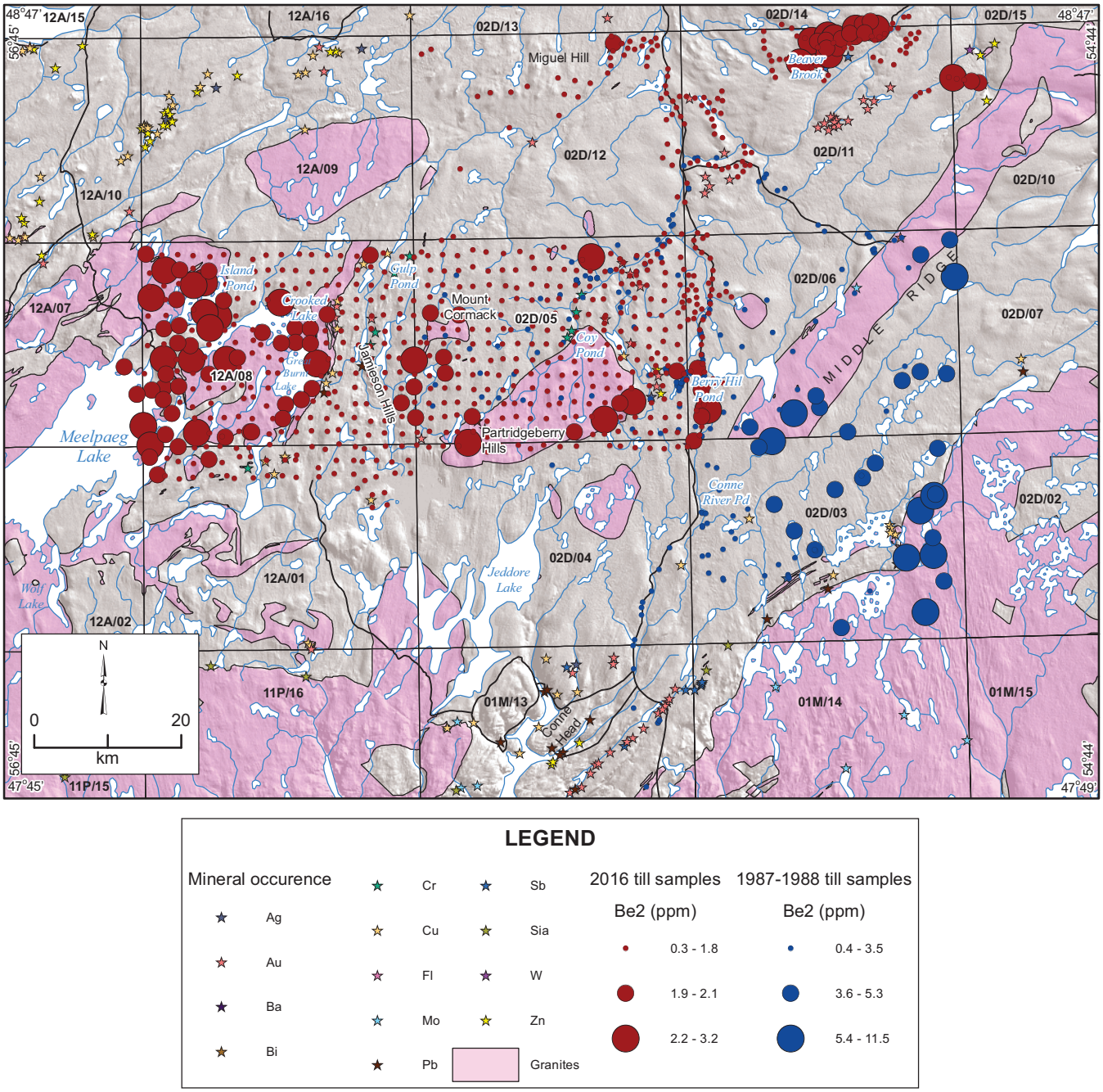

LEGEND

Mineral occurence

Ag
Au
Ba
Bi
Cr
Cu
Fl
Mo
Pb
Sb
Sia
W
Zn
Granites

2016 till samples
Be2 (ppm)
0.3 - 1.8
1.9 - 2.1
2.2 - 3.2

1987-1988 till samples
Be2 (ppm)
0.4 - 3.5
3.6 - 5.3
5.4 - 11.5

Figure 19. *Distribution of Be2 in tills from the 2016 and 1987–88 studies.*

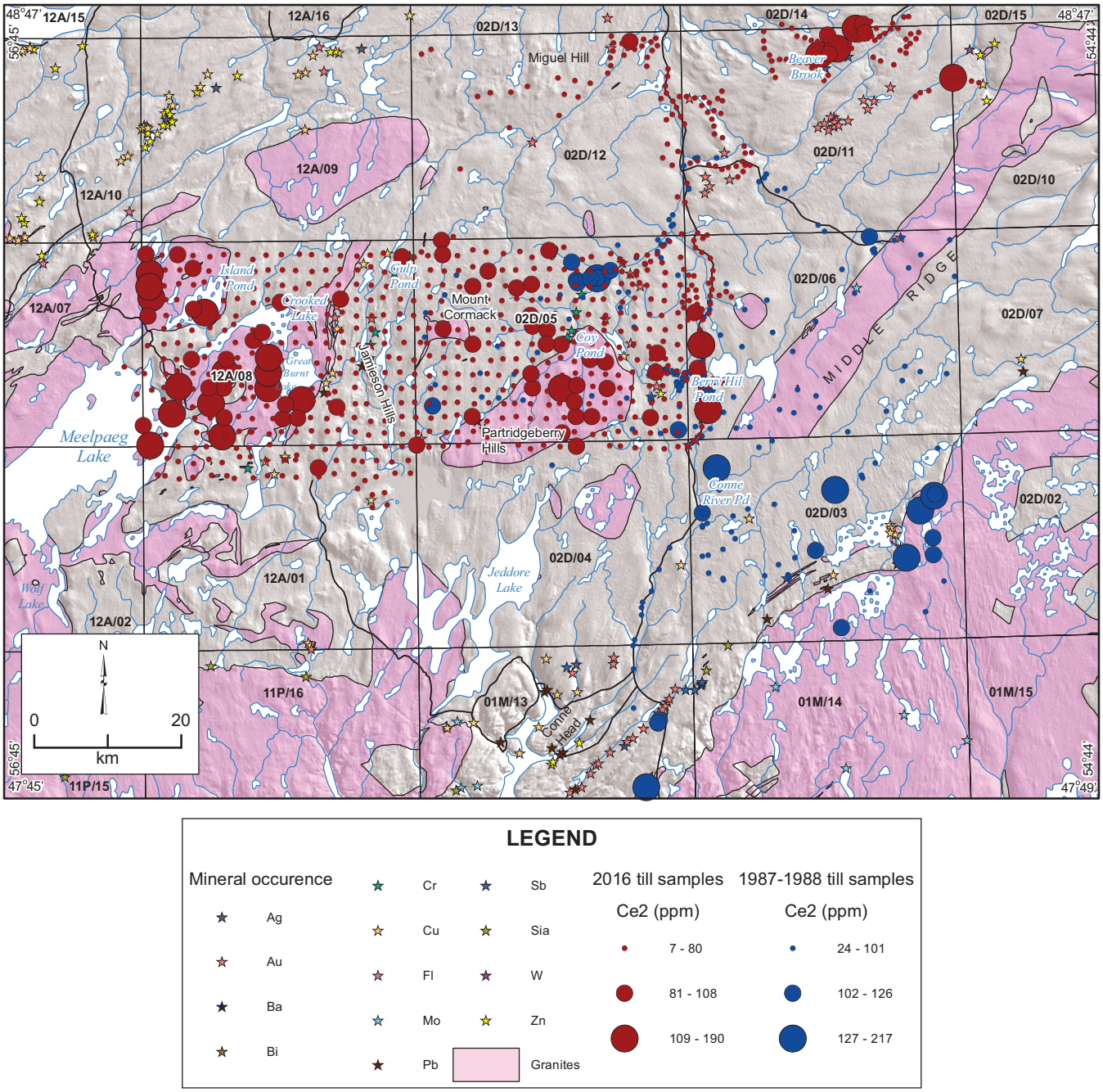

LEGEND

Mineral occurence

Ag
Au
Ba
Bi
Cr
Cu
Fl
Mo
Pb
Sb
Sia
W
Zn
Granites

2016 till samples
Ce2 (ppm)
7 - 80
81 - 108
109 - 190

1987-1988 till samples
Ce2 (ppm)
24 - 101
102 - 126
127 - 217

Figure 20. *Distribution of Ce2 in tills from the 2016 and 1987–88 studies.*

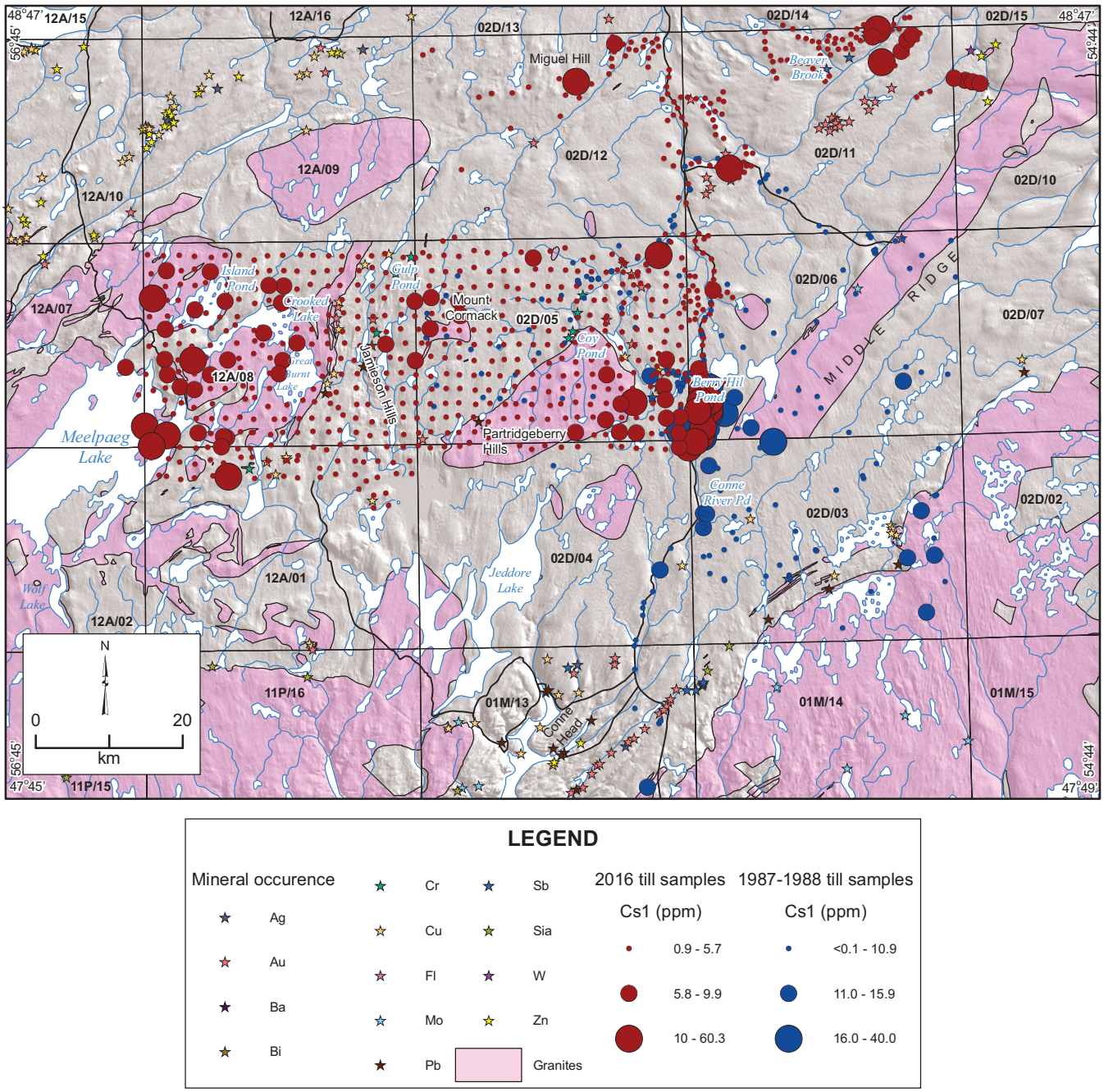

Figure 21. *Distribution of Cs1 in tills from the 2016 and 1987–88 studies.*

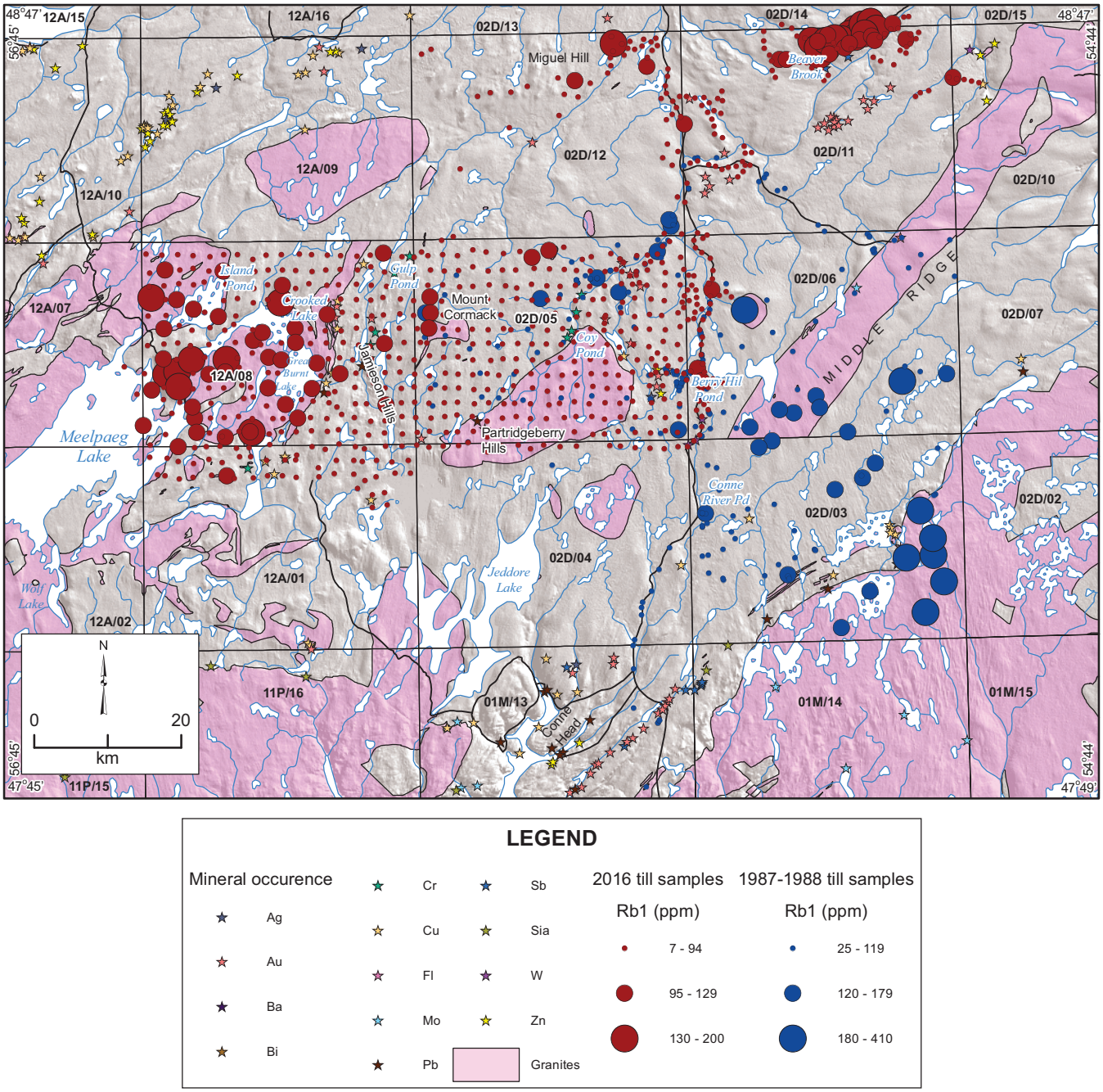

Figure 22. *Distribution of Rb1 in tills from the 2016 and 1987–88 studies.*

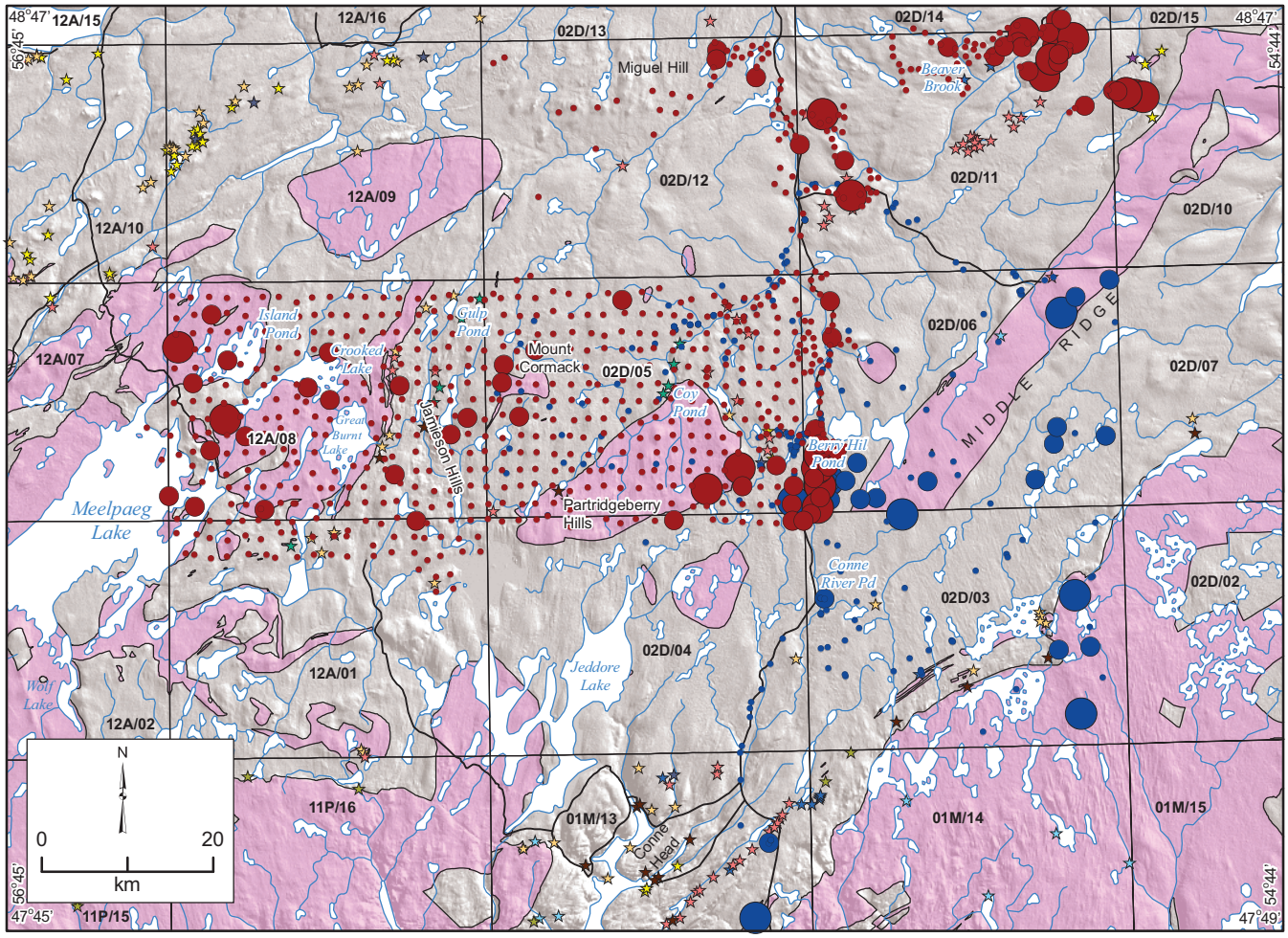

LEGEND

Mineral occurence

Ag
Au
Ba
Bi
Cr
Cu
Fl
Mo
Pb
Sb
Sia
W
Zn
Granites

2016 till samples
Li2 (ppm)
2.7 - 31.6
31.7 - 48.6
48.7 - 102.7

1987-1988 till samples
Li2 (ppm)
8.3 - 42.7
42.8 - 59.8
59.9 - 119.1

Figure 23. *Distribution of Li2 in tills from the 2016 and 1987–88 studies.*

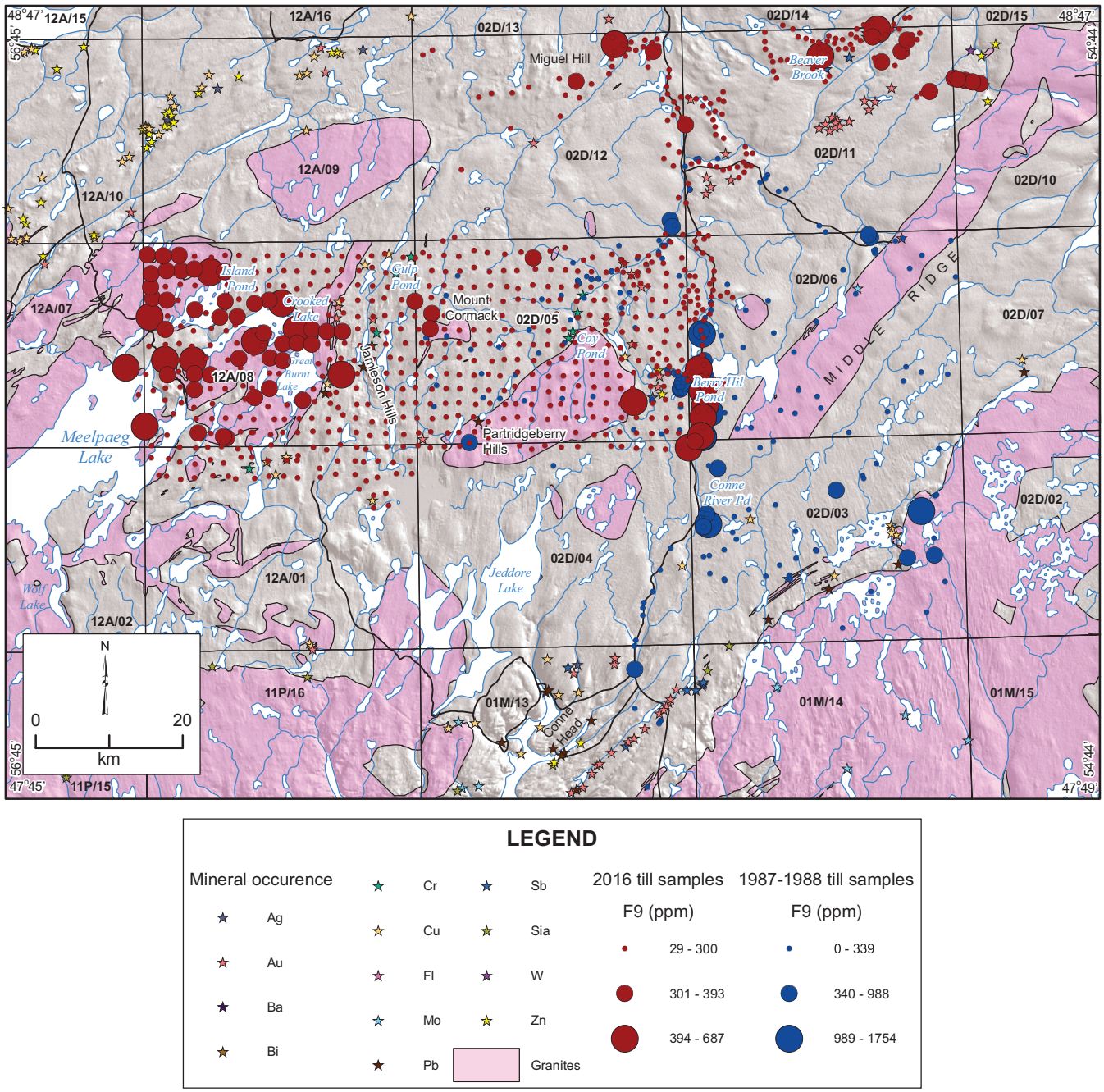

Figure 24. *Distribution of F9 in tills from the 2016 and 1987–88 studies.*

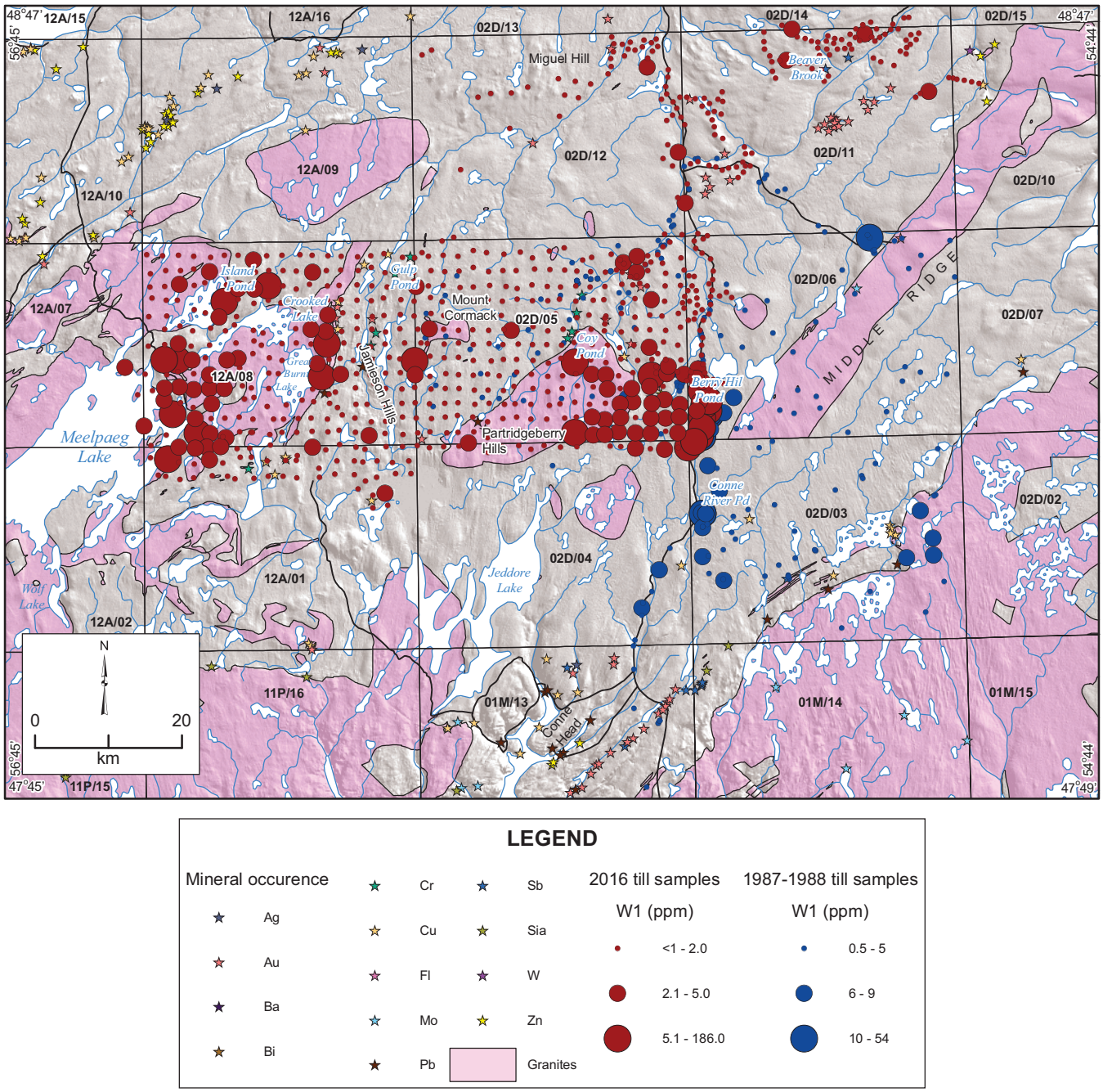

Figure 25. *Distribution of W1 in tills from the 2016 and 1987–88 studies.*

the Through Hill granite and the Spruce Brook Formation. The highest Pb anomaly in till (1326 ppm) is located 5 km south of the southern contact of the granite and the Spruce Brook Formation, and 8.7 km southeast of Pipestone Rapids (12A/ 08/Pb003) indication.

As1 and Sb1 (Figures 16 and 17)

Anomalous As and Sb are located in till samples 8 km west of the Coy Brook indication (2D/05/Cu001) and 1 km south of the Wolf Pond prospect (1M/13/Au008). Anomalous As is distributed in samples taken next to the Bay d'Espoir highway, north and south of Berry Hill Pond. A 3-km-linear southeast dispersal train of elevated As in till is located 4.5 km south of Berry Hill Pond. Anomalous As in till is located west of the Pipestone Pond Complex, and east of Partridgeberry Hills Granite. Anomalous and elevated Sb is located in tills northeast of the Coy Pond Complex, and in tills sampled around the Beaver Brook antimony mine. Samples with the highest Sb results (125–131 ppm) are located 1 km south of the Wolf Pond prospect.

K2, Be2 and Ce2, Cs1 and Rb1 (Figures 18–22)

Till samples with anomalous K, Be, Ce, Cs and Rb results are distributed around Great Burnt Lake, Meelpaeg Lake and overlying the Ackley Granite Suite. Anomalous Be results from till samples are located east and south of Middle Ridge. Cerium is dispersed in an 8.8-km-semi-linear southward direction in tills over the Partridgeberry Hills Granite. Anomalous Cs occurs in till taken next to the Bay d'Espoir highway north and south of Berry Hill Pond, whereas anomalous Rb is distributed in samples next to roads in the Beaver Brook antimony mine.

Li2 (Figure 23)

Anomalous Li occurs in till samples next to the Bay d'Espoir highway north and south of Berry Hill Pond, including a Li sample that returned 119.1 ppm. Anomalous Li values overlie the Ackley Granite Suite.

F9 and W1 (Figures 24 and 25)

A trend of high F values (1466–1754 ppm) and W (6–54 ppm) extends 25 km to the south-southeast from 4 km north of Berry Hill Pond. Although the anomalies are noted in both datasets in this region, the dataset from 1987–88 returned much higher values. Anomalous F and W is also noted above the Meelpaeg Lake Granite, with the highest W value of the 2016 dataset (186 ppm) directly east of the northeastern shoreline of Meelpaeg Lake. Anomalous W is noted west of the Pipestone Pond Complex overlying the Great Burnt Lake granite, and anomalous and elevated F in tills 4 km south of the Gulp Pond chromite indication (12A/08/Cr005), extending southward for 6 km. Elevated W in till extends eastward from the Partridgeberry Hills Granite toward the Bay D'Espoir highway.

DISCUSSION

Till samples having anomalous values of Au overlie (or are proximal to) inferred source occurrences (Figure 7), with the exception of the sample with 81 ppb Au, 12 km southeast of the Pipestone Pond gold showing, 8 ppb Au, northwest of Island Pond Lake and 22 ppb Au, immediately west of Great Burnt Lake. The magnitude of the 81 ppb Au anomaly at that distance suggests that it has not been dispersed, but may indicate an unknown source in the Pipestone Pond Complex closer to the location of the till sample.

Anomalous base-metal distribution in tills is presented in a pie-chart dotplot (Figure 26) that illustrates a combination of elements in a diagram rather than a single element. This figure, a combination of Cu + Pb + Zn values in till, suggests that material may have been dispersed to the east-southeast from known occurrences (*i.e.*, the Gulp Pond indication (12A/08/Cr005), the Great Burnt Lake developed prospect (12A/08/Cu001), the Pipestone Rapids indication (12A/08/Pb003), the Katie prospect (2D/05/Zn002), the Coy Brook indication (2D/05/Cu001) and the O'Reilly prospect (2D/11/Au021). However, the high anomalous till results east and southeast of the Pipestone Pond Complex (*e.g.*, three large circles) are located 5.5 km (624 ppm Zn), 8 km (1326 ppm Pb) and 12.5 km (471 ppm Zn) from the closest inferred source units. Potentially the magnitude of the anomalous values at these distances may indicate an unknown source, although, it is possible that the Zn- and Pb-rich till was initially dispersed by east-southeast glacial flow, with later southward dispersal.

The 8-km-southeastward linear extent of the elements Co (Figure 10), and Sc, V, Cu, Zn, Pb and As (Figures 11−16) from the Bay d'Espoir highway south of Berry Hill Pond toward Conne River Pond may indicate dispersal from a small, unmapped ophiolitic sliver. Alternatively, anomalous and elevated values of these elements in tills sampled beside the highway may be the result of anthropogenic transport of material from five local quarries located in a 10 km stretch east and west of the Bay d'Espoir highway. Material from these quarries represents ultramafic units and W-bearing rocks, used as aggregate for road building and construction. The distribution of anomalous elements in this same stretch of highway is also coincident with southward ice-flow direction (Proudfoot *et al.*, 1988), which further complicates matters. Thus, caution is advised when interpreting the results from these elements in this region.

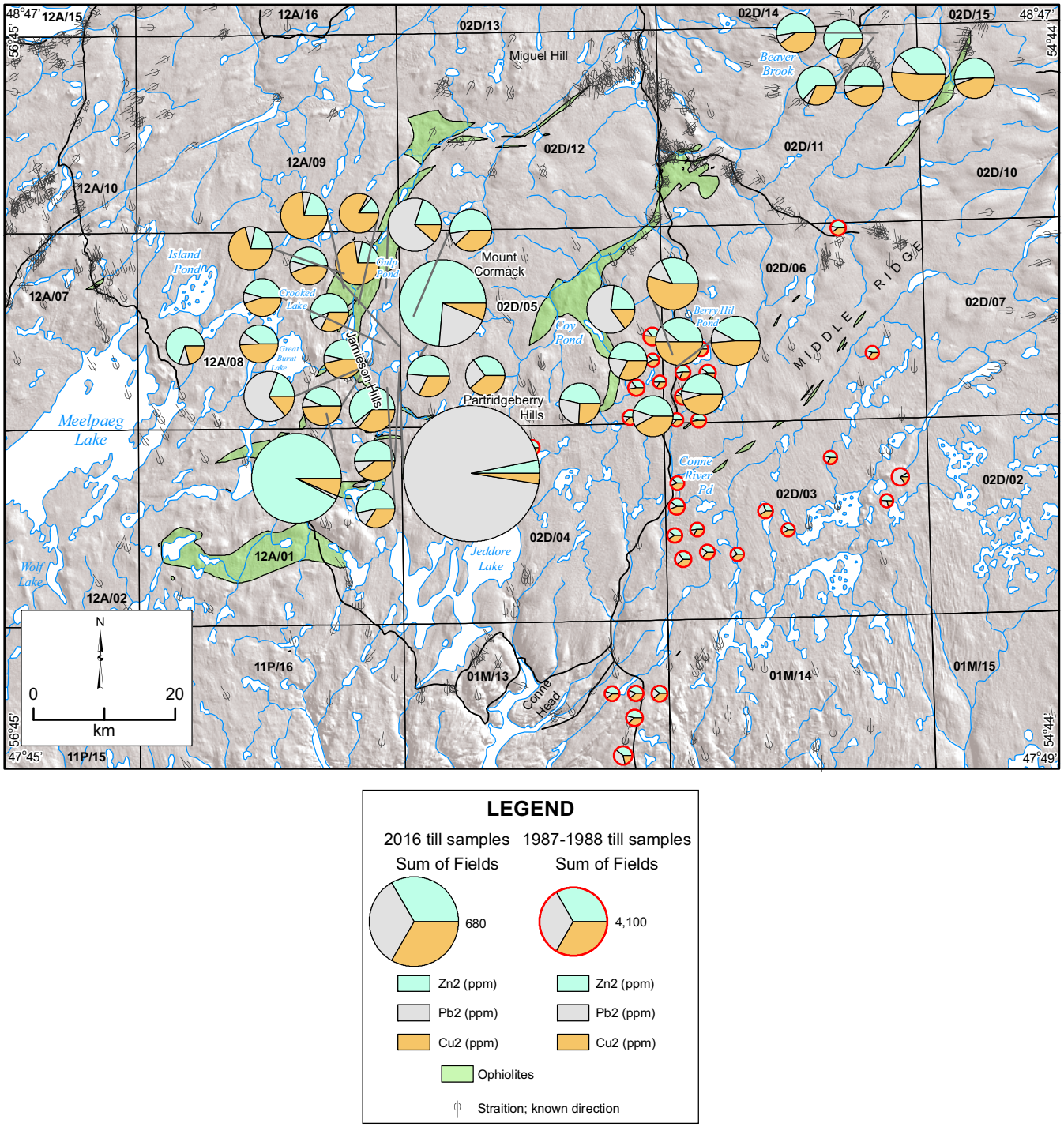

Figure 26. *Figure showing Pb + Zn + Cu anomalies in tills from the 2016 and 1987–88 studies. Data are filtered, with sample where the sum of the three elements is greater than 150 ppm. The dot sizes represent the sum of the elements, with larger circles representing higher values.*

Fluoride and tungsten are also anomalous and elevated in the aforementioned region, covering a larger linear extent (30 km) from 4 km north of Berry Hill Pond to 11 km south of Great Gull tungsten #1 (2D/04/W001) (Figure 27). Anomalous Cs (Figure 21) and Li (Figure 23) are distributed along the same trend but over a much shorter (10 km) distance. The same issues discussed in the previous paragraph apply to these anomalies as they are located next to the road. However, south-southeastward distribution of these elements off the highway is thought to be the result of glacial dispersal from known (*i.e.*, Great Gull tungsten #1 and #2 (2D/03/W001, W002) and South Quarry tungsten (2D/06/W001) and possibly unknown mineral occurrences (*i.e.*, southeast of Great Gull tungsten #1) along this extent. Elevated W (Figure 25) is dispersed from the Partridgeberry Hills Granite, to the south and southeast. The distribution of the elevated values indicate that they are derived from the low-silica main phase subunit of the Partridgeberry Hills Granite (Colman-Sadd, 1980), as the anomalies overlie and are dispersed from this unit.

Distribution of anomalous values of Li (Figure 23) southeast of Berry Hill Pond is perhaps the result of southeastward ice-flow, or dispersal from isolated bedrock units (pegmatites?) located in, and west of, the Middle Ridge Granite (Figure 24). Anomalous F in till from the 1987–88 (1400–1700 ppm) study is an order of magnitude higher than anomalous F in samples taken in the same proximity in 2016 (400–500 ppm). This may be due to 1) the difference in depth between the1987–88 and 2016 samples (*i.e.*, excavated by backhoe versus hand dug pits), and/or 2) comminution of fluorite into a finer grain size. Till excavated from backhoe sites is closer to the bedrock source, and thus may contain more anomalous bedrock material than hand-dug samples from shallower depth, such as those taken in 2016. Results from a study completed in Guangdong, China (Zhu *et al.*, 2007), revealed increasing fluoride concentrations with soil depth, where the highest geometric mean concentration in soils is above bedrock (120 cm down from the surface). However, the increase in fluoride with depth in the present study was minimal (about 60 ppm from the top soil horizon to the bottom), which is not sufficient to explain the difference in fluoride values from the 1987–88 and 2016 studies in Newfoundland. Fluoride in the finer grained portion of tills would be enhanced by the removal of coarse-grained minerals through the smaller sieve size (63 microns) used in the 1987–88 study. The difference in F concentrations from material sieved through the 177 and 63-micron sieve size would not be expected to be as large as those encountered in the results of the 1987–88 and 2016 surveys (S. Amor, personal communication, March 2019). Despite the differences in absolute F concentrations between the two survey datasets, there appears to be anomalous F in samples east of, and along, the 10 km stretch of highway south of Berry Pond and northeast and south of Conne River Pond. The anomalous values may represent dispersal from the tungsten occurrences mentioned in the previous paragraph, with the caution applied to samples that were collected near the highway.

The source of the 183-ppm W anomaly east of Meelpaeg Lake in the northwest corner of NTS map area 12A/01 is not known. Occurrences of W, Mo, F and Bi are noted in the Granite Lake area (Tuach and Delaney, 1987; Kerr *et al.*, 2009) but these are located 27 km to the east of the till anomaly, perpendicular to known ice-flow direction. Thus, this anomaly is thought to be related to a nearby, unknown occurrence.

Elevated concentrations of Ba, Be, Ca, Ce, Hf, K, La, Lu, Nb, P, Rb, Sm, Ta, Tb, Th, U and Yb are present in samples collected near and surrounding the Meelpaeg Lake Granite (Figures 18 to 25). Many of these elements are abundant in felsic plutonic rocks (Levinson, 1974) and the abundance of elemental anomalies is most likely due to the presence of minerals hosting these elements (*e.g.*, feldspars) in glacial material. In areas underlain by the granites (Figure 2), displacement of these elements in glacial material appears minimal (1–2 km), with anomalous concentrations of the K (Figure 19), Ce (Figure 20) and Rb (Figure 22) along the contact of the Meelpaeg Lake Granite and the quartzites, psammites and pelites of the Spruce Brook Formation (Figures, 2, 18, 20 and 22). Dispersal of these elements may occur to the southeast of Island Lake Pond and Crooked and Burnt lakes, although it is difficult to determine, as the distribution of the elements is in tills overlying inferred bedrock sources.

CONCLUSIONS

The geochemistry of till samples collected from both the 2016 and 1987–88 studies appear to reflect underlying bedrock compositions. Correlations between geochemical elements clearly indicate contributions from underlying mafic and felsic bedrock sources.

Most of the till samples that are anomalous in base- and precious-metals are overlying or dispersed from the Pipestone Pond and Coy Pond complexes. This is expected, as these complexes host most of the known mineral occurrences. Single anomalous base- and precious-metal values, in till southeast of the Pipestone Pond Complex, are thought to be located too far from known mineral occurrences to be derived from them. Further examination of the grains in till (*e.g.*, McClenaghan and Paulen, 2017), and the isotopic signature related to base metals (*e.g.*, Paulen *et al.*, 2011; Conliffe *et al.*, 2018) might clarify the source of the till anomalies. Although there are no recorded mineral occurrences in the Meelpaeg Lake Granite, anomalous W and F in till samples overlying this unit suggest that there may be potential in this area for further prospecting and sampling. Anomalous W and F south and

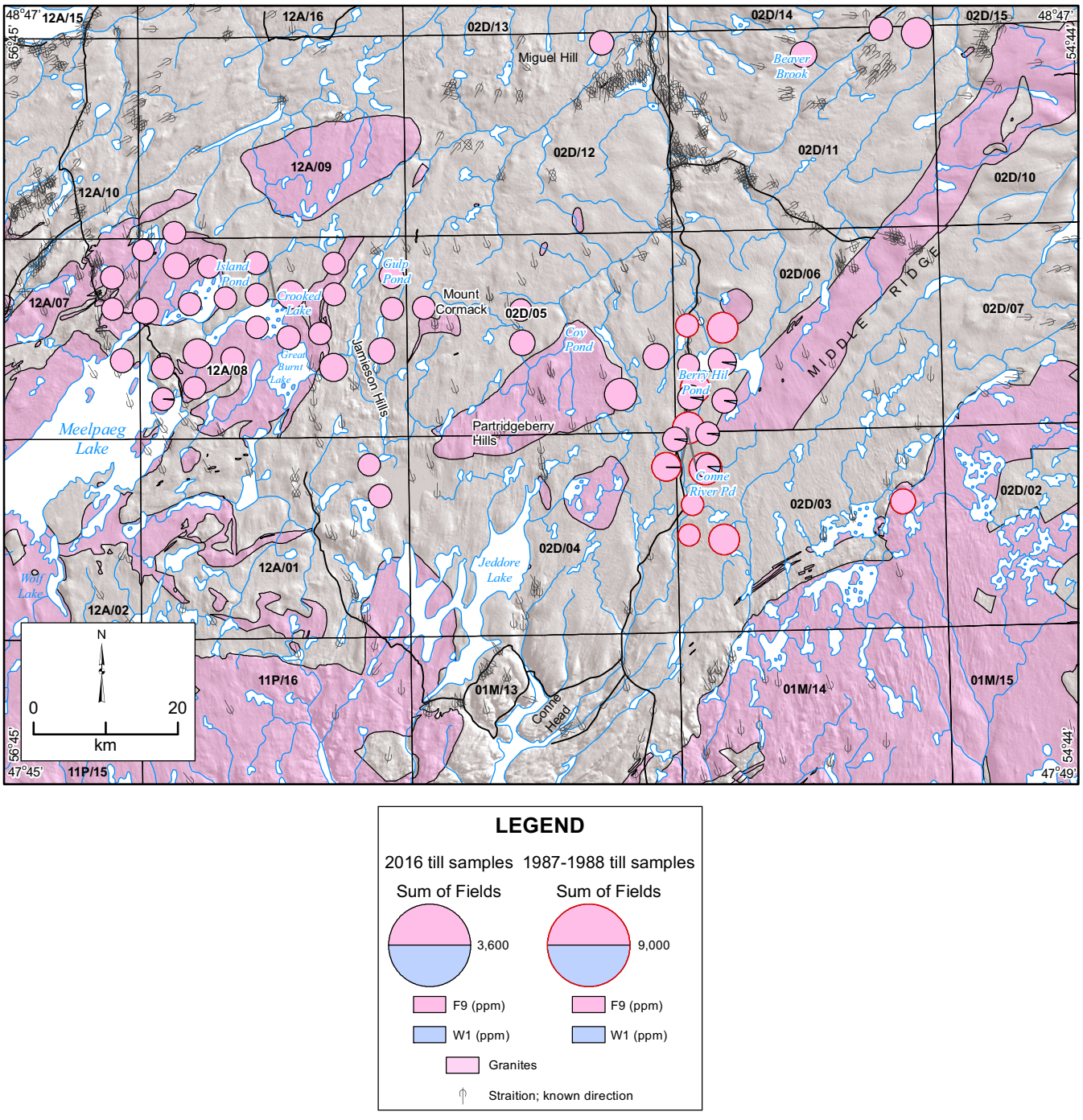

Figure 27. *Figure showing F + W anomalies in tills from the 2016 and 1987–88 studies. Data are filtered, with sample where the sum of the three elements is greater than 350 and 700 ppm for the two datasets, respectively. The dot sizes represent the sum of the elements, with larger circles representing higher values.*

southeast of the Bay d'Espoir highway are thought to be the result of dispersal from known and unknown mineral occurrences.

Further work, including the integration of surficial maps and regional geochemical data from nearby map areas, will allow for a more complete understanding of the geochemical distribution in the study area.

ACKNOWLEDGMENTS

Stephen Amor is thanked for his contributions of the control charts and his earlier editing of this document. The author is grateful to Gerry Hickey for his logistical support of the project. Kim Morgan is appreciated for her talent in drafting the figures. Joanne Rooney is thanked for her drafting and publishing of this paper. Brittany Baker, Brant Gaetz, Stephen Connolly, Dave Taylor, Jennifer Organ and Robyn Constantine are acknowledged for their assistance in the field. Many thanks to Hamish Sandeman for providing lithogeochemical data for the Pipestone Pond and Coy Pond complexes, and for showing the author mineral occurrences and geology related to the Coy Pond Complex. This paper benefitted from conversations with John Hinchey about the bedrock geology and mineral potential of the Pipestone Pond Complex. Many thanks are given to Crispin Pike, who provided information on the history of exploration efforts in the study area. Steve Amor is thanked for his earlier edits and suggestions for improving this paper.

REFERENCES

Amor, S.D.
2013: Identification of local maxima in regional geochemical datasets. *In* Current Research. Government of Newfoundland and Labrador, Department of Natural Resources, Geological Survey, Report 13-1, pages 5-33.

Batterson, M.J. and Liverman, D.G.
2000: The contrasting styles of glacial dispersal in Newfoundland and Labrador: Methods and case studies. Geological Society of London, Special Publication 185, pages 267-285.

Batterson M. and Taylor, D.
2008: Ice-flow history and regional till-geochemistry sampling of the southern part of the Red Indian Lake Basin. *In* Current Research. Government of Newfoundland and Labrador, Department of Natural Resources, Geological Survey, Report 08-1, pages 25-34.

Benn, D.L. and Evans, D.J.A.
2010: Glaciers and Glaciation. Second edition, Hodder Education, London, 802 pages.

Blackwood, R.F.
1981: West Gander Rivers (east half) and Dead Wolf Pond (northwest portion). Government of Newfoundland and Labrador, Department of Mines and Energy, Mineral Development Division, Map 81-100.

Blackwood, R.F. and Green, L.
1983: Geology of the Great Gull Lake (2D/6). Government of Newfoundland and Labrador, Department of Mines and Energy, Mineral Develoment Division, Map 82-71.

Blundon, P., Bell, T. and Batterson, M.
2010: Ice streaming in the Newfoundland Ice Cap: Implications for the reconstruction of ice flow and drift prospecting. *In* Current Research. Government of Newfoundland and Labrador, Department of Natural Resources, Geological Survey, Report 10-1, pages 143-157.

Brown, P.A. and Colman Sadd, S.P.
1976: Hermitage flexure: figment or fact? Geology, Volume 4, pages 561-564.

Brushett, D.
2015: Till-geochemistry sampling and Quaternary mapping in south-central Newfoundland, Eastern Pond (NTS 2D/11) and Miquel's Lake (NTS 2D/12) map areas. *In* Current Research. Government of Newfoundland and Labrador, Department of Natural Resources, Geological Survey, Report 15-1, pages 253-261.

Brushett, D. and Amor, S.D.
2016: Till geochemistry of Eastern Pond and Miguels Lake (NTS map areas 2D/11, 12), Jeddore Lake (NTS map areas 1M/13, 2D/04 and 12A/01) and surrounding areas. Government of Newfoundland and Labrador, Department of Natural Resources, Geological Survey, Open File NFLD/3273, 107 pages.

Campbell, H.
2018: Till-geochemistry survey in the Great Burnt Lake (NTS 12A/08), Burnt Hill (NTS 2D/05), northern Cold Spring Pond (NTS12A/01) and adjacent map areas. Government of Newfoundland and Labrador, Department of Natural Resources, Geological Survey, Open File NFLD/3341, 10 pages.

Campbell, H., Organ, J.S. and Taylor, D.
2017: Till-geochemistry sampling and quaternary mapping in south-central Newfoundland, Great Burnt Lake (NTS 12A/08), northern Cold Spring Pond (NTS 12A/01), and Burnt Hill (NTS 02D/05) map areas. *In* Current Research. Government of Newfoundland and Labrador, Department of Natural Resources, Geological Survey, Report 17-1, pages 105-117.

Canstar Resources Inc.
2018: website-https://www.canstarresources.com/projects/the-katie-project/geology.

Clifton, H.E., Hunter, R.E., Swanson, E.J. and Phillips, R.L.
1969: Sample size and meaningful gold analysis, USGS. Professional Paper, number 625-C. Pages C1-C17.

Colman-Sadd, S.P.
1976: Geology of the St. Alban's map-area, Newfoundland. Government of Newfoundland and Labrador, Department of Mines and Energy, Mineral Development Division, Report 76-4, 22 pages.

1980: Geology of south-central Newfoundland and evolution of the eastern margin of Iapetus. American Journal of Science, Volume 280, 33 pages.

1985: Geology of the west part of Great Burnt Lake (12A/08) area. *In* Current Research. Government of Newfoundland and Labrador, Department of Mines and Energy, Mineral Development Division, Report 85-1, pages 105-113.

Colman-Sadd, S.P., Hayes, J.P. and Knight, I. (compilers)
2000: Geology of the Island of Newfoundland (digital version of Map 90-01 with minor revisions). Map 2000-03. Scale 1:1 000 000. Government of Newfoundland and Labrador, Department of Mines and Energy, Geological Survey, Open File NFLD/2192.

Colman-Sadd, S.P. and Russell, H.A.J.
1988: Miguels Lake (02D/12), Newfoundland. Map 88-050. Scale: 1:50 000. Government of Newfoundland and Labrador, Department of Mines, Mineral Development Division, Open File 2D/12/0197.

Colman-Sadd, S.P. and Swinden, H.S.
1980: Geology and mineral potential of south-central Newfoundland. Government of Newfoundland and Labrador, Department of Mines and Energy, Mineral Development Division, Open File NFLD/1251, 91 pages.

1982: Geology and mineral potential of south-central Newfoundland. Government of Newfoundland and Labrador, Department of Mines and Energy, Mineral Development Division, Report 82-8, 102 pages.

1984a: Great Burnt Lake, Newfoundland. Map 84-066. Scale: 1:50 000. Government of Newfoundland and Labrador, Department of Mines and Energy, Mineral Development Division, Open File 012A/08/0412. Blueline paper. GS# 012A/08/0412.

1984b: A tectonic window in central Newfoundland? Geological evidence that the Appalachian Dunnage Zone may be allochthonous. Canadian Journal of Earth Sciences, Volume 21, pages 1349-1367.

Conliffe, J., King, R. and Wilton, D.
2018: Genesis of carbonate-hosted Zn mineralization in the Hare Bay and Pistolet Bay areas, Great Northern Peninsula, Newfoundland. *In* Current Research. Government of Newfoundland and Labrador, Department of Natural Resources, Geological Survey, Report 18-1, pages 71-93.

Dean, M.T. and Wilton, D.H.C.
2002: The Katie prospect and the potential for volcanogenic massive sulphides in the Baie D'Espoir Group, south-central Newfoundland: a metallogenic and lithogeochemical study. *In* Current Research. Government of Newfoundland and Labrador, Department of Natural Resources, Geological Survey, Report 02-1, pages 289-305.

Dickson, W.L.
1983: Geological map of the Ackley Granite, eastern Newfoundland. Government of Newfoundland and Labrador, Department of Mines and Energy, Mineral Development Division, Map 81-005.

1996: Geochemical sample sites in the Mount Peyton (2D/14) map area, central Newfoundland. Map 96-27. Scale: 1:50 000. *In* Whole-rock Geochemical and Field Data from the Mount Peyton Intrusive Suite, the Great Bend Complex and Miscellaneous Rocks, Central Newfoundland (NTS Map Areas 2D/11E, 2D/14, 2E/3 and Parts of 2D/13 and 2D/15). Government of Newfoundland and Labrador, Department of Mines and Energy, Geological Survey, Open File NFLD/2614.

2000: Geology of the Mount Sylvester map area, south-central Newfoundland. Map 2000-07. Government of Newfoundland and Labrador, Department of Mines and Energy, Geological Survey, Open File 2D/03/0349.

Evans, D.T.W.
1996: Epigenetic gold occurrences, eastern and central Dunnage Zone, Newfoundland. Government of Newfoundland and Labrador, Department of Mines and Energy, Geological Survey, Mineral Resources Report 9, 135 pages.

Evans, D.T.W., Kean, B.F. and Jayasinghe, N.R.
1994: Geology and mineral occurrences of Noel Paul's Brook. Map 94-222. Scale: 1:50 000. Government of

Newfoundland and Labrador, Department of Mines and Energy, Geological Survey Branch, Open File 012A/09/0685.

Finch, C., Roldan, R., Walsh, L., Kelly, J. and Amor, S.D.
2018: Analytical methods for chemical analysis of geological materials. Government of Newfoundland and Labrador, Department of Natural Resources, Geological Survey, Open File NFLD/3316, 67 pages.

Garrett, R.G., Reimann, C., Hron, K., Kynclova, P. and Filmoser, P.
2017: Finally, a correlation coefficient that tells the geochemical truth. Explore-Newsletter for the Association of Applied Geochemists, Number 176.

Giroux, G.H. and Froude, T.
2010: FORM 43-101F1 technical report for the Mosquito Hill zone resource estimate, Huxter Lane option Grand Falls–Windsor–Buchans Electoral District NTS: 2D/5 Newfoundland and Labrador for Golden Dory Resources Corp. and Paragon Minerals Corporation., SEDAR website.

Grant, D.R.
1974: Prospecting in Newfoundland and the theory of multiple shrinking ice caps. *In* Report of Activities. Geological Survey of Canada, Paper 74-1B, pages 215-216.

1977: Glacial style and ice limits, the Quaternary stratigraphic record, and changes of land and ocean level in the Atlantic Provinces, Canada. Geographie Physique et Quaternaire, Volume 31, Number 3-4, pages 247-250.

1989: Quaternary geology of the Atlantic Appalachian region of Canada. *In* Quaternary Geology of Canada and Greenland. *Edited by* R.J. Fulton. Geological Survey of Canada, Geology of Canada, Paper 76-1A, pages 283-285.

Howley, J.P.
1881: Chapter 10: Report for 1870 - survey of Bay East River - Mr Howley's examination of sundry parts of the coast. *In* Geological Surveys of Newfoundland. By A. Murray and J.P. Howley, pages 210-249

Jenness, S.E.
1960: Late Pleistocene glaciation of eastern Newfoundland. Geological Society of America Bulletin, Volume 71, pages 161-180.

Kerr, A., van Nostrand, T.S., Dickson, W.L. and Lynch, E.P.
2009: Molybdenum and tungsten in Newfoundland: A geological overview and a summary of recent exploration developments. *In* Current Research. Government of Newfoundland and Labrador, Department of Natural Resources, Geological Survey, Report 09-1, pages 43-80.

Kynčlova, P., Hron, K. and Filmozer, P.
2017: Correlation between compositional parts based on symmetric balances. Mathematical Geosciences, Volume 49, pages 777-796.

Lake, J. and Wilton, D.H.C.
2006: Structural and stratigraphic controls on mineralization at the Beaver Brook antimony deposit, central Newfoundland. *In* Current Research. Government of Newfoundland and Labrador, Department of Natural Resources, Geological Survey, Report 06-1, pages 135-146.

Levinson, A.A.
1974: Introduction to exploration geochemistry. 2nd Edition. Applied Publishing Co. Ltd. Wilmette, Illinois.

Liverman, D., Batterson, M., Bell, T., Marich, A. and Putt, M.
2006: Digital elevation models from Shuttle RadarTopography Mission data – new insights into the Quaternary history of Newfoundland. *In* Current Research. Government of Newfoundland and Labrador, Department of Natural Resources, Geological Survey, Report 06-1, pages 177-189.

Lynch, J.
1996: Provisional elemental values for four new geochemical soil and till reference materials, TILL-1, TILL-2, TILL-3 and TILL-4. Geostandards Newsletter, Volume 20, Number 2, pages 277-287.

MacClintock, P. and Twenhofel, W.
1940: Wisconsin glaciation of Newfoundland. Geological Society of America Bulletin, Volume 51, pages 1729-1756.

McBride, D.E.
1988: First year assessment report on geological, geochemical and geophysical exploration for licence 3115 on claim block 5351 in the Newfoundland Dog Pond area, south-central Newfoundland. Bitech Energy Resources Limited Unpublished report, 21 pages.

McClenaghan, M.B. and Paulen, R.C.
2017: Chapter 20: Mineral exploration in glaciated terrain. *In* Past Glacial Environments (Sediments, Forms and Techniques). *Edited by* J. Menzies and J.J.M. van der Meer. Elsevier, pages 689-751.

McNicoll, V.J., Squires, G.C., Wardle, R.J., Dunning, G.R. and O'Brien, B.H.
2006: U–Pb geochronological evidence for Devonian deformation and gold mineralization in the eastern Dunnage Zone, Newfoundland. *In* Current Research. Government of Newfoundland and Labrador, Department of Natural Resources, Geological Survey, Report 06-1, pages 45-61.

Murray, R.C.
1955: Directions of glacier ice motion in south-central Newfoundland. Journal of Geology, Volume 63, pages 268-274.

O'Brien, S.J.
1998: Geology of the Connaigre Peninsula and adjacent areas, southern Newfoundland (parts of NTS 1M/5, 6, 11, 12 and 14 and 11P/8 and 9). Map 98-002. Government of Newfoundland and Labrador, Department of Natural Resources, Geological Survey, Open File NFLD/2660.

Organ, J.S. and Amor, S.A.
2016a: Till geochemistry of Sheffield Lake, Springdale, Dawes Pond and The Topsails (NTS map areas 12H/07, 08, 01, 02). Government of Newfoundland and Labrador, Department of Natural Resources, Geological Survey, Open File 012H/2212, 34 pages.

2016b: Till geochemistry of The Topsails and Rainy Lake (NTS map areas 12H/02 and 12A/14) and surrounding areas. Government of Newfoundland and Labrador, Department of Natural Resources, Geological Survey, Open File NFLD/3301, 29 pages.

Paulen, R.C., Paradis, S., Plouffe, A. and Smith, I.R.
2011: Pb and S isotopic composition of indicator minerals in glacial sediments from NW Alberta, Canada: Implications for Zn-Pb base metal exploration. Geochemistry, Exploration, Environment, Analysis Volume 11, pages 309-320.

Primmer, S., Bell, T. and Batterson, M.
2015: The role of ice dynamics on drift dispersal in the Newfoundland Ice Cap: Preliminary investigations. *In* Current Research. Government of Newfoundland and Labrador, Department of Natural Resources, Geological Survey, Report 15-1, pages 277-285.

Proudfoot, D.N., Scott, S., St Croix, L. and Taylor, D.M.
1990: Quaternary geology of the Burnt Hill (NTS 2D/05) – Great Gull Lake (NTS 2D/6) map areas in southeast-central Newfoundland. *In* Current Research. Government of Newfoundland and Labrador, Department of Mines and Energy, Geological Survey Branch, Report 90-1, pages 49-64.

Proudfoot, D.N., Scott, S., St. Croix, L., Taylor, D.M. and Vanderveer, D.G.
1988: Glacial striations in southeast-central Newfoundland. Map 88-102. Scale 1:250 000. Government of Newfoundland and Labrador, Department of Mines and Energy, Mineral Development Division, Open File NFLD 1725.

Puritch, E. and Barry, J.
2015: FORM 43-101 and FORM 43-101F1 P and E Mining Consultants technical report number 297. Resource estimate on the Great Burnt Copper property, central Newfoundland for Pavey Ark Minerals Inc. Latitude 48°20'28" N Longitude 56°09'06" W UTM WGS84 Zone 21U 562869 mE 5354553 mN; NTS 12A/08.

R Project
2016: The R Project for Statistical Computing. http://www.r-project.org (accessed June 18th, 2018).

Rogerson, R.J.
1982: The glaciation of Newfoundland and Labrador. *In* Prospecting in Areas of Glaciated Terrain - 1982. *Edited by* P.H. Davenport. Canadian Institute of Mining and Metallurgy, pages 37-56.

Sandeman, H.A.I., Dunning, G.R., McCullough, C.K. and Peddle, C.
2017: U–Pb geochronology, petrogenetic relationships and intrusion-related precious-metal mineralization in the northern Mount Peyton intrusive suite: Implications for the origin of the Mount Peyton trend, central Newfoundland (NTS 2D/04). *In* Current Research. Government of Newfoundland and Labrador, Department of Natural Resources, Geological Survey, Report 17-1, pages 189-217.

Sandeman, H., McNicoll, V. and Evans, D.T.W.
2012: U–Pb geochronology and lithogeochemistry of the host rocks to the Reid gold deposit, Exploits Subzone–Mount Cormack Subzone boundary area, central Newfoundland. *In* Current Research. Government of Newfoundland and Labrador, Department of Natural Resources, Geological Survey, Report 12-1, pages 85-102.

Sandeman, H.A.I., Peddle, C. and Newman, R.
2018: Beaver Brook antimony mine revisited: an update on operations and new structural and geological observations. *In* Current Research. Government of Newfoundland and Labrador, Department of Natural Resources, Geological Survey, Report 18-1, pages 123-152.

Sandeman, H.A., Wilton, D.H.C., Conliffe, J., Froude, T. and O'Driscoll, J.M.
2013: Geological setting, geochronological constraints and the nature of mineralization at the Mosquito Hill (Huxter Lane) gold deposit, central Newfoundland. *In* Current Research. Government of Newfoundland and Labrador, Department of Mines and Energy Geological Survey, Report 13-1, pages 167-188.

Shaw, J., Piper, D.J.W., Fader, G.B.J., King, E.L., Todd, B.J., Bell, T., Batterson, M.J. and Liverman, D.G.E.
2006: A conceptual model of the deglaciation of Atlantic Canada. Quaternary Sciences Reviews, Volume 25 (17-18), pages 2059-2081.

Stapleton, G.J. and Smith, J.L.
2018: Mineral Inventory Project. *In* Current Research. Government of Newfoundland and Labrador, Department of Natural Resources, Geological Survey, Report 18-1, pages 185-191.

Swinden, H.S.
1988: Geology of the Pipestone Pond area (12A/1 NE; 12A/8 E), Newfoundland. Map 88-051. Scale: 1:50 000. *In* Geology and Economic Potential of the Pipestone Pond Area (12A/1 NE; 12A/8 E), Central Newfoundland. Government of Newfoundland and Labrador, Department of Mines, Mineral Development Division, Report 88-2, 101 pages, enclosure (map).

Swinden, H.S. and Collins, W.T.
1982: Geology and economic potential of the Great Burnt Lake area, Newfoundland. *In* Current Research. Government of Newfoundland and Labrador, Department of Mines and Energy, Mineral Development Division, Report 82-1, pages 188-207.

Taylor, D.M.
2001: Newfoundland and Labrador striation database. Government of Newfoundland and Labrador, Department of Mines and Energy, Geological Survey, (http://gis.geosurv.gov.nl.ca).

Thompson, M. and Howarth, R.J.
1978: A new approach to the estimation of analytical precision. Journal of Geochemical Exploration, Volume 9, pages 23-30.

Tuach, J. and Delaney, P.W.
1987: Tungsten–molybdenum in the Granite Lake–Meelpaeg Lake area, Newfoundland. *In* Current Research. Government of Newfoundland and Labrador, Department of Mines and Energy, Mineral Development Division, Report 87-1, pages 113-127.

Westhues, A.
2017: Updated geology of the St. Alban's map area (NTS 01M/13), Dunnage and Gander zones. *In* Current Research. Government of Newfoundland and Labrador, Department of Natural Resources, Geological Survey, Report 17-1, pages 87-103.

Westhues, A. and Hamilton, M.A.
2018: Geology, lithogeochemistry and U–Pb geochronology of the Baie d'Espoir Group and intrusive rocks, St. Alban's map area, Newfoundland. *In* Current Research. Government of Newfoundland and Labrador, Department of Natural Resources, Geological Survey, Report 18-1, pages 207-232.

Zhu, l. Zhang, H.H., Xia, B. and Xu, D.R.
2007: Total fluoride in Guangdong soil profiles, China: Spatial distribution and vertical variation. Environment International, Volume 33, pages 302-308.

APPENDICES

Appendices B–P are available as digital comma-separated files (.csv) and Appendices Q-S are available as pdf files through this link.

APPENDIX A: Open File NFLD/3341
The report and data are available as a pdf and digital comma-separated file through this link.

APPENDIX B: Analyses of CRM Till Standards TILL-1, TILL-2, TILL-3 and TILL-4, ICP-OES after 4-Acid (HCl-HNO_3-$HClO_4$-HF) Digestion

APPENDIX C: Analyses of CRM Till Standards TILL-1, TILL-2, TILL-3 and TILL-4, INAA

APPENDIX D: Analyses of CRM Till Standards TILL-1, TILL-2, TILL-3 and TILL-4, ICP-OES after HNO_3 Digestion

APPENDIX E: Analyses of CRM Till Standards TILL-1, TILL-2, TILL-3 and TILL-4, ISE after Alkaline Fusion

APPENDIX F: Analyses of CRM Till Standards TILL-1, TILL-2, TILL-3 and TILL-4, Gravimetry

APPENDIX G: Analyses of Lab Duplicates, ICP-OES after 4-Acid (HCl-HNO_3-$HClO_4$-HF) Digestion

APPENDIX H: Analyses of Lab Duplicates, INAA

APPENDIX I: Analyses of Lab Duplicates, ICP-OES after HNO_3 Digestion

APPENDIX J: Analyses of Lab Duplicates, ISE after Alkaline Fusion

APPENDIX K: Analyses of Lab Duplicates, Gravimetry

APPENDIX L: Analyses of Field Duplicates, ICP-OES after 4-Acid (HCl-HNO_3-$HClO_4$-HF) Digestion

APPENDIX M: Analyses of Field Duplicates, INAA

APPENDIX N: Analyses of Field Duplicates, ICP-OES after HNO_3 Digestion

APPENDIX O: Analyses of Field Duplicates, ISE after Alkaline Fusion

APPENDIX P: Analyses of Field Duplicates, Gravimetry

APPENDIX Q: Control Charts of Analyses of CRM Till Standards TILL-1, TILL-2, TILL-3 and TILL-4 from 1987–88, 2016 and 2017, for all Elements Listed in Appendix A

APPENDIX R: Thompson-Howarth Plots of Lab and Field Duplicate Data from all Elements listed in the 2016 Study

APPENDIX S: Thompson-Howarth Plots of Lab and Field Duplicate Data from all Elements listed in the 1987–88 Study